TAMPEREEN TEKNILLINEN YLIOPISTO
TAMPERE UNIVERSITY OF TECHNOLOGY

MIKKO TAPANI SAHINOJA

STUDY OF MAGNESIUM METAL AND ITS ALLOYS AS A BIODEGRADABLE MATERIAL FOR MEDICAL AND ELECTRICAL APPLICATIONS

Master's Thesis

Examiners: professors Minna Kellomäki and Jukka Lekkala, and postdoctoral researcher Ville Ellä
Reviewers and topic approved in the Engineering sciences Faculty council meeting in 6. March 2013

TIIVISTELMÄ

TAMPEREEN TEKNILLINEN YLIOPISTO
Materiaalitekniikan koulutusohjelma
SAHINOJA, MIKKO TAPANI: Magnesiummetallin ja sen lejeerinkien tutkimus biohajoavan materiaalin näkökulmasta lääketieteellisiin ja elektronisiin käyttösovelluksiin
Diplomityö, 80 sivua, 4 liitesivua
Lokakuu 2013
Pääaine: Biomaterials
Tarkastajat: Professorit Minna Kellomäki, Jukka Lekkala, sekä tutkijatohtori Ville Ellä
Avainsanat: Magnesium, polymeerikomposiitti, hajoaminen, fosfaattikerros

Diplomityön tarkoitus oli koota tietoa magnesiumista sekä materiaalina että sen käytöstä lääketieteellisiin tarkoituksiin ja tarkastella magnesium metallin ominaisuuksia. Käytännön työnä oli tarkoitus testata Mg-10Gd-1Nd-1Zn lejeeringin hajoavuutta poly(l-laktidi-co-dl-laktidi) (PLDLA) 50:50 polymeerikomposiitissa. Tavoitteena oli arvioida käytettyjen metallien asemaa lääketieteellisistä välineistä implanttituotteisiin asti ja tutkia, että onko biohajoavia metalleja käytössä näissä sovelluksissa. Kirjallisuustutkimuksen tarkoituksena oli selvittää voiko magnesiumia käyttää lääketieteellisesti ja kokeellisessa osiossa selvittää sen hajoamisprofiilia.

Magnesium on tunnettu materiaali, jonka ominaisuudet ovat tehneet siitä tärkeän monessa eri käyttökohteessa jossa materiaalin keveys on tärkeä ominaisuus. Magnesiummetallin bioyhteensopivuus on kiinnittänyt tutkijoiden huomiota. Nopea hajoaminen on kuitenkin aiheuttanut ongelmia implanttisovelluksissa. Viime aikoina huomio magnesiumia kohtaan on kasvanut luuimplanttien, stenttien sekä implanttien, jotka hyödyntävät sähköä toiminnassaan kuten ihon alle sijoitettavat anturit, suunnittelussa. Materiaalia on jo tutkittu prekliinisesti eräiden implanttisovellusten kohdalla. Nämä tutkimukset ovat olleet lupaavia, mutta ristiriitaiset tulokset tutkimusten välillä sekä metallin tai sen lejeerinkien turvallisuus kliinisessä käytössä ovat toistaiseksi estäneet tuotteiden laajemman kaupallisen käytön. Tutkimustulosten pohjalta on esitetty, että kehon sisäisenä implantti materiaalina magnesium on turvallista käyttää kun hajoamisnopeus on alle 0.01 ml/cm^2/päivä.

Käytännön työssä Mg-lejeerinkiä käytettiin sinänsä sekä siitä valmistettiin komposiitteja joissa oli 67–92 wt-% PLDLA 50:50 polymeeriä. Työ keskittyi pH-mittauksiin sekä visuaaliseen tarkasteluun mikroskoopilla. Tulokset osoittivat, että lejeerinki materiaali hajoaa tehokkaammin "Sørensen" puskuriliuoksessa kuin de-ionisoidussa vedessä. Lejeerinki saa fosfaatti-kerroksen päälleen jo muutaman päivän aikana puskuriliuoksessa. Polymeeri hidasti magnesium lejeeringin hajoavuustahtia verrattuna magnesium lejeerinki näytteisiin nähden. Implanttisovelluksia varten komposiittimateriaali vaatii lisää tutkimusta, jotta sen käyttöä ja soveltuvuutta voidaan määrittää tarkemmin.

ABSTRACT

TAMPERE UNIVERSITY OF TECHNOLOGY
Master's Degree Programme in Material Science
SAHINOJA, MIKKO TAPANI: Study of magnesium metal and its alloys as a biodegradable material for medical and electrical applications
Master of Science Thesis, 80 pages, 4 appendix pages
October 2013
Major: Biomaterials
Examiners: Professors Minna Kellomäki, Jukka Lekkala and postdoctoral researcher Ville Ellä
Keywords: Magnesium, polymer composite, degradation, phosphate layer.

The goal of the work was to review known metallic materials and especially magnesium that are used for medical purposes. The intention was to review the role of the current metallic materials, covering the field from medical utensils to actual implant products and to find if there are any degradable metals used. Other purpose was to determine if magnesium is suitable for medical applications with a focus on the alloy's degradation properties in the practical section. Here the Mg-10Gd-1Nd-1Zn alloy's degradation behavior was studied when it was used in composite structure with poly(l-lactide-co-dl-lactide) (PLDLA) 50:50.

Magnesium metal is well-known and commonly used material. Its influence in different fields has made it an important material with applications that are used due to the light weight of the material when compared to other metal materials. Magnesium's biocompatibility has made the material gain attention in the medical field. On the other hand, due to magnesium's fast degradation rate, it has been difficult to use the material for medical applications. Recently, though, magnesium has been studied and planned to be used for medical implants for bone and electrical applications. The material has been used for certain implant application already but only in pre-clinical testings. These tests have shown that the material is almost suitable as it is for some applications but conflicting results from different sources and safety aspects have prevented its use. Studies propose that, for safe in vivo use, a suitable degradation rate should be under 0.01 ml/cm^2/day.

Testing the Mg-10Gd-1Nd-1Zn alloy by itself and as a composite with 67-92 wt-% PLDLA 50:50 polymer resulted in various results. Work was focused on pH-measurements and microscope imaging. Results indicated that the alloy degraded more rapidly in a "Sørensen" buffer solution than in di-ionized water immersion. The alloy also gained a phosphate layer on top of the metal in a few days in the buffer solution. It was also noticed that the polymer was able to hinder degradation of the magnesium material heavily. In that respect the magnesium alloy in a composite might be promising for implant applications for its electrical properties but further research is needed to determine this.

PREFACE

The Master's Thesis was conducted to the Department of Electronics and Communicational Engineering (formerly known as the Department of Biomedical Engineering). It was a part of a project SpareParts where multiple researches from different fields were gathered.

Especial thanks are given to Ph.D. Ville Ellä for providing the guidance for the work and to professors Minna Kellomäki and Jukka Lekkala as well as to doctoral student Timo Salpavaara for providing suggestions and insight of their own during the meetings held together. Thanks to the researchers and personnel from the Department of Electronics and Communicational Engineering, Department of Automation Science and Engineering, and Department of Materials Science who also provided help and guidance in various ways.

Tampere 13.11.2013

_____

Mikko Tapani Sahinoja

TABLE OF CONTENTS

LIST OF SYMBOLS AND ABBREVIATIONS

BCC	Body-centered cubic crystal structure.
CIP	Cold isostatic pressing
CP-Ti	Commercially pure titanium
FCC	Face centered cubic crystal structure.
Gd	Gadolinium
HCl	Hydrochloride acid
HCP	Hexagonal close-packed crystal structure.
HIP	Hot isostatic pressing
HPM	High porosity membrane
LPM	Low porosity membrane
MDD	Mechanical disintegration and deposition method
Mg	Magnesium
Nd	Neodymium
PCL-HMW	Poly(e-caprolactone)-high molecular weight
PCL-LMW	Poly(e-caprolactone)-low molecular weight
PLDLA	Poly(l-lactide-co-dl-lactide)
PLLA-HMW	Poly(l-lactid acid)-high molecular weight
PLLA-LMW	Poly(l-lactid acid)-low molecular weight
SBF	Simulated body fluid
SMA	Shape memory alloy
Zn	Zinc

1 INTRODUCTION

Metal materials have an important role in the medical field. Choosing the right material can mean the success over a failure situation which is why metals have been used extensively even if they are not perfect for the purpose. One interesting metal is magnesium, which has low density when compared to other metals. It has been known for over two centuries now and has been widely used for several different applications by, different industrial fields but it has not been widely used in the medical field. Medical field, especially, thrives on innovation which is why new material solutions emerge constantly to solve existing problems. Magnesium is now gaining even more interest due to the improved technological capabilities and knowledge about the material.

A common property with metals is that most of them have one of the three different primary crystal structures. These three types, presented in Figure 1, are face centered cubic (FCC), hexagonal close-packed (HCP) and body-centered cubic (BCC). Some metals can have, though, other crystal structures like double hexagonal, monoclinic, orthorhombic, rhombohedral, tetragonal and trigonal crystal structures to name a few more.

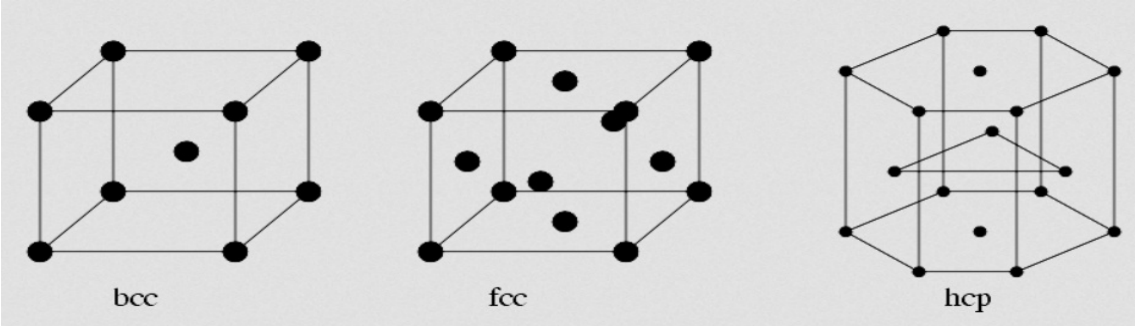

Figure 1. Unit cells of metal crystal structures: face centered cubic (FCC), hexagonal close-packed (HCP) and body-centered cubic (BCC).

Metal materials used in the medical field usually provide some kind of advantage over the other materials. These advantages are usually, strength, toughness, biostability and easy to make sterile. Due to these properties, metals are mainly used as utensils and other medical instruments. In some cases they are used as implants like hip prostheses and heart pacers. Biodegradable applications, though, usually fall outside the metal material group until recently. Iron and magnesium, being the exceptions in the metal materials, are biodegradable. This has led to multiple studies about them.

Magnesium's history shows that the material contains a lot of potential, which is not yet fully obtained. Magnesium has especially been studied due to its biocompatibility. Medical studies concentrating on magnesium have been around for over 100 years now.

These have ranged from in vitro to small animal studies and human studies. In some cases the results have been promising and in others not. Due to conflicting results, magnesium as a metal has not been commercialized in the medical field for implant applications. The promising results, though, have kept the interest in the material and its research.

Our research in this paper now focuses on magnesium and its possibilities as a biomedical material. The practical work is concentrated to study a magnesium alloy, its degradation properties and how it reacts under aqueous surrounding when embedded into a biodegradable polymer. What further is determined are the materials possibilities as an implant material in electrically conductive composites.

2 BIOSTABILE METALS AND ALLOYS IN BIOMEDICINE

In the field of materials science, there are a large number of metal materials and alloys. There are frequently new and unique material combinations used to solve technical problems. In this chapter, the focus is on metals that have been used to solve the technical problems in the medical field in ways that are known. The most common and some not so common metals and the applications they are used in are discussed to understand their role in the medical field.

When metals in biomedicine are discussed, stainless steels are the group of metals that stand out. This group consists of multiple different versions of the same larger group. Other metals are also in an important role in biomedicine. These materials are metals based on cobalt, titanium, nickel, tantalum, zirconium, tungsten and silver.

2.1 Stainless steels

Stainless steels are considered as one of the most important group of metal materials in biomedicine for the last few decades. This material group has kept its importance in the medical field because it is easy to manufacture and process for products. Stainless steels have different crystalline structures that include martensitic, ferritic, austenitic and duplex. Each of these structures has a different effect on the material's properties. Stainless steels also have good corrosion resistance in oxygen based environment, which is due to chromium and nickel, or molybdenum and nitrogen additions. [14; 53; 57.] This resistance comes from a protective oxide layer that these additions create. This layer works against pitting corrosion which is a very common type of corrosion in metal materials. These additions also improve the mechanical strength of these metals. [66.]

2.1.1 Martensitic

Martensitic stainless steels are alloys that consist of a Fe-Cr-C combination, where the chromium content is around 10.5 to 18 % and the carbon content is around 1.2 %. This material has a body-centered tetragonal crystal structure which is defined as a martensitic structure. The material is generally ferromagnetic in nature and can be hardened through heat treatment. As stated earlier, stainless steels have good corrosion resistance. With martensitic materials, this resistance is good in low moisture conditions. The addition of some specific chemical element into the martensitic stainless steels can alter certain properties of the metal. Adding niobium, silicon, tungsten or vanadium results to changes in tempering procedure that happens after the hardening process. If we want to improve the mechanical strength and toughness or corrosion resistance, then we can add nickel to the alloy. If we want to improve

machinability of the alloy, then we need to add small amounts of sulfur or selenium. [14; 57.]

Martensitic stainless steel is used in applications where high hardness is needed, like dental and surgical instruments. These include dental chisels, scalpels, bone chisels, bone gouges, and orthodontic pliers to name a few. Because of the limitations of the martensitic structure, other forms of stainless steels have been used for more corroding conditions. [14.]

2.1.2 Ferritic

With ferritic stainless steels materials, the structure combination is Fe-Cr. This alloy has a body-centered cubic (BCC) crystal structure. In contrast to martensitic materials, the ferritic alloy has 11 to 30 % of chromium. As with martensitic alloys, certain materials can be used to improve specific characteristics of ferritic stainless steels. Some of these materials are molybdenum, silicon, aluminum, titanium, niobium, sulfur and selenium. Materials like sulfur and selenium can for example improve the machinability of the alloy while molybdenum can improve toughness. [14; 57.]

Ferritic materials cannot be strengthened through heat treatment, additionally, they can strain-harden relatively slowly and with cold working, the materials ductility is greatly lowered. Because of these limitations, ferritic materials are not really used in medical applications. The material has been in use only in solid handles, guide pins and fasteners. [14.]

2.1.3 Austenitic

Austenitic stainless steels (ASS) is the most used stainless steel group in the medical field. The chronium content of austenitic steels is around 16 to 26 %, nickel content is 35 % or less and manganese content is 15% or less. These ratios are different compared to other stainless steels. Austenitic steels resemble ferritic steels since they cannot be hardened through heat treatment, although, austenitic steels are not magnetic in their annealed state compared to ferritic steels. Austenitic steels can only be hardened through cold working. Austenitic steels are good at cryogenic conditions and have good to high temperature strength and oxidation resistance. [14; 57.]

Austenitic steels can be modified by adding different metals like molybdenum, copper, silicon, aluminum, titanium or niobium to improve halide pitting resistance, oxidation resistance and formability. By altering nickel content you can adjust the response to deformation and gain better formability. [14.] Austenitic stainless steels are used where good corrosion resistance and moderate strength are the key factors. These applications include dental impression trays, hypodermic needles, work surfaces and steam sterilizer equipment. [14; 53.]

2.1.4 Duplex

Duplex alloys are two phase alloys based on Fe-Cr-Ni systems. This alloy is comprised of equal amounts of austenitic and ferritic phases in the alloys microstructure. The carbon content of this material is very low, under 0.03 %. The alloy can contain small amounts of molybdenum, nitrogen, tungsten and copper. The chromium content is from 20 to 30 % and nickel content is from 5 to 8 %. Small differences in the metal amounts and the different phases in the microstructure have led to specific properties. The duplex alloys have better tensile strength than austenitic stainless steels. Toughness and ductility values are improved when compared to ferritic grades. This alloy group also has superior chloride stress corrosion cracking resistance and pitting corrosion resistance. This alloy has not been used much in the medical field but they might prove to be important in the future. [14; 57.]

2.1.5 Precipitation-hardenable

Another not so common group is precipitation-hardenable stainless steels (PH stainless steels). In this group, chromium and nickel are the dominant materials. Hardening, of this alloy type, is done by aging treatment. With this method, austenitic to semi-austenitic or martensitic structures can be obtained. The classification of this group is due to their solution-annealed microstructure. [14.]

Semi-austenitic structures can be heat-treated to gain a martensitic structure. Utilizing cold working can speed up the aging process. The aging process itself can also be improved by adding aluminum, titanium, niobium or copper. In the field of medical applications, both semi-austenitic and martensitic precipitation-hardened steels are used. Applications range from neurosurgical aneurysm and micro-vascular clips to surgical and dental instruments. On the other hand, austenitic grades of precipitation-hardened steels are not used in the medical field. [14; 57.]

2.1.6 Implant grade

Most of the stainless steels are used for transient contact to the human skin and tissue. This has resulted to a additional classification of implant grade stainless steels that are suitable to be used in contact with the human tissue. This group consists of austenitic stainless steels (ASS). They are inexpensive as their manufacturing and processing is done through common techniques. Their mechanical properties can be adjusted to gain optimal strength and ductility for the alloy. The classification of these steels is wrought alloys since they are forged and machined. These alloys can additionally gain passivity by immersing them on nitric acid to create a protective layer, before they are sterilized and packaged. The corrosion behavior of the materials prevents long term implant use. Even with this critical limitation, they are being used as bone screws, plates, nails, rods and other temporary fixation devices that are removed after a desired time period postoperatively. [14.]

Implant grade stainless steels contain a additional group, which is low carbon stainless steels, typically named as type 316L which is comprised of under 0.08 % carbon, 18% of chromium, 14 % of nickel and about 2.5 % of molybdenum. These metals are vacuum melted to gain the low carbon variation from type 316 alloys. Utilizing vacuum melting also improves cleanliness of the process. Pitting corrosion resistance can be maximized with a ferrite free microstructure. Grain size should be uniform throughout the specimen so that any specifically wanted property can be obtained. [14; 53; 57.]

This group is generally used in the 30% cold worked state as this increases the yield and ultimate tensile strength and fatigue strengths of the material when compared to annealed metals. These properties result to the material's lower ductility. This group can be welded but this can sensitize the material which is not wanted. [14.] The 316L steels can be used as wires for temporary solutions. Vacuum melted 316L are used in temporary fixation applications like plates, screws, wires, sutures and clips for example. Additionally, the type 316L material is most common in total joint prostheses. [14; 53.]

2.1.7 Nitrogen-strengthened

Nitrogen-strengthened metal group is gained by utilizing nitrogen to increase the metals properties. These strengthened metals have increased corrosion resistance (both crevice and pitting). The mechanical properties like tensile strength, impact strength and fatigue strength are better when compared to 316L stainless steels. The improvement is gained by using the electro slag refining (ESR) process. Improvement over 316L steels has resulted these types of stainless steels to be used for bone plates, bone screws, spinal fixation components and other medical applications that require higher mechanical and corrosion resistance properties. Nitrogen-strengthened stainless steels have been utilized especially with fracture fixation as the material can gain high ultimate tensile strengths, nearing 1380 MPa. [14.]

2.2 Cobalt alloys

Cobalt-based metal alloys came into use in the 1930s. Cobalt metals have high mechanical properties when compared to other metals due to the existence of solid-solution elements and carbides in the alloy. The corrosion resistance is lower than with stainless steels even though their resistance ability comes from chromium as in stainless steels. Cobalt-based alloys still have had an important part in the development of medical materials even if wrought metals have started to replace them. [14.]

Cobalt-based materials have been divided into four main alloy groups and into three special groups in the medical field, seen in Table 1. Some of the composition ratios can differ from the mentioned in the table. For example, with ASTM F 75 the composition can alter from 27 to 30 wt-% Chromium and from 5 to 7 wt-% with Molybdenum. [14.]

Table 1. Alloy groups of cobalt in medical applications. [14.]

Alloy	Composition	Use
ASTM F 75	Co-28Cr-6Mo	Casting alloy
ASTM F 90	Co-20Cr-15W-10Ni	Wrought alloy
ASTM F 799	Co-28Cr-6Mo	Similar to ASTM F 75, but thermomechanically processed.
ASTM F 562	Co-35Ni-20Cr-10Mo	Wrought alloy
ASTM F 563	Co-Ni-Cr-Mo-Fe	Wrought alloy
ASTM F 1058	Co-Cr-Ni-Mo-Fe	Wrought alloy
UNS R30004	Co-Cr-Ni-W-Mo	Cast or Wrought alloy

The strength of cobalt-based wrought alloys can be enhanced through cold working just like austenitic alloys. Wrought alloys have about 0.05 % carbon when compared to casting alloys 0.25 % carbon. Difference between carbon amounts means that wrought alloys have less strength coming from carbides. Fabricability can be enhanced with cobalt-based alloys by decreasing the chromium content and increasing the nickel amount. [14; 57.]

Wrought alloys have the ability to be hot worked and some of them can be cold drawn. Yield strength is highly influenced by grain size and the degree of cold work done to the material. Forging of metal alloys for medical purposes will restrict the material to be used for structural applications and should be done only when optimal properties for tensile strength and toughness are desired. Forging can result to non-uniform grain sizes to the material which is not desired. [14; 53; 57.]

Cobalt-based alloys are more difficult to machine than stainless steel alloys. Closed-die forging can be utilized to make the process easier but wrought alloys required more machining than casting alloys. Investment casting can be used to create implants at lower cost range if the compression and tensile strength of the material is not an important factor. Investment casting causes the material to have larger grain sizes, lower strength, lower cost and possible problems with porosity. Porosity and grain sizes, though, can be adjusted by improving the casting molds and by utilizing hot isostatic pressing (HIP) in post-cast treatment of vacuum investment-cast alloys. HIP can be used with powder metallurgy to gain fine grains and very good properties but with higher cost. With HIP cobalt-chromium alloys can be used for applications like hip prostheses to some extent. These positive and negative aspects result to the fact that cost and properties are against each other in choosing the preferred method for the creation of any possible and wanted implant application. [14; 57.]

ASTM F 75 alloys are commercially named as Vitallium or Haynes 21. The alloy has good corrosion resistance in chloride environments due to the high chromium content seen in table 1. Another reason is the formation of a protective oxide layer consisting of Cr_2O_3. Casted cobalt implant alloys generally have large and coarse grain sizes due to large mold sizes during manufacturing, which results to poorer mechanical properties compared to methods that provide fine grain sizes. Structure of ASTM F 75

alloys consists of carbides in grain boundaries and grains that contain cobalt, chromium or molybdenum and carbon in the following way $X_{23}C_6$. The alloy can also consist of sigma and gamma phases based on cobalt, cobalt-base and molybdenum. [14; 57.]

ASTM F 90 alloys are commercially named as Haynes 25 and L-605. ASTM F 90 alloys have improved machinability and fabrication properties when compared to ASTM F 75 alloys, due to additions of tungsten and nickel. In the annealed state ASTM F 90 is similar to ASTM F 75 group. Differences between these groups arise when the F90 material is cold worked to 44 % which results to over doubling the machinability and fabrication properties. [14; 57.]

ASTM F 799 group is modified from the ASTM F 75 group through mechanical processing. This is done by hot forging rough billets in to the wanted shapes. ASTM F 799 has a more worked grain structure and a hexagonal close-packed phase (HCP), which is formed through shear-induced transformation of face-centered cubic (FCC) matrix. ASTM F 799 group has about twice the fatigue, yield and ultimate tensile strength when compared to ASTM F 75 alloys. Good mechanical properties can also be gained through the use of powder metallurgy with HIP due to finer microstructure of the alloy. Wear properties are also enhanced through HIP, which has been used in contact with ultra-high molecular weight polyethene (UHMWPE) or ASTM F 799 alloy cups in joint implants. [14; 57.]

ASTM F 562 alloys are commercially sometimes named as MP35N. These alloys have high strength, ductility, corrosion resistance and stress-corrosion cracking resistance compared to other cobalt-based alloys. Higher strength of the alloy is gained from the phase transformation of the material which changes from FCC crystal structure to a HCP crystal structure through the use of cold working due to high cobalt content. Different crystal structures in the alloy make the material harder as the structures prevent dislocation movement through the crystal structure barriers. Tensile strength can be increased with cold-working and aging to over 1795 MPa. This tensile strength is higher than the current highest surgical implant. [14.] The alloy can experience over 8 % of elongations, which can create unwanted problems if [57].

ASTM F 563, ASTM F 1058 and UNS R30004 have been standardized for the use of medical devices and have no harmful effects in terms of cytotoxicity, systemic toxicity, intracutaneous irritation, intramuscular implantation, skin sensitization, blood hemolysis or pyrogenicity. ASTM F 563 has been used in bars, wires and forgings. ASTM F 1058 has higher chromium content than nickel. ASTM F 1058 has been used in heart springs and in neurosurgery and vascular surgery if the material has been aged. These two metals can be strengthened through cold working and aging. UNS R30004, also known as Havar, has been in consideration for medical implants but has not been used in applications yet. [14; 57.]

2.3 Titanium and titanium alloys

Titanium is a commonly used material in the medical field due to its use in joint implants because of its biocompatibility. The densities of titanium alloys are low when compared for example to stainless steels, around 50 to 60 % of 316L stainless steels density. Titanium can be strengthened by alloying and deformation processing. Corrosion behavior for the material is low due to a protective oxide layer. This oxide layer can reform itself if it is damaged even under low loads and slow sliding speeds in articulating conditions. If the protective film is removed and does not generate back, the material will experience galling that causes metal-to-metal contact and cold welding for example in joint implant situations. This then will result in high friction and wear rates. Titanium's wear can prevented with methods like: coating with vapor deposition of titanium-nickel (TiN) or titanium-carbon (TiC), ion implantation of N^+, thermal treatments like nitriding and oxygen diffusion hardening, and laser alloying with TiC. Titanium also has a low modulus when compared to stainless-steel and cobalt based alloys. Due to these properties, pure titanium (CP-Ti), α + β (Ti-6Al-4V) alloys and recently new compositions and orthopedic metastable β alloys have been used more in the medical field. [14; 57.]

Titanium has different crystal structures depending on the temperature used during the manufacturing. The α-phase of titanium causes HCP crystal structure and β-phase causes BCC crystal structure for the material. Temperature limit in which this change happens (allotropic transformation) is highly influenced by the interstitial elements of α- and β-stabilizers. The α- and β-phases divide the material into four different types which are α-, near-α, α-β and β-alloys. [14; 53; 57.]

Materials like tantalum, vanadium, molybdenum and niobium are β-isomorphous, with similar phase relations, with BCC titanium. Titanium does not form intermetallic compounds with these kinds of materials. For α-β alloys the elements are distributed equally between the two phases. Commercial titanium alloys typically contains one or more elements as they generally improve creep strength in the α-phase. Additions like iron and chronium can be used in β-rich, α-β or in β-alloys to improve hardenability and response to heat-treatment as they are β-stabilizers. Improving corrosion resistance of non-alloyed titanium can be done by adding nickel, molybdenum, palladium or ruthenium. [14; 57.]

Commercial titanium grades for medical purposes are divided to three groups which are unalloyed commercially pure (CP-Ti) grades, α-β alloys and β-alloys. α-β alloy group contains the Ti-6Al-4V alloy that is used in hip prostheses and which is used when evaluating fatigue resistance of orthopedic titanium alloys. Ti-6Al-4V alloy has about 45 % section of titanium production. Unalloyed titanium holds about 30 % section and the rest hold the 25 % amount. [14; 53; 57.]

2.3.1 Commercially pure titanium

Commercially pure titanium consists of 98.9 % to 99.6 % pure titanium and has the α-phase with the HCP crystal structure. The material has low strength and high ductility but good corrosion resistance due to low amount of impurities in the structure. Yield strength of the material can range from 170 to 480 MPa, depending on the impurity amount. Increasing the oxygen and iron content in the material increases the strength and fatigue strength of the material. High solubility of elements like oxygen and nitrogen causes titanium to have oxidation and solid-solution hardening on surface. This is caused by the inward diffusion of these elements. The surface-hardened layer can be removed by machining, chemical milling or other mechanical ways if needed. This layer is sometimes removed as it has a α-phase which reduces fatigue strength and ductility. [14; 57.]

Commercially pure titanium is used in applications like pacemaker cases, housings for ventricular-assist devices and implantable infusion drug pumps. Other applications include dental implants, maxillofacial implants, craniomaxillofacial implants, screws and stables for spinal surgery. [14; 53; 57.]

2.3.2 Alpha-beta alloys

The α-β alloys consist of α- and β-phases in which the β-phase is present due to retained structure or transformed structure of the alloy. Solution-treating and aging can increase the α-β alloys tensile strength from 30 to 50 % over the annealed or over-aged conditions. Alpha-beta alloys have high notch sensitivity as they can lose to 40% of their rotating bending fatigue strength. The fatigue limit is reduced with notched surfaces and porous samples. [14; 57.]

At this time, there are at least four different α-β alloys that have been standardized by the ASTM. Ti-6Al-4V and Ti-6Al-4V ELI are the most commonly used out of the four alloys due to their use in total joint replacement arthroplasty. Ti-6Al-7Nb has been used for femoral hip stems, fracture fixation plates, spinal components, fasteners, nails, rods, screws and wire. Ti-3Al-2.5V has been used for tubing and intramedullary nails because it has 20 to 50 % higher tensile properties than CP-Ti. [14.]

2.3.3 Beta alloys

The β-alloys retain their β-phase on cooling to room temperatures but can precipitate secondary phases when heat-treated. Beta alloys have higher hardenability properties than α-alloys. Beta alloys also have excellent forgeability, cold-rolling capabilities and in sheet form they can be cold brake-formed more readily than the other titanium alloys. Beta alloys cannot be work hardened much as they experience necking in complex forming operations. Solution treating and aging can be used to improve the tensile strength, ductility, toughness and formability of the alloy when compared to aged α-β alloys. The density of β-alloys is higher than α-β alloys and they have lower creep

strength and lower tensile ductility when aged. Fracture toughness of an aged beta alloy is higher than that of an α-β alloy with similar yield strength. [14; 57.]

Beta alloys are not suited for elevated-temperature applications or services unless they are stabilized or overaged treated before use. Beta alloys are used in applications that require lower elastic moduli and enhanced biocompatibility when compared to α-β alloys. Beta alloys have been used also in joint applications due to their properties. [14; 53; 57.]

2.4 Nickel-titanium

Nickel-titanium (NiTi) alloys are used as shape memory alloys (SMA) for biomedical devices. Shape memory alloys have the ability to return to some previously determined shape or size when the material is subjected to a certain thermal procedure. This deformation happens plastically. When the shape memory effect is only caused by heating the material is a one-way shape memory material. Two-way shape memory materials have the reverse effect when cooled. These materials can recover from a state that has a substantial amount of strain. The shape memory reaction with nickel-titanium alloys react through martensitic transformation which allows the alloys to be deformed by a twinning mechanism below the transformation temperature. The transformation of the martensitic structure yields a thermoelastic martensite that develops from a high-temperature austenitic phase with a long-range order. The shape memory transformation process happens in a narrow temperature range and has s hysteresis loop to it which means that the cooling and heating process transformation happens at different temperatures. [14; 57.]

For nickel-titanium systems the alloy is binary equiatomic with about 49 to 51 % Ni in the alloy. NiTi alloys have a moderate solubility range for excess nickel or titanium, as well as other metallic elements. The alloys ductility is very comparable to other metal alloys. Alloying with iron and chromium can lead to lower transformation temperature. With copper the alloy has decreased hysteresis loop and lower deformation stress of the martensite structure. Oxygen and carbon shift the transformation temperature and lower the mechanical properties of the alloy which is why these elements should be minimized or avoided completely. [14; 57.]

Work hardening and heat-treatment improve the ease of the deformation of the martensite structure. These processes also provide much greater tensile strength to the austenite structure and the property to move itself spontaneously on heating and on cooling. [14; 57.]

Processing is done in a vacuum or an inert atmosphere due to the reactivity of the oxide surface to the titanium material. Plasma arc melting, electron beam melting and vacuum induction melting are commonly used with NiTi alloys. The alloy can be hot-formed with methods like forging, bar rolling and extrusion. Cold-working can be used but requires frequent annealing due to fast work hardening. The most common method

for NiTi alloys is wire drawing as it provides excellent surface properties and the sizes of the wire can be made as small as 0.05 mm. [14.]

NiTi alloys can be used as osteosynthesis plates where the plate contracts and pulls the fractured surfaces together. Applications also include medical staples for broken bones, blood-clot filters to anchor themselves to the vein walls and catch passing clots. Other applications for SMAs are orthodontic wires and endodontic instruments. Potential applications that are not yet used are for example hip prostheses, anterior cruciate ligament prostheses and endoprostheses. [14; 53; 57.]

2.5 Tantalum

Tantalum belongs to a group named refractory metals. These metals like niobium, molybdenum and tungsten are mostly used as alloying elements in the medical field. They have the highest melting temperatures, usually above 2000 ^{o}C, and lowest vapor pressures of all metals. Tantalum differs from the rest in that commercially pure and unalloyed tantalum that is at least 99.90 % pure is used for a variety of different medical devices. Tantalum has excellent corrosion resistance against a large number of acids, aqueous solutions of salts, organic chemicals, and various combinations and mixtures of these agents. The high corrosion resistance of the metal can be compared to the level of glass. Tantalum additionally has a good biocompatibility. [14; 57.]

Tantalum is used for example in general surgery and neurosurgery as a monofilament suture. It is also used as a braided suture wire for skin closure and tendon repair. It is also used as foils and sheets for nerve anastomoses. Tantalum is additionally used as clips for the ligation of vessels, staples for abdominal surgery and as pliable sheets and plates for cranioplasty and reconstructive surgery. The metal in sintered state is also used as capacitor electrodes in electrical stimulation devices. It can be utilized as coatings for carbon foam skeletons that are used as biocompatible replacements for vertebral bodies in the spinal column. The coating is around 70 to 80 % porous and resembles the appearance of cancellous bone. Tantalum is also currently being considered as an alloy with carbon for hip and knee construction and a bone scaffold for void-filling products and applications. [14; 57.]

2.6 Zirconium

Zirconium resembles titanium as it is a reactive metal in an oxygen environment, forming a protective oxide layer on the surface of the material. Formation of this layer happens spontaneously in air or in water at ambient temperatures and below it. Just like titanium, this oxide layer heals itself when it is damaged. The oxide layer can protect the material up to temperatures of 300 ^{o}C. The protective layer enables the metal to have good corrosion resistance against mineral and organic acids, strong alkaline and saline solutions. Zirconium's biocompatibility is superior to other stable metals. [14; 57.]

Due to the corrosion resistance and biocompatibility properties, zirconium has been used as an alloying additive in other metals like β-titanium alloys. Zirconium has also been used for knee implants with a hard ceramic zirconium oxide (zirconia) surface that is gained through heating the metal to 500 ^{o}C. The material has been Zr-2.5Nb alloy in these cases with small additions of oxygen to increase the materials strength. Depth of this layer is around 5 µm. After this depth, the material transitions to zirconium through several micrometers. Zr-2.5Nb material has relatively low modulus out of the other metal materials in medical applications, being at 100 GPa. [14; 57.]

2.7 Silver

Silver has been used in applications like structural devices that include cranial support plates, suture wires, aneurysm clips and tracheostomy tubes. The metal has been used also in prostheses like silicon-silver penile implants. Silver has an antimicrobial tendency which is why it has been used as silver salts and complexes, which break down to silver ions (Ag^{+}), and also for polymeric coatings. Further development of the material has been concentrating on the prevention of the growth of micro-organisms responsible for diseases. [14.]

2.8 Electrical applications

Electrical applications are a subsection in the medical field that is recently growing. Medical electrode applications mentioned with the tantalum metal section indicates a role that metals have in electrical applications. Metals like tungsten, vacuum melted type 316L stainless steel, cobalt alloys Elgiloy and MP35N, as well as pure metals like zirconium and titanium are considered for these types of applications. These metals have high mechanical strength and fatigue resistances that are demanded in intramuscular electrodes. [14.]

Currently metals materials used for electrode applications are the noble or precious metals like platinum, iridium, rhodium, gold and palladium. These materials are used in devices meant for neural control implants like cardiac pacemakers, phrenic stimulators for respiratory control, spinal cord stimulators for bladder control, auditory prostheses, visual prostheses and neuromuscular prostheses for mobility of the limbs. These materials have good electrochemical corrosion resistance even if each of them shows some corrosion in vitro and in vivo in the electrical stimulation tests. Platinum and platinum-iridium alloys containing 10 to 30 % Ir are the usual materials in use for electrical stimulation. Other metal like tungsten are in consideration for more demanding applications where the mechanical properties are also of importance. [14.]

3 METALS AND ALLOYS FOR BIODEGRADABLE APPLICATIONS

Metals tend to corrode under body environment and the degradation products are usually toxic at least in large amounts when they do degrade. Due to these two reasons, there are only two viable metal materials for biodegradable solutions in biomedicine that are known. One of these materials is magnesium, the other is iron.

3.1 Iron alloys

Iron has been the first biodegradable metallic material used for implant purposes. Iron has been used to manufacture stents even though the corrosion rate of the material still needs some improvement. Iron's corrosion method is a localized one. The iron content in the stent materials is over 99.8 %. The metal's property to interconvert between ferric (Fe^{2+}) and ferrous (Fe^{3+}) ions by accepting and donating electrons readily enables it to be compatible with biological reactions. This makes the metal ions useful for different molecules like hemoglobin, myoglobin and many enzymes. Some research [50] have shown that metal does not completely degrade before the material is eventually released to the blood stream. Excess amount of the material through degradation can still be a negative aspect, though, which needs to be considered. [62.]

Iron's mechanical properties like high radial strength due to high elastic modulus and ductility are considered beneficial for medical implants. High radial strength enables easier manufacturing of stents with thinner struts and the ductility enables the more gentle implantation. A few of the tested iron materials and alloys for stent purposes are shown in Table 2. [26; 27; 51]

Table 2. Mechanical properties with in vitro degradation rate and average grain size for different iron-based materials. [51.]

Material	Yield Strength (MPa)	Tensile Strength (MPa)	Elongation (%)	In vitro degradation rate (mm/y)	Average grain size (µm)
316L SS: annealed (ASTM F138) [3]	190	490	40	_	12-30
Fe: annealed [26]	150	200	40	0.19	40
Fe-35Mn alloy: annealed [25]	230	430	30	0.44	<100
Fe-10Mn-1Pd alloy: heat treated [62]	850-950	1450-1550	2-8	_	_
Fe-30Mn-6Si alloy: solution treated [43]	180	450	16	0.3	<100

Iron is a ferromagnetic material which makes it unsuitable for magnetic resonance imaging (MRI). This can be changed with alloying elements like manganese with content amount from 30 % and up. This type of alloying enables higher mechanical properties that can be compared to 316L stainless steel. Manufacturing the alloy can be done with methods like powder metallurgy and different rolling-sintering steps. Degradation rate of this type of alloy, though, is twice as fast as with pure iron. Choosing the correct alloying element is thus a very important aspect when controlling material properties. Processing also has an impact in controlling different properties for the alloys. [26; 27; 51]

Iron can be manufactured and processed in many different ways, just like other metallic materials. Vacuum induction furnace casting, heat treatments, rolling-sintering steps and extrusion techniques are a few that can be used with iron. Iron can be alloyed with elements like Manganese, Cobalt, Tungsten, Boron, Carbon and Silicon to improve yield strength and ultimate tensile strength. Elements like Tin can lower the mechanical properties of the iron metal if needed. Microstructure modification techniques like electroforming processes causes finer microstructure of the material compared to other techniques. This can increase properties like yield and tensile strength but at the same time can lead to higher corrosion rates depending on the corrosion type, as the grain size is smaller and the microstructure is orientated to columnar grains [26; 27; 51]. Just like with NiTi alloys, certain iron based alloys with specific processing technologies can create memory shape materials for different applications [43]. Iron's properties make it a very promising material for biodegradable stents. Iron is not a good choice for electrical applications since its conductivity is only 18% from coppers conductivity. [26; 51]

4 MAGNESIUM AND ITS ALLOYS

Magnesium has been known for over two centuries now. Due to this fact, the material has been used in many different application and studies in different fields. As magnesium is used a lot, at the same time, it has shown its own problematic areas that prevent it from being utilized in certain situations, for example for medical purposes.

4.1 Production of magnesium

Magnesium is the eight most abundant element in the Earth's crust and the fourth most common in Earth, right after elements like iron, silicon and oxygen. Just like any other metal material, magnesium needs to be extracted from the varying sources it is in before we can use it for any applications.

Elemental magnesium was first discovered by Sir Humphrey Davy in England in 1808 by producing a mixture of magnesia and mercuric oxide. After Sir Humphrey's discovery of the oxide version of magnesium, it took about twenty years until the metal form of magnesium was isolated by a French scientist named Antoine-Alexander Bussy, in the years of 1828 to 1831. Bussy did this by fusing magnesium chloride with metallic potassium. In 1833, Sir Humphrey's assistant, Michael Faraday was able to produce magnesium metal by electrolysis of fused anhydrous $MgCl_2$. [6; 85]

In 1852 Robert Bunsen created a small laboratory for the electrolysis of fused $MgCl_2$. This was the start of commercial production of magnesium through electrolysis. In 1862 magnesium was produced at a larger scale and the material was being used for pyrotechnical and photographical applications. The world exhibition in London at that time was one of the outlets that presented this new material to even wider audiences. In the years of 1886 to 1940, several companies around the Europe and USA started expanding the commercial production of magnesium through electrolytic production and modifications of the Bunsen's laboratory cell method. Companies like "The Aluminium und Magnesium Farbik" in Germany, "Chemische Fabrik Griesheim-Elektron" the main producer of magnesium until 1916, American Magnesium Corporate and the Dow Chemical Company enabled the wide use of the material during that time. The large amount of companies around the world was due to the transportation limitations and cost. For medical studies and trials, purity requirements resulted to the use of the closest possible material provider. [85.]

4.1.1 Production methods

Magnesium does not exist in a metallic form in the nature but as in compounds. Magnesium can be found for example in some ores like carbonates: dolomite ($MgCO_3$*$CaCO_3$) and magnesite ($MgCO_3$). Magnesium also exists in a compound

named double chloride carnallite ($MgCl_2$*KCl*$6H_2O$) that is found in salt deposits in natural brines and evaporites. These can be found in the Great Salt Lake in Utah for instance. The most common and abundant source for magnesium is ocean water as 0.13 % of the world's oceans contain magnesium. [6.]

One of the first ways to produce magnesium for commercial purposes was in the middle of the nineteenth century by using the Deville-Caron process. This method uses potassium to reduce magnesium chloride in a heated closed container. First the production was done to create wires or powders. Later magnesium was also produced by electrolysis of the fused chloride. Currently there are about three different methods for the production of magnesium metal. One of these methods is electrolysis of fused anhydrous magnesium chloride ($MgCl_2$) derived from magnesite, brine or seawater. This method was used the most at least prior to the year of 2000, at an amount of 80 % of the entire magnesium output of the world. The second method is the thermal reduction of magnesium oxide (MgO) by ferrosilicon derived from carbonate ores. The last method appeared in the 1990's, which uses electrolysis of fused anhydrous $MgCl_2$ derived from serpentine ores. [6.]

The common electrolytic process that is used resembles the Dow seawater process that is presented in Figure 2. Difference to the Dow seawater process appears in the methods used to produce the anhydrous $MgCl_2$. The difficulty of the process is in the complete removal of the water from the $MgCl_2$*$6H_2O$ compound. First four moles of water can be extracted by heating it in the air so that the water evaporates. Further heating after this will result to undesirable oxides and oxychlorides. The last parts of water are difficult to remove. Methods to remove these two moles were created by various companies. The water can be flashed off by adding small quantities of partially dehydrated chloride which is added directly into a large mass of liquid mixture of magnesium, sodium and calcium chlorides contained in the electrolytic cell in the process. Another method uses dry hydrochloride acid (HCl) as an atmosphere to the process and heat to dehydrate the compound. A different approach uses a cell feed of dehydrated carnallite, which reduces the compound to a anhydrous form. [6.]

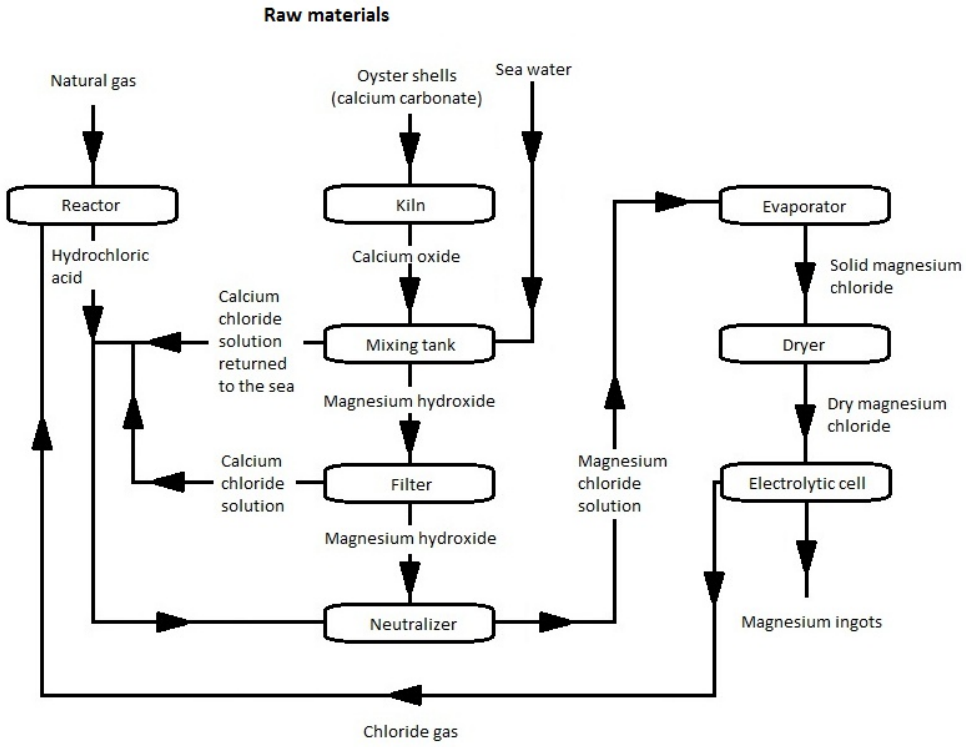

Figure 2. Dow seawater process to produce magnesium ingots. [6.]

Producing anhydrous $MgCl_2$ can be done by adding ethylene glycol to the solution. The water is removed by distillation, which will produce magnesium chloride hexammoniate by sparging with ammonia. This is then calcified to gain high-quality anhydrous $MgCl_2$. The solvents in the production method can be additionally recycled. [6.]

The Magnola process, presented in Figure 3, uses serpentine ore as a source of magnesium. The process is electrolytic as it uses magnesium chloride. The material in this method contains magnesium silicate. This material is leached with a strong hydrochloric acid in a specific process to produce $MgCl_2$ solution, which is purified by pH adjustments and ion exchange techniques. The result is concentrated ultra-high-purity brine. This brine is dehydrated and used for electrolysis. [6.]

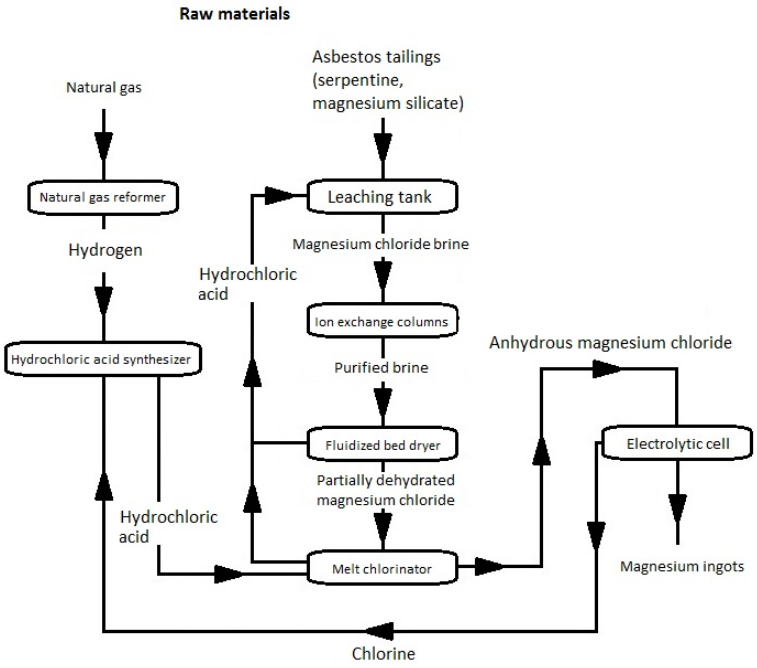

Figure 3. The Magnola process. [6.]

Thermic-reaction processes can be used for the production of magnesium metal. These processes are batch operations that are done in a vacuum environment and generally use dolomite as the starting ore. Ferrosilicon is usually used as a reductant. The process creates volatile magnesium, which distills off and is collected in a container. One of these methods is the Pidgeon process presented in Figure 4. This method uses externally heated retorts of relatively small diameter that each produces about 120 kg of magnesium per day. [6.]

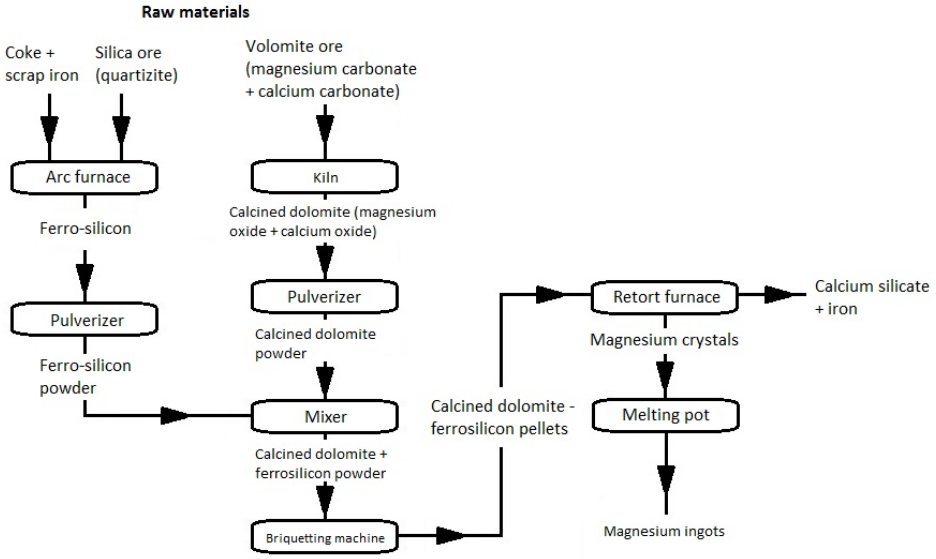

Figure 4. Pidgeon process to produce magnesium ingots. [6.]

Alternative way for the Pidgeon process is the Magnetherm process, presented in Figure 5. The difference is in that it produces a molten slag that can be then tapped off without breaking the vacuum. The furnace is electrically heated internally and alumina is used as a flux to reduce the melting point of the slag. Batch sizes of this method can go as high as 11,000 kg. [6.]

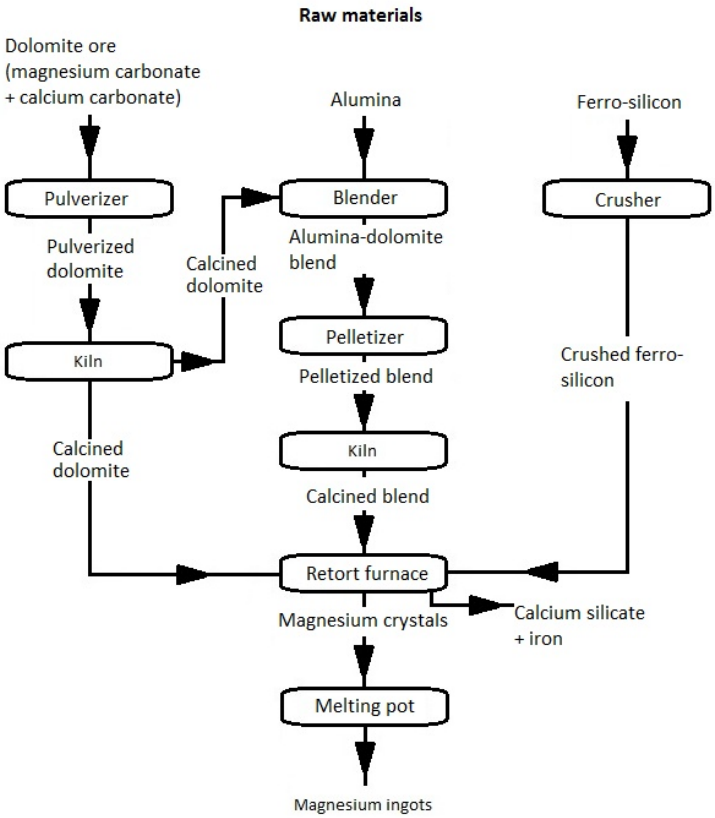

Figure 5. The Magnetherm process. [6.]

These methods indicate the complexity of producing magnesium to metal form. Other production methods also exist but the above mentioned methods are the most common ones.

4.2 Properties of magnesium

Magnesium's mechanical properties can be considered beneficial in many fields. Magnesium's light weight compared to other metal materials is a common reason for the materials use. Magnesium's reactivity in corrosive environment is another factor that has made it usual for corrosion protection for other materials.

4.2.1 Basic properties

Magnesium belongs to the alkaline earth metal group with elements like beryllium and calcium. The atomic weight of the element is 24.3050 u and the volume is 14.0 cm^3/mol. Magnesium is comprised of hexagonal close-packed unit cells in its structure,

when the material is in its pure state under atmospheric pressure, presented in Figure 6. Pure magnesium at 25 ^{o}C has almost perfect closed packed hexagonal crystal structure with a c/a ratio (c and a can be seen from the Figure 6. (a)) of 1.6236 to 1.633. Heating the material causes thermal expansion which changes this property at higher temperatures. Slip reactions happen at room temperatures primarily on the (0001) basal plane and in the [11-20] direction that is the most closely packed direction of the plane. Secondary slip occurs in the [11-20] direction on the (10-10) vertical face planes. At elevated temperatures slip will also occur in the [11-20] direction on the (10-11) pyramidal planes. [6; 23.]

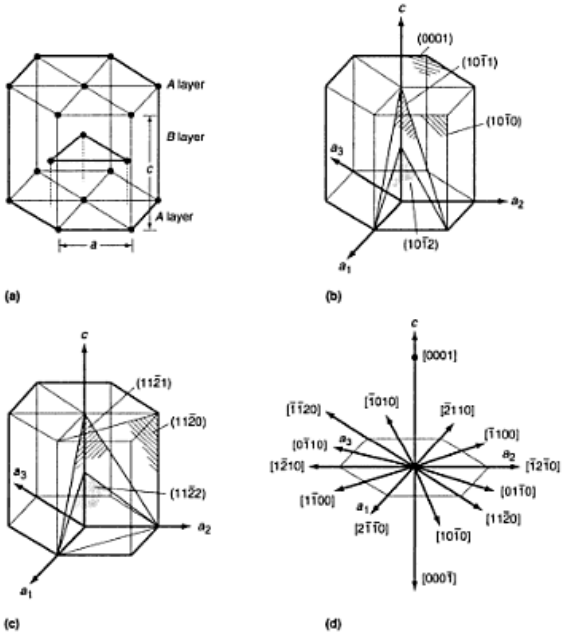

Figure 6. Magnesium's unit cell crystal: (a) Atomic positions in hcp structure, (b) Basal plane, face plane, and principal planes of the [1-210] zone, (c) Principal planes of the [1-100] zone, and (d) Principal directions. [6.]

Twinning, which is that two different crystal share a same crystal section, can occur to pure magnesium at room temperatures across the (10-12) planes and secondary twinning can occur across the (30-34) planes, according to Avedesian and Baker [6]. At elevated temperatures twinning can additionally happen across the (10-13) planes showing that heating the material affects multiple aspects of metal material structures. [6.]

Fractures are common in metal materials. They can happen in different ways, presented in Figure 7. For pure magnesium, at room temperatures and below, fractures will occur mainly because of the joining of intragranular cracks that have formed on the (30-34) twinned planes and on higher-order planes like (10-14), (10-15) and (11-24), by a moderate amount of intergranular cracking. At higher temperatures cracking and cavitation will generally happen at grain boundaries. [6; 57.]

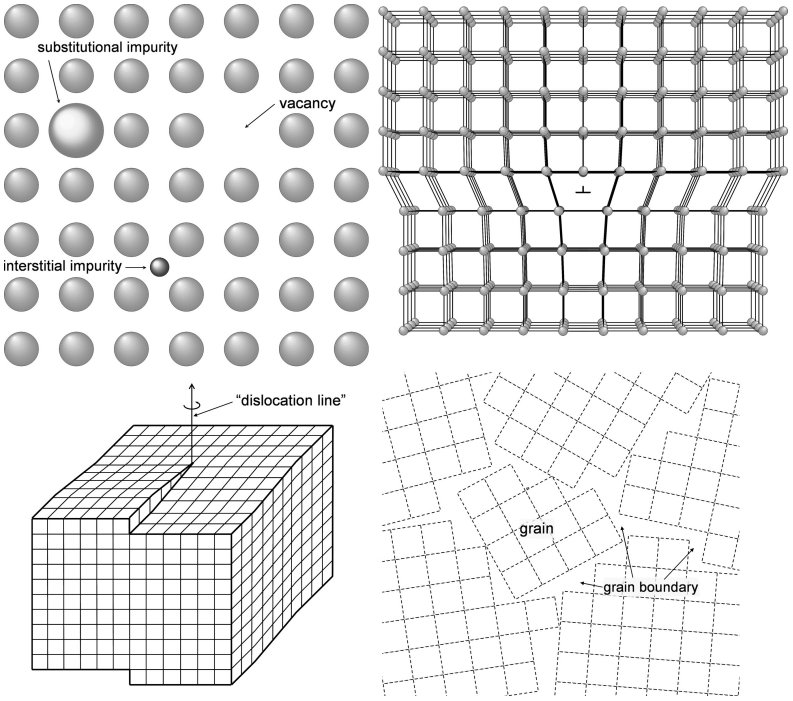

Figure 7. Metal material crystal structures that show point defects (substitutional or interstitial elements, vacancies), line defects (edge and screw dislocations) and planar defects (grain boundaries). [57.]

Mass characteristics of magnesium are an important aspect when creating applications from the material. The density of magnesium is the lightest of all structural metals which has made it a key material for applications that require light weight. The density of pure magnesium at 20 ^{o}C is 1.738 g/cm^3 [23]. Density has a linear tendency when compared to temperature until it reaches the melting point. The melting temperature of magnesium is 650 ^{o}C and the density in that point in the solid state is about 1.65g/cm^3 and in the liquid state it is about 1.58 g/cm^3. On cooling the volumetric shrinkage of magnesium is around 5 %, when it is done from 650 ^{o}C to 20 ^{o}C. Linear shrinkage on cooling is about 1.7 %. This shows that the thermal behavior of metals needs to be taken into account when designing products. The melting point of magnesium increases when the pressure increases. The increase is linear with the increase in pressure in that in 10kbar the temperature is about 725 ^{o}C and at 20 kbar it is almost 800 ^{o}C. Boiling point for pure magnesium under atmospheric pressure is about 1090 ^{o}C. [6.]

Magnesium's thermal expansion coefficient of magnesium increases as the temperature of the material increases. Thermal conductivity of magnesium peeks at about -64^{o}C. The values, though, for the material changes depending on the temperature. Magnesium's magnetic properties are very weak. The relative magnetic permeability (μ/μ_0) of magnesium is 1.000012, which is near woods permeability. Magnesium color due to its optical properties is bright silvery white. Table 3, presents additionally some of the thermal, magnetic and optical properties of magnesium. [6.]

Table 3. Thermal, magnetic and optical properties of magnesium. [6.]

Property	Value	Unit
Thermal conductivity (20 °C)	148-171	W/m*K
Enthalpy (formation of solid, 25 °C)	0	J/mol
Enthalpy (heat fusion, 25 °C)	32.7 ± 0.1	J/mol
Entropy (25 °C)	32.7± 0.1	J/mol*K
Specific heat capacity (20 °C)	1.025	kJ/kg*K
Latent heat of fusion	360-377	kJ/kg
Latent heat of sublimation (25 °C)	6113-6238	kJ/kg
Latent heat of vaporization	5150-5400	kJ/kg
Latent heat of combustion	24,900-25,200	kJ/kg
Magnetic susceptibility (Mg)	+13.1	$Xm/10^{-6}cm^3mol^{-1}$
Magnetic susceptibility ($Mg(OH)_2$)	-22.1	$Xm/10^{-6}cm^3mol^{-1}$
Magnetic susceptibility (FeO)	+7200	$Xm/10^{-6}cm^3mol^{-1}$
Magnetic susceptibility (GdO)	+53200	$Xm/10^{-6}cm^3mol^{-1}$
Reflectivity (Mg, λ = **0.500 µm**)	0.72	
Reflectivity (Mg, λ = **1.000 µm**)	0.74	
Solar absorptivity (Mg)	0.31	
Emissivity (Mg, 22 °C)	0.07	
Absorption constant (λ = 0.589 µm)	4.42	
Refractive index (λ = 0.589 µm)	0.37	
X-ray absorption coefficient (µm)	32.9	m^2/kg

Magnesium mechanical and other properties are presented in Table 4. The elasticity of magnesium is different at different temperatures and changes linearly in the way that the value is about 42 to 46 GPa at 100 °C and 37 to 39 GPa at 300 °C. The Poisson's ratio for magnesium is 0.35 and the friction coefficient for magnesium versus magnesium is 0.36 at 20°C. Surface tension of magnesium at temperatures of 660 to 852 °C range from values of 0.545 to 0.563 N/m. For temperatures at 894 to 1120 °C the values range about 0.502 to 0.504 N/m. [6.]

Table 4. Mechanical and viscosity properties of magnesium. [6.]

Property	Value	Unit
Elastic modulus (dynamic,99.98% Mg, 20 °C)	44	GPa
Elastic modulus (static, 99.98% Mg, 20 °C)	40	GPa
Elastic modulus (dynamic,99.80% Mg, 20 °C)	45	GPa
Elastic modulus (static, 99.80% Mg, 20 °C)	43	GPa
Shear modulus	17	GPa
Dynamic viscosity (liquid Mg, **650 °C**)	1.23	mPa*s
Dynamic viscosity (liquid Mg, **700 °C**)	1.13	mPa*s

Mechanical properties of magnesium metal changes depending on the processing history that has been used. Tensile strength, compressive yield strength, elongation and hardness values at room-temperature values with different processing histories can be seen in the Table 5 and 6.

Table 5. Mechanical properties of unalloyed magnesium at 20 °C. [6.]

Form	Tensile strength MPa	0.2% tensile yield strength MPa	0.2% compressive yield strength MPa	Elongation in %	Hardness HRE	Hardness HB (a)
Sand cast, 13mm diam.	90	21	21	2-6	16	30
Extrusion, 13mm diam.	165-205	69-105	35-55	5-8	26	35
Hard rolled sheet	180-220	115-140	105-115	2-10	48-54	45-47
Annealed sheet	160-195	90-105	69-83	3-15	37-39	40-41

(a) 500kg load with 10mm diameter ball.

Table 6. Mechanical properties of magnesium in 20 °C, with different processing histories. [23.]

Pure Magnesium	Annealed Sheet	Hand-Rolled Sheet	Sand Cast	Extruded	PM-Extruded	DMD-Extruded
0.2% Compressive yield strength (MPa)	69-83	105-115	21	34-55	92±12 (a)	74±4 (b)
0.2% Tensile yield strength (MPa)	90-105	115-140	21	69-105	132±7 (c)	97±2 (d)
Ultimate tensile strength (MPa)	160-195	180-220	90	165-205	193±2 (c)	173±1 (d)
Hardness HB (e)	40-41	45-47	30	35	-	-

(a) PM: powder metallurgy method, extruded at 350 °C, extrusion ratio 20,25:1,
(b) DMD: disintegrated melt deposition method, extruded at 350 °C, extrusion ratio 20,25:1,
(c) PM: powder metallurgy method, extruded at 250 °C, extrusion ratio 20,25:1,
(d) DMD: disintegrated melt deposition method, extruded at 250 °C, extrusion ratio 20,25:1,
(e) Using 10mm diameter ball and 500 kg load.

Magnesium's properties are highly dependent on temperature, which is seen from previous values. The yield strength of magnesium is 130 MPa and density ~1.8 g/cm^3, which is close to the bone value of ~110 MPa and ~1.6 g/cm^3. When compared to other metallic materials like Ti-6Al-4V with corresponding values of ~970 MPa and ~4.50 g/cm^3, it indicates that magnesium could be used as a non-stress shielding material for bone healing applications. [6.]

4.2.2 Corrosion property of magnesium

Corrosion has been generally considered a negative aspect when metals are designed for stable applications under corrosive environment. Corrosion is the degradation of a metal material that causes the mechanical and structural properties to fail. This can lead to problems if the material is used in critical structural applications. Corrosion is also a problem with magnesium metal, although, the problem has been solved in general use by coatings and alloying the material. Magnesium's corrosion has not been, though, solved in the medical field in implant use due to toxic alloying elements and coatings. As the degradation property is a positive aspect for some medical implants, this is why magnesium has also been studied for this kind of use. [84.]

Magnesium's corrosion effects have been studied after Prof. Dr. Erwin Payr started to the material research for medical purposes in the 1900's. According to Payr and Siegfried Vordemann, the studies on vessels and subcutaneous tissue revealed that magnesium had severe influence on the tissue around the material. In the studies the surrounding tissues had a large number of round cells and granulation tissue due to the corroding magnesium. This granulation tissue had mucous consistence and foreign body giant cells with metallic particles. These particles were also seen in leucocytes and the granulation tissue was observed to be vascularized. Payr's studies indicated that the corroding magnesium can cause severe blood clotting. Payr was one of the first researchers to observe the corrosion of magnesium in a living tissue, according to Witte [85]. Payr's studies indicated that the corrosion does not happen uniformly but by pitting corrosion. His studies revealed that pure 0.1g magnesium piece can degrade completely in three to four weeks in humans. Additionally, the location had distinctive effects and that high-purity magnesium had a more uniform corrosion behavior in vivo than non-pure magnesium. [85.]

Later studies by Höpfner [32], according to Witte [85] using anastomosis treatment with dog vessels, supported the previous studies showing that the location of the implant is important when considering the corrosion rate. The corrosion was faster in the limbs due to the limb movement that enables more active blood flow. Wexler [78], according to Witte [85] reported in 1980 that magnesium alloy wires with aluminum can cause an increase in adrenal glandular weight, thymic involution, depression of the abnormally elevated blood pressure and a retarded gain in weight with operated rats. Certain serum enzyme levels of creatine phosphokinase (CPK), serum glutamic-oxaloacetic transaminase (SGOT), serum glutamic-pyruvic transaminase (SGPT) and lactic dehydrogenase (LDH), and corticosterone and deoxycorticosterone secretion were reported to become elevated due to the use of this kind of alloy. The circulating levels of triglycerides and cholesterols were reduced. These two studies [32; 78] already showed the importance of knowing the corrosion of the material. [85.]

Magnesium does not corrode much in ambient environment as it gains a protective oxide layer to it. Unlike some of the other metals, the oxide layer on magnesium is not as protective as it is unstable and can easily be destroyed. The oxide layer can also be

created through heat treatment. In a solution environment the corrosion of magnesium is fast due to the degradation of the oxide layer. [103.]

In a solution based environment the metal releases Mg^{2+} ions due to the surrounding solution and other ions. The pH of the solution has been reported to have a major effect on the corrosion tendency of the material as higher pH results to the formation of a passivation layer of MgO and $Mg(OH)_2$, presented in Figure 8. The MgO layer has been found out to be constant in thickness of about 2.5 nm and the outer $Mg(OH)_2$ layer to be variable in the range of 2.2 nm to several nanometers more [29; 95]. The passivation layer on the surface of the material is created in a stable pH of 11 or higher solution. It has been suggested that a solution of NaOH can effectively create the $MgO/Mg(OH)_2$ layer. The protective layer can slow down the initial corrosion rate of the material. If the solution has Cl^- -ions or the solution is a buffer solution then the layer is destroyed due to the pH stability at a lower level. [1; 29; 58; 95]

The degradation rate of magnesium is, additionally, highly dependent on the concentration of HCO_3^- ions in a solution. Higher concentrations of HCO_3^- enhance the degradation of the material. It also creates a protective layer which lowers the total degradation rate of the material significantly. Xin et.al [89] have reported that about 27 mmol/L of HCO_3^- should be present in SBF solutions to acquire more accurate corrosion results. [88.]

The potential of magnesium also has an effect as magnesium is nobler in water than in simulated body fluid (SBF) [76; 95]. During the corrosion process, magnesium releases hydrogen bubbles (H_2) from the surrounding solution, presented in Figure 8 [29; 95]. The release of the hydrogen has a negative effect to surrounding tissue as it can cause cell death. On the other hand, this corrosion tendency has been used in studies as a positive aspect by Payr [56] according to Witte [85]. Different solutions have been reported to have different effect on the degradation rate of magnesium. Pure Mg has a lower potential of -2.37 V when compared to -1.53 V for $Mg(OH)_2$, which explains the protective nature of the layer. [96.]

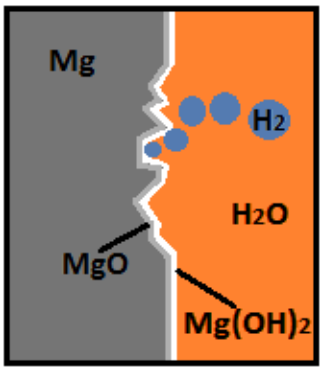

$$Mg^{2+} + 2e^-$$

$$H_2O + 2e^- \rightarrow H_2 + 2OH^-$$

$$Mg^{2+} + 2OH^- \rightarrow Mg(OH)_2$$

Figure 8. Corrosion of Magnesium metal (Mg^{2+}) in water creating a passive interlayer of $Mg(OH)_2$ or MgO on the degradation surface. [96.]

The fast rate of corrosion in solutions containing chloride ions can change the surrounding pH level of the solution to 10. This can happen in a 250 ml neutral Hank

solution in a 15 hour time span. This kind of reaction can lead to alkaline poisoning in a body environment due to high amounts of metal material released to the surrounding tissue. [68.]

Lespinasse [40] found out in 1910, according to Witte [85], that since the corrosive environment has an effect on the Mg corrosion, the in vitro and in vivo studies gave different results for the corrosion rate. Andrews in 1917 [2], according to Witte [85], revealed that the surface area is more important for the corrosion rate than the materials weight/volume for in vitro and in vivo studies. Different studies [2; 19; 49; 55] have resulted in different corrosion rates with different animal species, according to Witte [85] and Song [68]. This has made comparisons between different study results difficult. Heinzhoff's and Dimitroff's study in 1928 revealed that limited local fluid exchange, gas exchange and autolytic changes in blood have a factor in the corrosion rate, according to Witte [85].

Corrosion rate is also dependent on the oxygen content [16] of the blood and protein presence [93]. The local hydrogen carbonic acid content has an effect due to the formation of magnesium carbonate on the material surface. In a bone tissue environment a carbonate layer is formed on the material surface which slows the corrosion rate of the material. Magnesium phosphate can also be formed in to the surface of the magnesium material in a bone tissue environment or in a solution where phosphates are present. Additionally, in a environment that contains phosphates the pH increase can enable the formation of a hydroxide apatite layer to the surface of the material. This type of apatite layer does not form if the corrosion rate is fast and a large amount of magnesium ions are released in a short period of time. [83.] Fontenier's et. al. [17] revealed in 1975 that the composition of the corrosion layer stays very much the same with different magnesium metals. The layer was determined to be about 60 % of phosphates (likely $MgNH_4PO_4*6H_2O$, 20 % of $MgCO_3$, 10 % of $Mg(OH)_2$ and 10 % of $CaCO_3$). [85.]

Magnesium can experience a degradation rate of 19-44 mg/cm^2/day in an area of 1 cm^2. The hydrogen release rate was determined to be around 25 ml/day. This hydrogen release rate has been reported to be too fast. [68.] The typical magnesium aluminum alloy that is used in different industries has the rate of hydrogen formation at a 1.5 ml/cm^2/day level. For AZ91D material (Mg-9Al-0.5Zn-0.5Mn) the rate is about 0.068 ml/cm^2/day. Alloying can thus decrease the degradation rate. The mentioned degradation rates are still too fast due to the hydrogen release that creates gas pockets on the areas of implantation. The gas can disappear after a few weeks when the hydrogen release is 0.068 ml/cm^2/day which means that the rate is very close to an ideal level. The study [68] indicates that the body can remove the hydrogen at a certain rate. The rate of hydrogen formation for a safe implant use has been suggested to be around 0.01 ml/cm^2/day. According to Song [68], human blood plasma can tolerate magnesium from 85- to 121 mg/L. These results have been gained by the use of hot distilled water as sterilization to gain the $Mg(OH)_2$ protective layer prior to implantation, alloying or other protective layer use. Studies also indicate that larger animals and humans tend to

be able to dissolve the gas cyst areas and degraded magnesium particles effectively when compared to small animals. The degradation rate of the each material in vitro tends to be higher than in vivo. [68.]

Some magnesium alloys that have been reported to have low degradation rates are not actually preferable as implant materials due to biocompatible and toxicity problems. Aluminum for example can be used for biostabile material applications but for biodegradable applications it is not recommended. Choosing the correct alloying elements is thus important for biocompatibility. Elements like calcium, zinc, manganese and low amounts of rare earth elements like yttrium can be tolerated but toxicity test are important to perform with magnesium alloys. Increasing the purity of the magnesium material can be used to lower the corrosion rate of magnesium to an acceptable rate. High purity magnesium, though, has low mechanical properties and machinability when compared to alloy versions. [68.]

Due to the difficulties of solving the degradation rate of the material, several studies in the recent years have been made, according to Xin et.al. [88]. Some of the degradation studies are summarized in Figures 9 and 10. Due to the variation between the studies, the results are very difficult to compare. Processing is a very influential to the corrosion rate of magnesium, which has been noticed by multiple researchers including Bonora et.al. [7] study about stressed magnesium alloys, Sun et.al. [70] study about extrusion drawn pure magnesium, Wang et.al. [75] study about the bio-corrosion of a magnesium alloy with different processing histories, and Xu et.al. [91] study about chromium and oxygen plasma-modified magnesium.

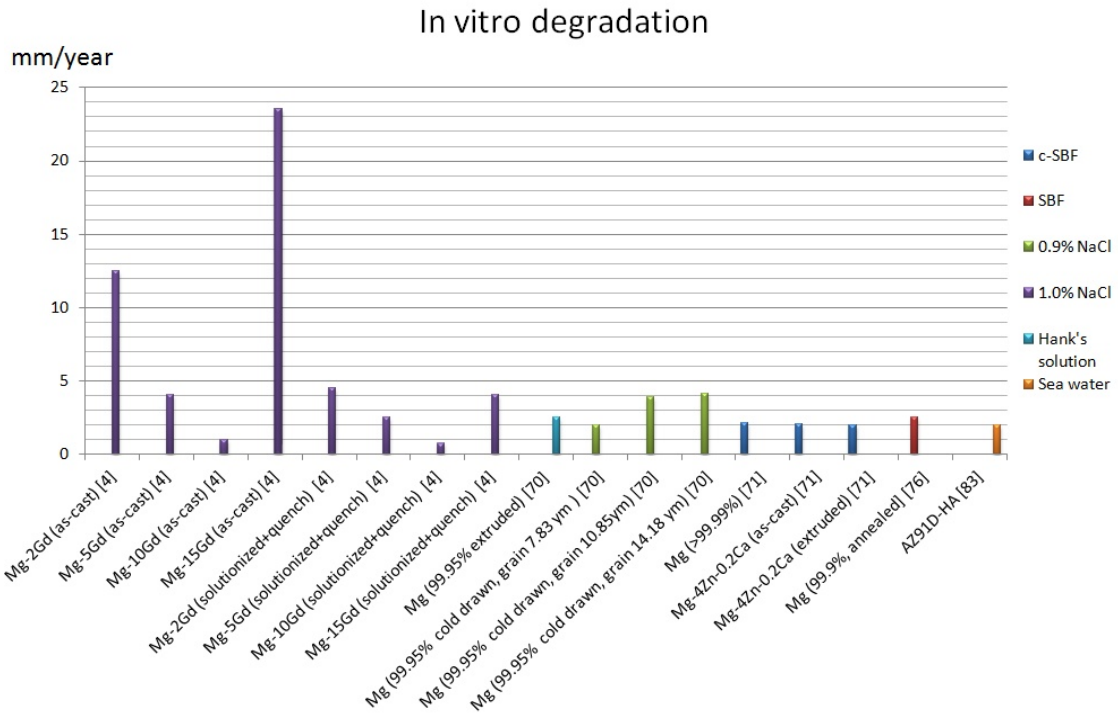

Figure 9. In vitro degradation of magnesium alloy samples in different solutions. [4; 70; 71; 76; 83]

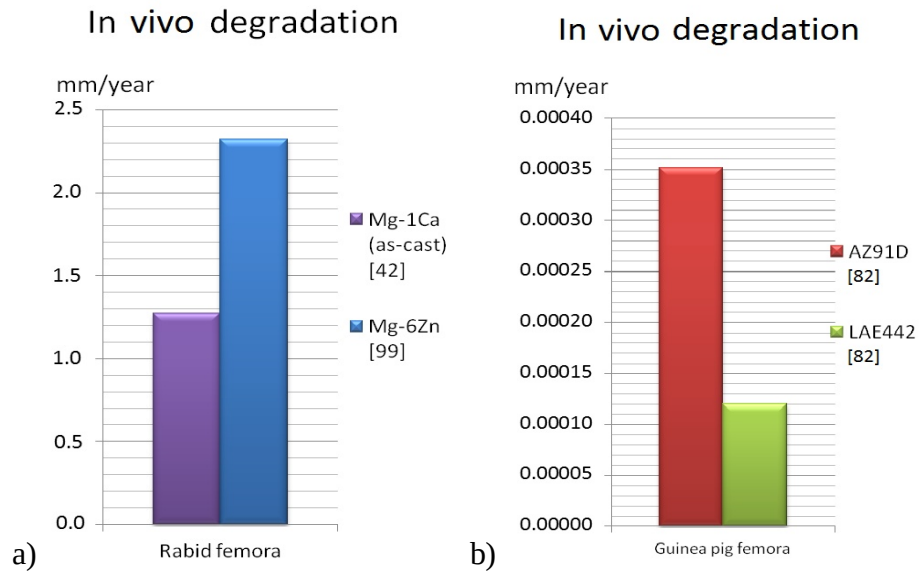

Figure 10. In vivo degradation of magnesium alloy implants in different animals. [42; 82; 99]

An alternative way of indicating the degradation compared to the surface erosion depth rate of the magnesium samples is through hydrogen evolution from the solutions. This way of indicating the degradation, is through hydrogen evolution from the solutions. The degradation rate comparison is different here, since the degraded magnesium is presented as a volume of hydrogen. The method, though, is a more accurate method as the degradation causes hydrogen release. Degradation rate estimates through weighting the samples can give false results due to the formed oxide or phosphate layers if they are not removed prior to weighing. Stating the degradation rate through hydrogen release is usually preferred as the hydrogen release rate is more prominent for the success of in vivo tests. Both results can be converted to each other but hydrogen evolution samples can be additionally weight. A hydrogen evolution study by Gu et.al. [21], which consisted of multiple different alloys in a SBF and Hank's solutions can be seen in Figure 11. The results were from a 250 h time period. Mg-1Al (as-rolled) results are not seen due to too high degradation rate before the 100 h time point. The degradation rate is an estimate from the results during the test period as the degradation rate was almost linear for the samples. The degradation rate, though, is higher at the start of the test, which is why these values are not accurate for the first 12 hours.

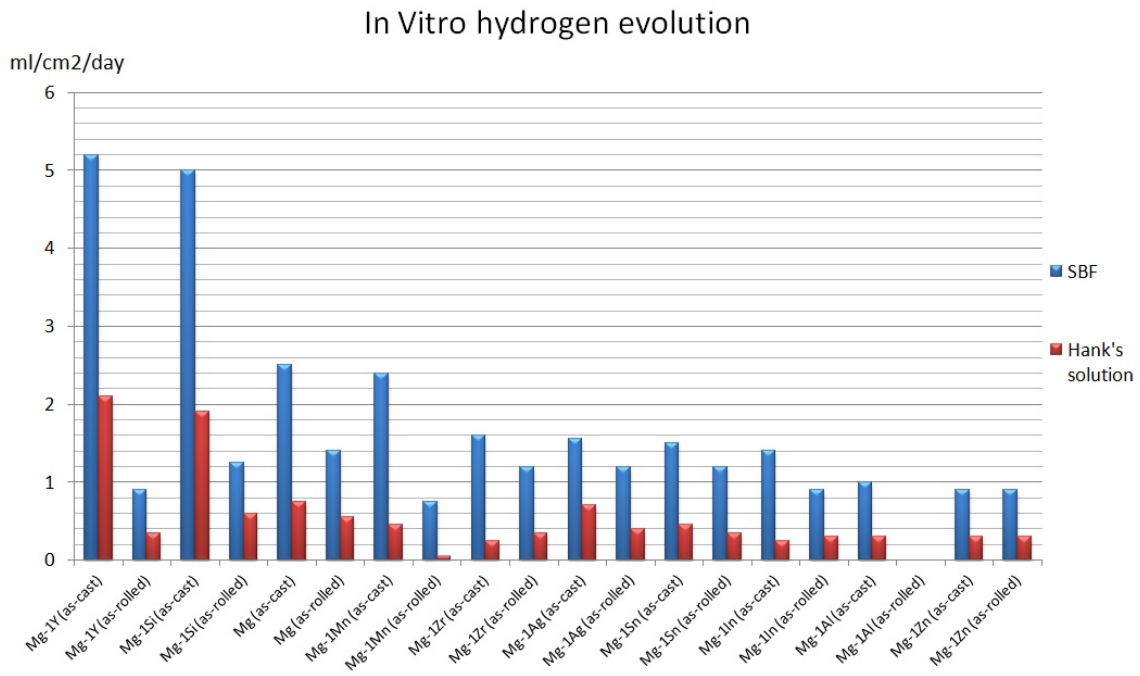

Figure 11. In vitro hydrogen evolution results from magnesium alloy degradation in SBF and in Hank's solution environments. [21.]

Processing effects seen in Figure 11 indicate that a more uniform, refined and compact material with smaller grain sizes structure can withstand degradation more due to smaller amount of defects and pitting corrosion locations [5]. The degradation rates are evidently different between materials and processing methods when comparing the results seen in Figures 9, 10 and 11. The in vitro solutions are fixed to certain ions and changed periodically, thus they do not have similar ways of buffering the pH change compared to in vivo.

Tissue response to degradation

Magnesium is an essential element in the human body to its functioning. Magnesium has been reported to be important for over 300 different reactions as it is a substantial intercellular cation. Magnesium is also very important for the health of the human heart, and for the maintenance of blood pressure and blood sugar levels. It has been reported that the systemic toxic level of magnesium is about 7 to 10 mmol/L in serum. [85.]

Magnesium's corrosion rate, though, is very high which can lead to overloading the surrounding tissue with the material and leading to neointimal formation. The high degradation rate combined with the neointimal formation tendency at high rates can cause restenosis to blood vessels if the material is used as a stent material. [85.]

The surrounding tissue can respond to the degrading magnesium in different ways depending on the tissue type. Tissues like bone have been studied by researchers like Lambotte [38; 39], McBride [49], Nicole [52] and Nogara [54], according to Witte [85].

Lambotte's studies have indicated periostal proliferation progresses with magnesium at 3 to 7 week time before returning back to normal. Lambotte claimed that the material is able to enhance bone regeneration, when on the other hand Zierold [104] stated the opposite. Verbrugge's study [74] resulted to bone marrow replacement by granulation tissue and new bone without osteoclasts. His studies also indicate cystic cavities in the newly formed bone tissue. McBride's study [49] found out that corrosion of the magnesium material is slower in intramedullar pegs than in transcortical applications. Nogara's study in 1939 [54] reported that the hydrogen gas cavity formation in the surrounding bone tissue leads to a small amount of bone damage that eventually is healed after the material is completely corroded. Nicole's studies also report favorable degradation rates for magnesium in bone when compared to other environments and that the metallic corrosion products from the material cannot be observed after a certain period of time. Nicole's study [52] also indicated the usual fibrous capsule formation with magnesium implants in other locations and the sponge like tissue formation due to the gas cyst formation. [85.]

Studies done in the nerve and muscle tissue area by Dr. Wilflinseder in 1981 [79] were inspired by Payr's studies [56] on haemangioma treatments, according to Witte [85]. Wilflinseder's study [79] reported that even though the gas formation is present with magnesium wires with diameters of 0.25mm and 0.50mm subcutaneously and intramuscularly, the material does not have negative effects that prevent the material to be used for haemangioma treatment. [85.]

It was noticed by several studies that the degradation of magnesium does not create any severe infections to the surrounding tissue even in non-sterile conditions [38; 49; 52; 54]. Although, in non-sterile conditions, it has been reported that the hydrogen gas formation can possibly lead to a reduced local immunity of the tissue and pose a higher infection risk from other sources. [85.]

4.2.3 Electrical conductivity of magnesium

The electrical conductivity of magnesium is 38.6 % IACS to that of annealed copper (100%, $5.8001*10^7$ S/m) [73]. Magnesium's conductivity is about $2.2388*10^7$ S/m. A comparison table of different materials with their electrical conductivity and resistivity is represented in Table 7.

Table 7. Comparison table of electrical conductivity and resistivity of certain materials. [9; 10; 11; 12; 13]

Material	Conductivity (% IACS)	Conductivity (Siemens/m))	Resistivity (Ohm-m)
Aluminum (pure)	61.00	3.54E+07	2.83E-08
Aluminum (99.99%)	64.94	3.77E+07	2.66E-08
Aluminum (As Cast)	27.00	1.57E+07	6.39E-08
Aluminum (Stress Relieved)	30.00	1.74E+07	5.75E-08
Copper (pure, annealed)	100.00	5.80E+07	1.72E-08
Copper (Deoxidized, annealed)	85.00	4.93E+07	2.03E-08
Gadolinium	1.32		1.31E-06
Iron (pure)	18.00	1.04E+07	9.58E-08
Iron Ingot (99.9%)	15.60	9.05E+06	1.11E-07
Iron 304 (Wrought Stainless Steel, annealed)	2.50	1.45E+06	6.90E-07
Magnesium (pure)	38.60	2.24E+07	4.47E-08
Magnesium (Cast)	15.00	8.70E+06	1.15E-07
Neodymium	2.68		6.43E-07
Titanium	3.10	1.80E+06	5.56E-07
Titanium (Ti-6Al-4V)	1.00	5.80E+05	1.72E-06
Zinc (Commercial Rolled)	28.00	1.62E+07	6.16E-08
Zinc (Die Cast)	25.00	1.45E+07	6.90E-08

The electrical resistivity for single crystals of magnesium at 20 ^{o}C is 45.3 nΩ*m along the c-axis. The temperature coefficient at this temperature is 0.165 nΩ*m/K along the a-axis and 0.143 nΩ*m/K along the c axis. Contact potential of the material is +44 mV versus saturated calomel electrode at 25 ^{o}C and -0.222 mV against copper at 27^{o}C. The electrochemical equivalent for the material is 126 mg/C and the standard electrode potential is -2.40 V against hydrogen. Ionization potential is 7.65 eV for Mg^{+} and 15.05 eV for Mg^{2+}. Electrolytic solution potential for magnesium is 1.63 mV against saturated calomel electrode at 25 ^{o}C in an aerated NaCl solution. The work function of magnesium is about 3.61 to 3.66 eV. [6.]

The given values indicate that magnesium is not as good as copper or aluminum in regards to pure electrical conductivity. Magnesium's density value, though, makes the material very appealing for electrical applications as it is around one fifth of that of copper. The degradation tendency of the metal has hindered the materials use as electrodes and other electrical parts. The biocompatibility aspect of magnesium, though, makes it very interesting as a possible biodegradable electrical material. Due to this potential, studies have emerged to create a magnesium based device that could degrade over time. A study done by Hwang et.al. [31] has already created a degradable circuit out of magnesium, silicon and silk, presented in Figure 12 f). Another study done by Sebaa et.al. [63] has tested if an electrically conductive polymer coating could be used as a medium for conductivity and for slowing down the degradation rate of the magnesium implant.

4.3 Alloying, processing and coating

Alloying and processing techniques are used to create a specific form to a material. They have an effect to the overall properties of a metal material. This can be a crucial part for modifying a material for implant applications.

A few methods are used more actively with magnesium for medical studies than others. Coating techniques are also important for magnesium as they can effectively prevent degradation at the start of the immersion period.

4.3.1 Alloying of magnesium material

Alloying is a typical method to modify metals for different applications. Alloying is the adding of certain chemical elements to the material to gain desired properties. Magnesium is no different in this regard. Alloying can have a major effect on the properties of the original material. Some of these changes can be seen in Table 8, where a stent material of 316L stainless steel is compared to magnesium alloys.

Table 8. Mechanical properties of different magnesium based materials in comparison to 316L stainless steel with in vitro degradation rate and average grain size for biodegradable stent use. [51.]

Material	Yield Strength (Mpa)	Tensile Strength (MPa)	Elongation (%)	In vitro Degradation Rate (mm/y)(a)	Average Grain Size (ym)
316L SS: annealed (ASTM F138)	190	490	40	-	12-30
Pure Mg: as cast	20	86	13	407	-
WE43 alloy: extruded T5	195	280	2	1.35	10
AM60B-F: die cast	-	220	6-8	8.97	25
ZW21: extruded	200	270	17	-	4
WZ21: extruded	140	250	20	-	7

(a) The degradation rate is calculated from potentiodynamic polarization test.

Mechanical alloying is based on the use of powder processing in a ball-mill. In the ball-mill, the material is repeatedly welded and fractured as the powder undergoes high-energy collisions with the balls. The powder, alloying powder elements and the balls are inside jars that are placed inside the mill. The alloying process happens inside the jars while keeping the mill intact of contaminants. A control agent like stearic acid is used to prevent excess welding that forms of lumps of material. With magnesium, solid solution hardening and precipitation hardening are the mechanisms that improve the mechanical properties of the metal. This is based on alloying elements that create intermetallic compounds with magnesium. These compounds have their own phases which influence the microstructure of the material and which can be seen in the alloy. [23.]

Alloying elements for improving magnesium can include elements like rare earth elements and metallic elements like lithium, zirconium and calcium [30; 57]. Lithium can be used to enhance ductility and formability of magnesium alloys as it changes the lattice structure from hexagonal close packed to body-centered cubic one. Zirconium can be used to grain-refine magnesium alloys, which has an effect to the grain boundary strengthening. [30; 57]

The limiting factor in alloying with magnesium is the liquid solubility of the element in molten magnesium and the interference between competing alloying elements. Each alloying element, additionally, has different effects to the magnesium material and to the overall alloy. [6.]

The change, that an alloy material causes to magnesium, needs to be known extensively so that the alloy does not gain toxicity, the degradation rate is in reasonable values and that the material can be still machined in a decent way. Processing of the alloy also has an effect to the end product, which is why it needs to be accounted for when designing applications from the metal material.

Alloying elements

Aluminum is considered to be one of the most used alloying elements with magnesium. Use of this material is due to its favorable influence on magnesium. Aluminum increases the hardness, strength and castability of magnesium [23; 84]. Aluminum itself is used in several implant studies and has shown good biocompatibility most of the time. Some studies, though, report that the material has negative effects to the body and to the corrosion resistance. High aluminum content increases the $Mg_{17}Al_{12}$ phase which enhances pitting corrosion for the alloy. Studies also report that aluminum is related to reduction in osteoblast [37] and osteoclast [60] numbers, and macrophage-related muscle diseases [67]. High aluminum content in a serum can also cause harmful effects to neurons and be linked to dementia and Alzheimer's disease [15]. High aluminum content can also suppress cell growth on the material surface. This can be changed through surface treatment though. [37; 60; 67]

Calcium improves the strength and creep resistance of magnesium. Calcium is also used to assist magnesium's grain refinement and creep-resistance. Corrosion resistance, thermal properties and mechanical properties are also improved by the addition of calcium. With casting alloys, the material reduces melt oxidation and oxidation during heat treatment process, and gives better rollability of magnesium sheets. Calcium can only be added up to 0.3 wt% to magnesium. [23.] Calcium can be, though, used with magnesium in composites. In these cases calcium can increase the corrosion resistance of the magnesium metal with up to 5 wt% of calcium without increased cytotoxicity due to formations of various layers that includes a calcium carbonate layer and magnesium carbonate and hydroxide layers. [102.]

Copper is used to improve the room temperature and high temperature strength of the magnesium metal. Copper just like aluminum is not a preferred alloying element

with biodegradable materials in implant solutions. Additionally, additions of copper cause lower ductility and corrosion resistance to magnesium metal. [23.]

Iron is a harmful alloying element with magnesium. Iron lowers magnesium corrosion resistance even with small amounts and only up to 0.005 % is acceptable for corrosion protection. [6; 23]

Manganese can increase the yield strength property slightly. It also improves the saltwater resistance of certain magnesium alloys by removing iron and other heavy-metal elements to harmless intermetallic compounds. The limiting factor for the use of manganese is its low solubility to magnesium. The material is usually incorporated to alloys that have aluminum in them. [6; 23.]

Molybdenum is an allying element does not alloy or interact with magnesium properly. Small increases, of 0.7 to 3.6 wt% amount molybdenum, results to improvements in hardness, elastic modulus, and ductility with magnesium. Molybdenum reduces the tensile strength of magnesium slightly. [23.]

Rare earth metals (RE) like yttrium are used to improve the high temperature strength, creep resistance and corrosion resistance of metal materials. They reduce the freeze range of the alloys which lowers the casting porosity and the weld cracking during processing. RE's high cost is usually the limiting factor of alloying them with magnesium. [23.]

Silicon is used to increase the fluidity of molten alloys. It used with iron, though, in electrical applications. Magnesium's corrosion resistance is lowered more than in the case of pure iron alloying. [23.]

Titanium has a limited solubility interaction with magnesium which makes it difficult to alloy. 2.2 to 4.0 wt% additions of titanium increases magnesium's yield strength and ductility only by 0.2 %. Titanium does not create intermetallic compounds in the magnesium alloy. [23.]

Yttrium has a high solid solubility in magnesium. This can be around 12.6 wt%, [23]. Adding yttrium to magnesium enhances the alloy's high temperature strength and creep performance with other RE materials [44]. Yttrium can additionally increase corrosion resistance due to the formation of an yttrium based oxide layer on the surface of the alloy. [6; 24.]

The alloy in the practical sections consists of about 10 wt-% of Gadolinium, 1 wt-% of Neodymium and 1 wt-% of Zinc which is why these are reviewed more than the other alloying elements. The provided material amount was too small to determine alloying effects when compared to pure magnesium. Understanding the alloying elements is still preferable for result discussion as small additions of another element can have a large effect for the metal.

Gadolinium

Gadolinium has been known for over one hundred years now as it was discovered by J.C. Galissard in Geneva, Switzerland in 1880. The material is part of the lanthanide

group and its abundance in the Earth's crust is about 7.7 ppm. Gadolinium is silvery white in appearance and is ductile and malleable. It is very similar to magnesium in appearance. Gadolinium reacts in moist air and forms an oxide coating. Reaction to water is slow but happens and the material is soluble in acids. [45.]

Gadolinium is used as an alloying material with metals like chromium and iron to improve workability and corrosion resistance. Gadolinium is, additionally, used to manufacture magnets and electrical component. [45.]

Gadolinium's crystal structure is hexagonal close packed; the electrical resistivity at 20 ^{o}C is 134 µOhmcm and is ferromagnetic. The bulk modulus is 39.1 GPA, hardness is 55 Vickers, tensile modulus is 56.2 GPa, tensile strength is 193 MPA and the yield strength is 179 MPa. Density for gadolinium is around 7.9 g/cm^3. [45.]

Neodymium

Neodymium was discovered in 1885 by Baron Auer von Weisbach. The material is used to produce permanent magnets and flints. Neodymium is also part of the lanthanide group. The material is reactive in air and forms an oxide layer. This layer can spall away easily revealing more metal to form the oxide layer again. Neodymium reacts slowly in cold water but quite fast in hot water. The abundance of the material in the earth's crust is around 38 ppm. [46.]

Neodymium is used to improve the tensile and compression strength of the material. This happens due to the solubility limits that it has with certain materials. The material can form stable precipitates within the grain structures and at grain boundaries. [46.]

Neodymium's crystal structure is hexagonal close packed. The electrical resistivity is 64 µOhmcm at 20 ^{o}C. The bulk modulus is 33.3 GPA, hardness is 35 Vickers, tensile modulus is 37.9 GPa, tensile strength is 172 MPA and the yield strength is 165 MPa. Density for gadolinium is around 7.0 g/cm^3. [46.]

Zinc

Zinc was discovered in the 16th century by Paracelcus. The material is used currently by different industries. It is used as a galvanic coating on steel to prevent corrosion and in alloys as a constituent. It is also used in zinc-base alloys for die-casting solutions and in dry batteries, zinc oxide as a pigment for paints and as a stabilizer for certain grades of rubbers and plastics. [48.]

Zinc is a brittle material. The material is abundant in the earth's crust at about 75 ppm and occurs as concentrated ores. Reactivity to air causes it to have a tarnished surface. It also reacts with acids and alkalis. Zinc has the hexagonal close packed crystal structure. The electrical resistivity is 5.96 µOhmcm at 20 ^{o}C. The bulk modulus is 69.4 GPA, hardness is 2.5Mohs and the tensile modulus is 104.5 GPa. Density for zinc is around 7.14 g/cm^3. [48.]

Zinc increases the tensile strength of the magnesium material without reducing its ductility [98]. Usually aluminum is with these alloys but in our study it is not present and as was mentioned it is not preferable for biodegradable implants. Adding zinc to magnesium, that has iron and nickel impurities, improves the alloys corrosion resistance. [23; 35; 99.]

4.3.2 Processing methods

Due to magnesium being a metallic material, it has several methods available for processing like sand casting, die casting, squeeze casting, spray forming, mechanical alloying, powder consolidation, sintering, heat treating, spin forming, hot forming, welding, and machining. There are also other techniques available. [6; 18; 23; 92]

Die casting is based on utilizing high-pressure when a molten metal material is forced through a small gap to fill a mold of a wanted shape and size. The method is fast but highly dependent on wall thickness, alloy type, flow distance and temperature of the material. When the mold is filled enough with the molten material, a high pressure of 40 to 1000 MPa is used to solidify the molten material, remove any gas inclusions and reduce the shrinkage that happens during solidification. Cooling rate for this method is around 100-1000 ^{o}C/s, resulting in a fine-grained microstructure. The method is used for variable of different products but usually for thin-walled parts. [23.]

Squeeze casting is divided between direct and indirect methods. Squeeze casting itself combines forging and casting processes but very much resembles die casting in the end. In direct method a molten material is poured into a mold. This mold is sealed with the upper half of the mold. A high unidirectional pressure is used to solidify the material. Preheat-temperature of the melt material, additions, infiltration speed, infiltration pressure and spacing between fibers need to be accounted for to gain a wanted result. Direct method is used for metal matrix composites, especially for fiber forced ones. In indirect method, the molten metal is poured into the sleeve of the equipment. The speed of the molten material is controlled more than in direct method. The method has higher material loss and therefore limits its use in situations where material is not abundant. [23.]

Powder consolidation (compaction method) is based on powder-pressing. This method is being divided into two different methods that are uniaxial and isostatic pressing. In uniaxial pressing, the powder is poured into a metal die cavity and pressed to a piece by a single direction pressure. Uniaxial pressing is divided additionally to two different compaction choices which are hot compaction and cold compaction. In hot compaction the die is heated to a wanted temperature during the pressure compaction process. The method uses inert gasses to avoid oxidation. In isostatic pressing, there is a pressuring medium between the die wall and the powder. This medium is used to apply uniform pressure from all directions. Isostatic pressing is divided two different sub groups that are cold isostatic pressing (CIP) and hot isostatic pressing (HIP). Both uniaxial and isostatic pressing have negative aspects to them that dictate which of them

is used at a given time. Uniaxial is used for cheaper and larger pieces. Isostatic is used to achieve uniform densification but at a higher cost and slower processing speed. [23.]

Mechanical disintegration and deposition method (MDD) is used to lower the cost of spray processes. MDD method uses a mechanical device to disintegrate the molten slurry before it is deposited. In normal spray processes the disintegration is done through inert gasses. In MDD method, the molten slurry of desired material is mixed mechanically to obtain uniform distribution. The slurry is released through a 10mm-diameter orifice at the base of the graphite crucible. Using a mechanical device below the crucible, at a preheated temperature of 1000 ^{o}C, causes the slurry to be disintegrated to multiple uniform streams. These streams are deposited to their own metallic substrate holders for ingot creation. [23.]

4.3.3 Coatings on magnesium

Improving the degradation properties of magnesium is a prevalent problem that needs to be solved. One solution to this is the incorporation of a polymer or a ceramic coating on top of the material or a modification of the material itself to form a protective layer. The goal is to enable small places of the underlying magnesium material to interact with the surrounding solution and degrade in a slower rate than a material without a coating. Coating processes that have been used with magnesium include spray coating and dip coating. [90.]

The idea of a coating being utilized as a protective barrier has been studied for a while now with promising results. Studies from Wong et.al. [86], and Xu and Yamamoto [90] indicate that different types of polymer coatings can slow down magnesium's corrosion rate. Wong et.al. [86] reported that utilizing a polymer coating that consists of polycaprolactone (PCL) and dichloromethane (DCM) with low porosity membrane (LPM) and high porosity membrane (HPM) coatings version. The coatings improved the corrosion resistance of magnesium significantly with improvements to the pH change of the surrounding solution and the cell growth to the material surface.

The study done by Wong et.al. [86] reported that a uncoated AZ91 magnesium material has around six times more weight loss than with a low porosity membrane sample and around two time higher weight loss than with a high porosity membrane sample. The study also indicated that weight loss of the material was about 0.017 g of magnesium ions after 60 days. The degradation rate is fast at the first few days but after 10 days its start to slow down. After 30 to 60 days the rate is becoming very minimal as the weight loss is slowing down. With the coated samples, the weight loss stayed very linear during the 60 days testing period and reached around 0.0025 g with low porosity membrane samples and 0.0060 g for high porosity membrane samples. [86.]

The pH values from Wong et.al. [86] indicates that the weight loss is relatable to the pH increase graphs that are attained from the measurements. The pH from the uncoated magnesium material lowers resulted to an end pH of 8.2. With the low porosity membrane sample the pH reached a value of 7.6 and the high porosity membrane sample reached 7.8 pH. The starting pH for the solutions was reported to be 7.2 pH,

which in turn indicates that there is a rise on the pH-values of the solutions. The imaging results from the study [86] indicate that after 3 days the magnesium samples do not have much mouse osteoblasts cell growth on the surface of the samples due to the violent pH rise from the degradation process. With both membrane coated samples, the cell growth was evident. [86.] A study by Witecka et.al. [80] reported that silanizing AZ91 alloy with different silanes can improve the alloys cytocompatibility and cell growth on the alloy surface.

Xu and Yamamoto's [90] study concentrated on four different polymer coatings which were poly (L-lactid acid) (PLLA)-high molecular weight (HMW), PLLA-low molecular weight (LMW), poly (e-caprolactone) (PCL)-HMW and PCL-LMW. The PCL-LMW coating caused the pitting corrosion depth for the magnesium material to be three times larger than with a PLLA-LMW coating. The corrosion rates from the test after 10 days indicate that the PLLA-HMW has the lowest corrosion rate out of the tested coatings, which was around 1.7 µm/day. With PLLA-LMW the rate was reported to be around 2.3 µm/day. For PCL-HMW the rate was around 3.0 µm/day and for PCL-LMW around 3.8 µm/day. All of these values were lower than the uncoated magnesium samples that had around 4.8 µm/day rate for the degradation. [90.]

Other coatings like PLGA, PLLA and micro-arc osidation/poly-l-lactid acid (MAO/PLLA) composites have also been studied with magnesium metal, according to Wong et.al. [86]. These coatings have been able to control the degradation of magnesium based alloys. Other methods for coating on the magnesium surface have been micro oxidation coatings, various Ca-P coatings and fluoride coatings. [86.]

These studies emphasize the importance of choosing the right type of coating regulate the degradation rate of the underlying magnesium material. The pitting corrosion type with the magnesium material can also have changes in its pitting corrosion depth depending on which coating material is used. Problem is that there is not enough relevant studies that indicate how well these coatings have attached to the magnesium surface. Obtaining uniform nonporous coatings have been a problem and the thicknesses of these coatings have not been reported clearly, which indicate the need for more accurate and extensive studies with these methods. Each coating should be thus considered differently and not discarded immediately. [86.]

4.3.4 Thin coatings from magnesium

Creating thing coatings from magnesium and for magnesium is a difficult process as the metal tends to create a hydroxide layer easily in a moist environment or an oxide layer when heated. These layers are brittle, yet beneficial when trying to lower the initial degradation rates in implants.

Coatings can be formed to the surface of the magnesium metal at least in two different ways. These include sputtering and electron beam evaporation techniques. Sputtering has been studied by Ibasco et.al. [33] and Wu et.al. [87]. Ibasco et.al. [33] studied a 3 µm thick magnesium coating on top of a titanium material by sputtering technique. This coating was created from a 20 cm diameter metallic targets that were

99.5 wt-% magnesium. Coated titanium pieces were sizes of 25.0 mm*25.0 mm*0.5 mm and they were rinsed with ethanol/acetone (50/50 wt-%) solution for 15 min. The coated material study was immersed in different solutions containing KCl, $NaHPO_4*7H_2O$, $MgCl_2*6H_2O$, K_2HPO_4 and $NH_4H_2PO_4$ to study the creation of stable phosphate precipitates. Immersion in ammonium diphosphate (ADP) formed struvite crystals ($NH_4MgPO_4*6H_2O$) in a few seconds, coating the material completely in a few minutes. The study reports that the creation of a struvite coating on top of a titanium material is possible. The coating is later replaced by a calcium phosphate layer (CaP) that enhances cell survival and adhesion to the material when compared to pure titanium material. It was also indicated that sputtering magnesium on top of material is possible as the coating is firmly attached to the titanium material. The underlying coating layer was determined to be MgO from the sputtering process. [33.] The effect of phosphate coating has also been proven by Ishizaki et.al. [34].

Electron beam evaporation method was studied by Chowdhury and Kumar [8]. A magnesium based films was created from MgO powder that was obtained from magnesium ribbons by burning the magnesium material or by sol-gel technique. The thin films were created on glass substrates that were the size of 25*25*1-3 mm. The electron beam had a 6 kV gun and a ~10-5 torr pressure was used during the coating process. Current was in the range of 60-80 mA for the evaporation. Deposition time for the coating went up to 15 min in the study. The e-beam evaporation technique is based on a magnetic field and electron beam use where the magnetic field directs the beam to the powder material which is then deposited at a high speed to the substrate. The target material itself is located in a ingot that is water cooled and the filament is away from the whole process so that it is not contaminated but from which the magnetic field can direct the beam correctly. Some of the films were later annealed in different conditions to determine the effect of annealing to the created coating. The study reported that e-beam evaporation is a viable technique to create coatings of magnesium and that annealing the surface causes the films to have different types of formations in them. [8.]

4.4 Applications consisting magnesium

Magnesium is the lightest structural metallic material. Due to this property, magnesium has been used for different applications that require light weight. The degradation property of the metal has prevented the metal to be used as the primary material for medical and electronic applications when. This has not, though, prevented the study of the material in these fields due to the positive sides the metal has.

The development of magnesium has concentrated on general applications outside of the medical field which is reviewed now. Studies and development of the material in the medical section is also an important part so that the history of the metal is known before the practical part of the work.

4.4.1 General applications

Magnesium has been used widely in different fields. One of the first applications that it has been used was in pyrotechnics and photography. Other areas have been in metallurgical, chemical, electrochemical and structural applications.

Pyrotechnics was the first application area of the material for wider use. Pyrotechnical use of the material is due to the burning nature of finely divided powder of magnesium-aluminum alloy containing over 30 % of aluminum. The powder burns in a very bright white light. This aspect made the alloy desirable for photography flashlights as it was more suitable for photography than natural light. The bright light in some fine magnesium powders can cause damage to the eyes if the material was not used properly. Other application for this light property has been in flares for night aerial photography, miscellaneous fireworks, high-energy fuels and incendiary devices. [6.]

Magnesium is also used to manufacture nodular iron as it removes some of the sulfur and spheroidizes the graphite from iron ore. Magnesium can also desulfurize steel and be used as a deoxidizer in the manufacturing of copper-based alloys like brass and bronze. Magnesium is used to improve the strength and corrosion resistance of metal materials like aluminum through alloying. [6; 47.]

Magnesium can be used in the production of complex and specialized organic and organometallic compounds. Magnesium is used in the production of magnesium alkyls and aryls and as a neutralizer in lubricating oils. It can also be used in the purification of argon and hydrogen gases. [18.]

Magnesium has, additionally, been used in electrochemical applications. Magnesium and its casted and wrought alloy products can be used in for example in cathodic protection, batteries and photoengraving. Magnesium can act as a sacrificial galvanic anode to extend the working life of household and industrial water heaters; underground structures like cables, pipelines, well casings, tanks, and tower footings; and seawater condensers, ship hulls, ballast tanks, and steel pilling in marine environments. Magnesium has also been used to construct batteries of dry-cell and reserve-cell types such as seawater activated cells. [6; 47.]

As a structural metal material, magnesium has been used due to its lightness. This has made it appealing for products that are carried, need lightness to reduce fuel consumption or need of a light material for lifting or thrust power requiring aspects. These applications include hand held device casings, laptop casings, car body parts, and airplane and missile parts. Lightness also enables lower inertia for rapidly moving parts. Magnesium's good elevated-temperature properties have also made it desirable for aircraft, missile and oven applications. Fatigue strength in wheels, damping in electronic housings for aircraft and missiles, dimensional stability in electronic housings and in jigs, and fixtures have had preferable use with magnesium. [18; 23.]

These applications indicate the diverse use of magnesium. Limitations of the material in the mind of the environment emissions and service forces that are applied to the product need to be considered when creating products from magnesium. Aqueous

environment in most cases is limited due to the corrosion tendency of the metal. Magnesium importance in each of these applications is different. For some applications the use of magnesium has lowered due to new materials as in the aeronautical market. Currently magnesium's role in aeronautical applications has been in cast engines and transmission housings for helicopters. In the automobile and hand held device market that use of die casted magnesium products has been growing. This is due to fuel consumption and the need for lighter hand held devices. Also magnesium's property to shield from electromagnetic forces has been an important factor for electrical equipment casings.

4.4.2 Medical applications

Edward C. Huse was the first to try the magnesium metal for implants, according to Witte [85]. His tests consisted of wire ligatures to stop the bleeding of blood vessels in three patients. These included one radial artery test and two varicocele operations. According to Avedesian and Baker [6] and Witte [85], Huse discovered during these operations that the material was able to stop the bleeding successfully but that the degradation aspect of the material seemed problematic.

Following Huse's experiments in 1900, Payr studied tubular, thin-walled cylinders made of magnesium for connecting vessel anastomosis, presented in Figure 12 a). Later in 1924 Seelig started to experiment with pure magnesium as wire material. The wires were produced from 99.99 % pure magnesium that were extruded and drawn to 0.005 inch and larger sizes. Seelig's studies resulted to similar low tensile strength results as previous commercial grade magnesium wires had. The low tensile strength of magnesium was overcome to some extend by Gotthard Gossrau in 1935 when he patented a magnesium rope consisting of a mesh of smaller than 0.1 mm thin wires around the inner stronger guiding wire or wire bundle. The outer wire mesh provided a better attachment surface that is required by suture material with the inner material having better mechanical property. Eventually, in 1986, Richard Jorgensen filed a patent of modified haemostatic clip design that had inspiration from metal clip designs that Andrews had published in 1917 for ligatures and deep sutures. Andrews designed magnesium medical clips and staples were reported to be useful in closing vessels, deep wounds and intestinal anastomosis cases. The alloys were not suitable, though, due to toxicity or due to the mechanical properties were lacking for medical purposes in 1917. These studies, though, created the ground work that is being continued currently. [85.]

Magnesium as a medical material has been studied extensively in the past already, additionally to the people and tests mentioned earlier. In the Table 9, there is a summary of some tests done by researchers from the 1870's to 1980's.

Table 9. Historical table of some of the authors investigating magnesium for medical purposes in chronological order. [85.]

Year	Author	Magnesium or alloy	Application	Human model	Animal model
1878	Huse	Pure magnesium	Wires as ligature	Humans	_
1892-1905	Payr	High-purity Mg	Tubes, plates, wire, rods	Humans	Guinea pigs, rabbits, pigs and dogs
1903	Höpfner	Pure magnesium	Cylinders as vessel connectors	_	Dogs
1906-1932	Lambotte	Pure Mg (99.70 %)	Rods, plates, screws	Humans	Rabbits and dogs
1910	Lespinasse	Metallic magnesium	Ring-plates for anastomosis	_	Dogs
1917	Andrews	Pure Mg and Mg/Al, Mg/Cd, Mg/Zn	Wires, clips as ligature	_	Dogs
1924	Seelig	Pure Mg (99.99 %)	Wires, strips, bands	_	Rabbits
1933-1937	Verbrugge	Mg-6Al-3Zn-0.2Mn and Mg-8Al	Plate, band, screws, pegs	Humans	Dogs, rats, rabbits
1951	Stone	Mg-2Al and Pure magnesium	Wires for clotting aneurysms	_	Dogs
1980	Wexler	Mg-2Al	Wires intravascular	_	Rats
1981	Wilflingseder	Pure Mg (99.80 %)	Wires for hemangioma	Humans	_

Payr studies in 1900 concentrated on repairing vessel anastomosis with magnesium connectors. These test indicated that the vessel ends became attached and solid in 8 days. Payr's tests, additionally, indicated that the intravascularly placed magnesium tubes enabled some thrombotic blood clotting at the end of the tubes but not to the point of closing the lumen. Extravascularly placed tubes on the other hand did not cause any thrombosis on the blood. Similar results were found by Höpfner in his own studies after Payr. Höpfner's cylinder studies were based on Payr's designs but modified to some extent. Höpfner noticed, though, that the thrombosis effect was present only in vessels of less than 3 mm diameter and even in these cases because of extensive intima lesions during operations. With larger vessels, Höpfner did not notice thrombosis with dogs even after 4 weeks of study. Later in 1910, Lespinasse studied with extravasal sutures and magnesium ring plates for anastomosis repair [40]. He found out that the ring plates degraded completely after 80 to 100 days. The original shapes of the rings were maintained for about 30 days before clear breaking down happened. In the 1920's to 1950's, Seelig studied the use of magnesium based wires for aneurysm treatment with rabbits. He found out that alloyed magnesium wires with aluminum resulted in higher

thrombosis chance than with stainless steel wires. With pure magnesium wires he noticed the brittle nature of the material to be a problem. Seelig reported collagenous tissue formation around the wire and the intima for attachment. The alloyed magnesium wires showed fast degradation in 21 days. [85.]

The study of musculoskeletal area with magnesium materials started with Payr's suggested possibilities of using plates and sheets in joint arthoplastics. His studies with animal and clinical experiments, unfortunately, did not have positive results but they did inspire others to study the subject more. One of these researchers was Chlumský, who studied magnesium for regaining motion in stiff joints. Chlumský's animal studies concentrated on knee joints of dogs and rabbits, by using 0.1-0.8 mm thick sheets. His tests revealed that these sheets degraded in 18 days to few weeks depending on sheet thickness. During these studies he was successful in preventing joint stiffness. His experiment extended to a human case eventually and was able to preserve a 2 mm wide joint space even after 8 months from the operation. [85.]

In 1909, Lambotte [38] experimented magnesium implants with a 17 year old child who had over a year old fracture on the lower leg. Lambotte decided to use magnesium based plates with iron wire and steels screws. This unfortunately, though, resulted in extensive subcutaneous gas cavity formation, swelling and pain after one day. Lambotte's discovery resulted him to research more of the matter with his assistant Verbrugge. Lambotte's experiments continued for some time with animal tests and eventually with increasing test cases to humans. He reported that even, though, the magnesium degradation does cause gas formation, it was not a problematic or painful as the gas cavities disappeared after a few weeks. He eventually understood that the problem was the combination of other metallic materials that resulted to a higher rate of electrolytic corrosion in his first test with the child. His studies also resulted that a magnesium screw in a supracondylar fracture healing treatment had degraded completely after one year of the operation without any hypertrophic bone. These results eventually made him recommend the material for certain bone healing areas like carpus fractures, lower arm diaphyseal fractures, humerus head fractures, malleolus fractures and others. This recommendation was also shared by Heschen and Gerlach in 1934. [85]

There has been, though, conflicting results. In 1913, Groves discovered abscess cavities and too fast degradation of the material for implants. In 1924, Zierold had the same opinion and concluded that magnesium is only a connective tissue stimulant, theorizing that the material is promoting but at the same time retarding new bone formation. [85.]

Verbrugge's work was continued by McBride in 1938 [49] with plates and screw, presented in Figure 12 b). McBride's studies showed that the material was not suitable in certain types of applications as plates showed a too fast degradation rate and with medullar pegs the gas formation became a problem because it was not able to exit into soft tissue. McBride concluded in his studies that magnesium does create a local disturbance even if the material is not toxic, and that the material is mostly suitable in

cases where the absorption of the material is needed and where the stress of the fragments is slight after a few weeks. [85.]

In 1940, Maier was investigating magnesium pins made of spindle-shaped sheets. Maier reported that there were no clear healing processes seen and the gas cavity formation was too large for the safety of the patient. What he noticed, though, was that the functional results were good after 14 years which resulted him to study more about the material with animal tests. His recommendation was to use magnesium for arthorodesis of joints and in spinal surgery. In 1948, Troitskii and Tsitrin experimented an Mg-Cd alloy for plate and screw applications. They reported that the material stimulated the formation of callus bone which was due to the formation of $MgCO_3$ in the corrosion layer. The use of this type of alloy was suggested for rod and plate use for severe osteomyelitis cases. The patent for improving the corrosion resistance of magnesium by alloying it with Cadmium, which enabled faster recovery of patients, happened in 1969 by Stroganov. [85.]

Payr's and Martina's studies also extended to operating a 54 year old woman's cancerous gall bladder with significant parts of the liver. The bleeding tissue was stopped by using magnesium plates with iodine-catgut sutures. In their previous studies with animals, they had noticed that the degrading magnesium material caused the hydrogen bubbles to penetrate the extensive fibrous tissue around the material and stop the local bleeding by a tamponade effect. After two weeks, the fibrous tissue formation slowed with the 54 year old woman. [85.]

Payr's has also suggested magnesium to be used for treating cavernous haemangioma and large-vessel aneurysms. Payr's idea of destroying the haemangiomas and lymphangioma tumors with magnesium pieces, presented in Figure 12 c). This was based on the principle of enhanced blood clotting in the tumor area through the metal's degradation. Payr later summarized that this method only seemed to work with subcutaneous cavernotic haemangioma. This method was later tested again in 1981 by plastic surgeon Wilflingseder [79] with 27 different haemangioma patients. Wilflingseder's clinical results showed that about 50 % of the cases were treated successfully. [85.]

Magnesium's suitability in medical implant applications have seen some doubt even in the researchers own study periods as was seen with Chlumský at one point. He had reported at one point that the material is not suitable for intestinal anastomosis treatment but after seeing Payr's work he saw that the purity of the material has a impact on the suitability. He reported that high-purity magnesium corrodes homogenously in vivo and that it is more suitable even though the connectors were significantly corroded after 8 days to a few weeks depending on the location. [85.]

Magnesium has also seen some studies regarding it being as a suture material, presented in Figure 12 d). The metal has also been suggested for connectors for neurography and for biobatteries for pacemakers. Studies have reported that magnesium can be used as a suture material but only as an alloy due to the brittle nature of the

metal. Magnesium has been studied extensively based on these researches. Figure 12 presents some of the applications that metal material have been used in.

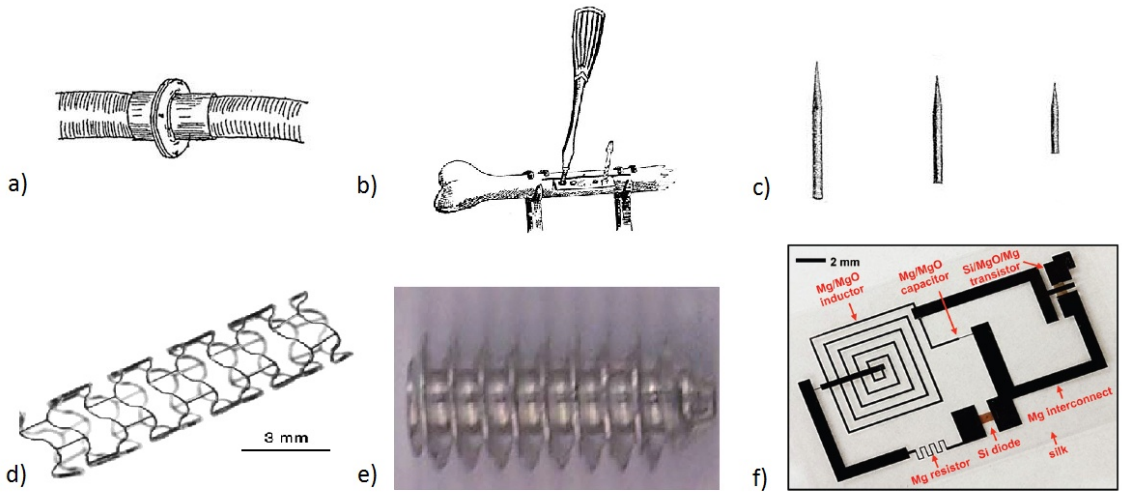

Figure 12. Researched magnesium based medical applications. a) Tubal magnesium connector designed by Payr for vessel anastomosis [85], b) Mg-Mn plate for rotation-resistant osteosynthesis by McBride [85], c) Magnesium rods for haemangioma treatment by Payr [85], d) Lekton Magic's expanded WE43 magnesium alloy coronary stent [51], e) Mg-4Y alloy screw for joint reconstruction surgery [95] and f) Biodegradable transient electronic silk sheet with magnesium and silicon based structure [31].

As the medical and implant field has been moving towards biodegradation products, magnesium's unique tendency to degrade as a metal has made it an interesting choice for certain application. The biocompatibility of the material has resulted to recent studies that are concentrating on applications like blood vessel stents, bone healing products and electrical electrodes, according to Li and Zheng [41]. The degradation rate of the material is still though unsolved. Studies done by Guan et.al. [22] about Mg-Zn-Sr alloy, Johnson and Liu [36] about Mg-Y alloy, Salahshoor and Guo [61] about Mg-Ca, Shadanbaz et.al. [64] about calcium phosphates on magnesium, Tang et.al. [72] about calcium phosphate/titania coatings on AZ31 magnesium alloy and Yu [94] copper containing carbon films on magnesium alloys are only a few of the new studies done to solve magnesium's problems. When these aspects are solved, it can mean huge possibilities and novel ideas to the implant field.

5 Mg-ALLOY's DEGRADATION AND CONDUCTIVITY STUDY.

The practical work centered on the idea of testing a magnesium alloy, to determine if a polymer coating could be used to lower the degradation rate of the magnesium alloy. The modification and preparation methods that the material needs were also in a focus to evaluate if the original material shape could utilized for powder creation.

Degradation tests are focused on pH measurements that are used to calculate mass and hydrogen release rates for the alloy material. The mass is also measured through weighting the samples to determine if the calculation results can be used accurately. Alternative approaches to how future testing could be done are discussed at the end.

5.1 Materials

The material provided for the study was a magnesium based alloy. The alloy consisted of 88wt-% of Mg, 10wt-% of Gadolinium (Gd), 1wt-% of Neodymium (Nd) and 1wt-% of Zinc (Zn). The material amount provided for testing was 6 grams of the alloy from the supplier.

The pieces all were different shaped with a similar form from cutting processes for other purposes. These pieces can be seen in Figure 13.

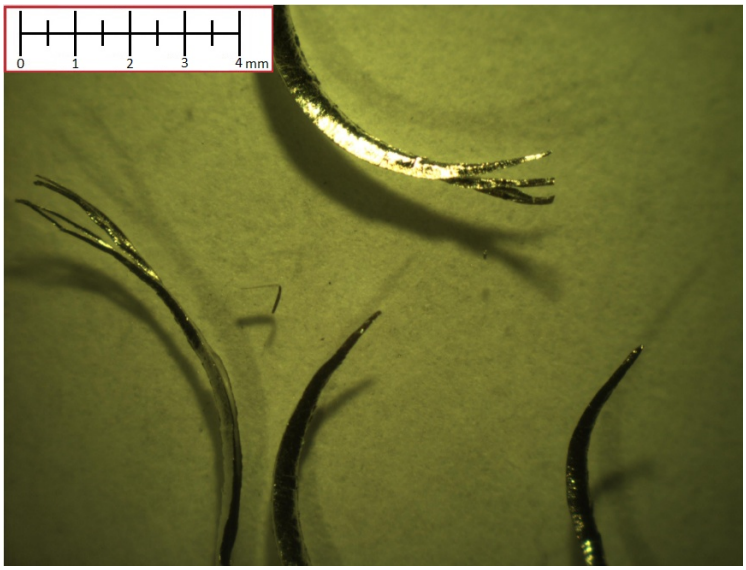

Figure 13. Provided material pieces for testing purposes.

The original pieces were cut with a utility knife as the material tended to break quite easily through bending and cutting forces. The pieces were also grinded between two files two obtain small particle sizes. Particle forming resulted to four different particle size groups for further testing. These groups were achieved by using sieves of different

hole diameters that resulted on size groups of >500 µm, <500 µm, <315 µm and <125 µm. The groups had alloy of about 1.808 g, 1.336 g, 0.586 g and 0.076 g respectively. Weighting was completely done in each phase with a "GWP Mettler PM400" weighting machine. The machine has a ±0.002 g error range for its readings.

The preparation and test phase also had a polymer material that was poly(l-lactide-co-dl-lactide) (PLDLA) 50:50 powder.

5.2 Composite preparation

A "Nike Hydraulics Type ZB110" compression machine, presented in Figure 14 a), was used to achieve similar composite pieces. During the composite formation the compression pads were heated to around 150 ^{o}C. Compression during this preparation was done so that it did not exceed 10 MPa of compression force. Cooling was done by either water or air, depending on if the water cooling was an option at that time.

a) 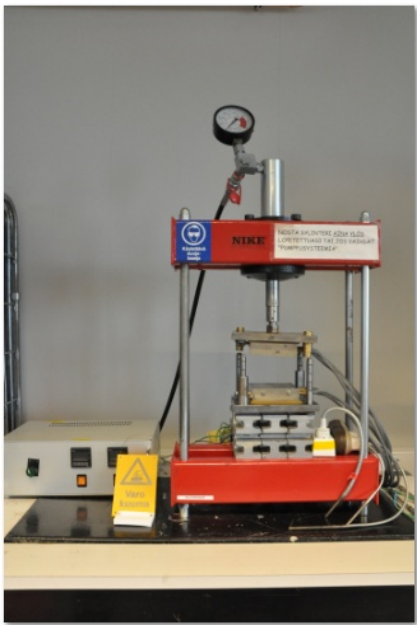 b) 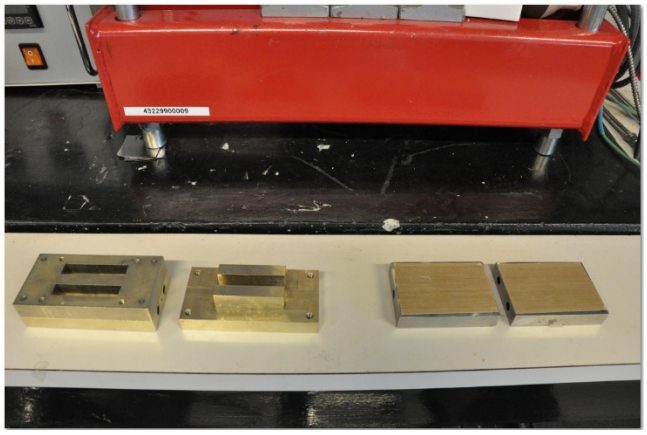

Figure 14. Nike Hydraulics Type ZB110 compression machine and molds used for composite forming.

Two different molds were used during the compression processes to get the needed composite pieces. First mold was a simple compression pads seen on the right of Figure 14 b). These compression pads were used to create flat polymer pieces that were cut into narrow strips that were able to fit into the mold seen on the left of Figure 14 b).

After acquiring the narrow polymer pieces from the compression and cutting process, the weighting machine was used to divide the pieces so that each composite sample had similar amounts of polymer. The magnesium amounts were not measured due to the difficulty of controlling them during the composite forming. This was due to the static electricity of the material.

Polymer pieces of 50*10*1.0 mm size were created with the molds. A small indent of 25*4*0.5 mm size was created onto the middle are of the polymer pieces. This indent was then filled with the magnesium alloy to mildly contain the alloy during the composite formation. Polymer pieces without the indent were placed on top of the polymer and magnesium material. This was then compressed together to create a solid composite piece that had the magnesium alloy generally in the middle of the polymer material.

5.3 Samples

Composite formation resulted to 10 composite pieces and 6 pure polymer pieces. Samples named Mg-PLDLA-s (surface) were composites where the polymer did not cover the magnesium material properly. Mg-PLDLA-e (embedded) named composite samples had polymer covering almost completely the magnesium alloy. PLDLA named samples had only polymer material in them. 6 magnesium particle samples and 4 original magnesium piece samples were, additionally, chosen for testing. Magnesium samples were named as Mg and 2 original samples were named as Mg-Original. Composite, particle and 2 original samples were used for testing the degradation in a “Sørensen” buffer solution. Two other original pieces were named as Mg-Original-water and were used for degradation testing in de-ionized water environment. Magnesium amounts were weighted so that they generally were in the same weight range for getting similar results. Result from the composite and particle sample formation can be seen in Table 10.

Table 10. Test samples and their material amounts.

	Diameter	Magnesium	Polymer:	Total	Ratio
Sample:	Size (µm)	Weight (g)	Weight (g)	Weight (g)	Mg/polymer (%)
Mg-PLDLA-s 1	>500	0.083	0.283	0.366	22.7 / 77.3
Mg-PLDLA-s 2	>500	0.090	0.302	0.392	23.0 / 77.0
Mg-PLDLA-s 3	<500	0.142	0.292	0.434	32.7 / 67.3
Mg-PLDLA-s 4	<315	0.060	0.282	0.342	17.5 / 82.5
Mg-PLDLA-s 5	<315	0.065	0.282	0.347	18.7 / 81.3
Mg-PLDLA-s 6	<125	0.031	0.268	0.299	10.4 / 89.6
Mg-PLDLA-e 1	>500	0.040	0.464	0.504	7.9 / 92.1
Mg-PLDLA-e 2	<500	0.056	0.462	0.518	10.8 / 89.2
Mg-PLDLA-e 3	<315	0.049	0.425	0.474	10.3 / 89.7
Mg-PLDLA-e 4	<125	0.039	0.415	0.454	8.6 / 91.4
PLDLA-s 1			0.292		
PLDLA-s 2			0.294		
PLDLA-s 3			0.296		
PLDLA-e 1			0.456		
PLDLA-e 2			0.429		
PLDLA-e 3			0.434		
Mg -1	>500	0.070			
Mg -2	>500	0.099			
Mg -3	<500	0.045			
Mg -4	<500	0.107			
Mg -5	<315	0.056			
Mg -6	<315	0.070			
Mg-Original 1	Original	0.076			
Mg-Original 2	Original	0.097			
Mg-Original-water 1	Original	0.085			
Mg-Original-water 2	Original	0.085			

For PLDLA samples the s and e letter at the end of the name refer to the polymer amount that is similar with the composite samples. This was done so that any effect of the polymer could be seen in the results.

5.4 Testing methods

Testing was focused on a simple resistivity test by using a "Fluke 112 True RMS Multimeter" machine, pH measurements by using a "Mettler Toledo SevenMulti" machine with a ±0.002 pH error range. A microscope was used to monitor the samples

visually during the hydrolysation testing by “Zeiss West Germany”, camera part was “BestScope” and a light source was “Schott KL1500”.

The buffer used in our test samples, except for the two Mg-Original-water samples, was a “Sørensen” buffer created from 15.48 g of Na_2HPO_4, 3.3 g of KH_2PO_4 and de-ionized water to get 2 liters of 7.48 pH buffer solution. Each sample was placed inside of test tubes with 30 ml of buffer or de-ionized water, depending on the sample. The 30ml amount of liquid was chosen based on the 1:30 ratio that is used for hydrolysis tests as there was less than 1 g of material for each sample.

During the testing period the pH of the samples was measured. The pH measurements were done during a four week time period in room temperature of about (19-22 ^{o}C). The buffer was changed to samples that had higher pH at 190 hour time point when compared to their pair in their magnesium particle size. Another buffer change happened at 528 hour time point, which was done to the samples that had the previous buffer change. Composites samples of Mg-PLDLA-s 1, Mg-PLDLA-s 3 and Mg-PLDLA-s 4 had the buffer changed due to these reasons. Magnesium samples of Mg-2, Mg-4, Mg-6 and Mg-Original 2 also received a buffer change. Buffer change was, additionally done to polymer samples of PLDLA-s 1, PLDLA-s 3 and PLDLA-e 1 to make sure the polymer does not have any real effect on the pH. De-ionized water sample of Mg-Original-water 1 got a solution change at 144 hour time point and the test period for the samples was 624 hours long. Mg-Original-water 2 sample had a test period of 480 hours and no solution change.

Wet weight of composite and polymer samples were done 672 hour time point after the first immersion to the solutions. Microscope and camera pictures were taken from key areas of the samples at before the start of the pH tests, after 190 hours from immersion and at the end of the hydrolysis test. Dry weights were measured after the hydrolysis test was over. Composite and polymer samples we dried for 24 hours and magnesium samples were dried for 72 hours.

Due to the limit of just weight measurements and pH change results, calculations from the pH change results were done to determine the degradation amounts that samples could relatively have. The buffer solution can prevent some material from being seen from the actual pH-changes, which is why its effect was calculated.

The degradation reaction that takes place happens according to formula (1) [95]. Presence of buffer can add reactions to the process which can be seen in formula (1) [24; 88] with the potassium phosphate reaction.

$$
\begin{aligned}
&Mg^{2+} + 2e^{-} \\
&H_2O + 2e^{-} \rightarrow H_2 + 2OH^{-} \\
&Mg^{2+} + 2OH^{-} \rightarrow Mg(OH)_2 \\
&or \\
&KH_2PO_4 + 2OH^{-} \rightarrow KPO_4^{2-} + 2H_2O \\
&Mg^{2+} + KPO_4^{2-} \rightarrow MgKPO_4 * nH_2 0
\end{aligned}
\qquad (1)
$$

The degradation calculation can be done by according to the formula (2). The concentration of the buffer element is the same amount as magnesium's. This is because the buffer can neutralize both hydroxide ions that evolve from the magnesium's degradation.

$$
\begin{aligned}
&[KH_2PO_4]_{2L} = m(KH_2PO_4) / M(KH_2PO_4) \\
&[KH_2PO_4]_{0,03L} = ([KH_2PO_4]_{2L} / 2) * 0{,}03 \\
&[Mg^{2+}] = [KH_2PO_4]_{0,03L} \\
&m(Mg^{2+}) = M(Mg^{2+}) * [Mg^{2+}]
\end{aligned}
\qquad (2)
$$

The mass change results from the pH changes can be calculated by using formula (3). The phosphate and hydroxide concentrations are multiplied by 0.03 to get the correct amount of ions in the test tubes (30 ml of liquid).

$$
\begin{aligned}
&pOH = 14 - pH \\
&[OH^-] = e^{-(pOH)} \\
&[OH^-]_{change} = [OH^-]_{result} - [OH^-]_{start} \\
&[OH^-]_{solution} = [OH^-]_{change} * 0{,}03 \\
&m(Mg^{2+}) = 0{,}5 * M(Mg^{2+}) * [OH^-]_{solution}
\end{aligned}
\qquad (3)
$$

Calculations to determine the hydrogen release of the sample materials were also done. As with the mass loss calculation, calculation of the hydrogen release was done first due to the buffer effect. Calculating hydrogen gas release is done through volume, which can be done according to the formula (4).

$$
\begin{aligned}
&PV = nRT \\
&\frac{V}{n} = RT / P \\
&V = n * \frac{V}{n}
\end{aligned}
\qquad (4)
$$

In formula 4 the R is the gas constant that is 0.08314510 bar*dm^3/(mol*K), P is the air pressure in sea level that is 1.01325 bar and T is the temperature from the lab room which was about 21 ^{o}C (294.15 K). Volume from the buffer effect can be calculated according to formula (5).

$$
\begin{aligned}
&[KH_2PO_4]_{2L} = m(KH_2PO_4) / M(KH_2PO_4) \\
&[KH_2PO_4]_{0,03L} = ([KH_2PO_4]_{2L} / 2) * 0{,}03 \\
&[H_2]_{buffer} = [KH_2PO_4]_{0,03L} \\
&V(H_2) = [H_2] * (\frac{V}{n}(H_2)) * (1000ml / 1l)
\end{aligned}
\tag{5}
$$

Calculating the released hydrogen from pH change is done according to formula (6), when the buffer effect is minimal and the pH rises. The calculation is based on both formula 3 and 5 calculations.

$$
\begin{aligned}
&pOH = 14 - pH \\
&[OH^-] = e^{-(pOH)} \\
&[OH^-]_{change} = [OH^-]_{result} - [OH^-]_{start} \\
&[OH^-]_{solution} = [OH^-]_{change} * 0{,}03 \\
&[H_2] = [OH^-]_{solution} * 0{,}5 \\
&V(H_2) = [H_2] * (\frac{V}{n}(H_2)) * (1000ml / 1l)
\end{aligned}
\tag{6}
$$

The resistivity tests were done by using a "Fluke 112 True RMS Multimeter" machine. Original alloy pieces that were not used for composites were used to determine if the alloys resistivity can be measured. Additional measurements were done with the particles gained from the particle forming process.

Imaging was done with the microscope at three different time points for most of the samples with magnifications of 0.8, 3.2 and 6.4. Imaging was done at room temperature (20-22 ^{o}C). Composite and polymer samples surface were dried lightly before imaging with a soft tissue paper. Each composite sample was imaged before the start of the hydrolysis test. The second time point for imaging was done at 190 h after immersion of the test samples. Third time point was done at the end of the hydrolysis test at 672 h after immersion. Mg-Original-water 1 sample had the imaging done at 144 h time point after immersion with a camera. Both Mg-Original-water samples were imaged at the end of the test at 624 h for Mg-Original-water 1 and 480 h for Mg-Original-water 2. Additionally, other magnesium samples in the test tubes were imaged with a camera at the 190 hour time point.

5.5 Results

Testing concentrated to a 4 week testing period of hydrolysis tests in the test tubes. The pH measurements during the time period provide the degradation information for later discussion and calculations.

Calculations were done to determine the mass loss and hydrogen release of the samples. These results were, additionally, compared to pH results and weighting results

to determine if the calculations are the effective way to determine the degradation of the samples. Figures from imaging provided further insight to the degradation.

5.5.1 pH results

During the first few hours of immersion to de-ionized water and buffer, magnesium creates a very active reaction with the solution. The reaction from formula (1) indicates that the degradation releases hydrogen. The hydrogen evolution started immediately after immersion to the solutions. This can be seen as hydrogen bubbles forming from the sample surfaces and rising to the surface of the solution. The hydrogen bubbles tended to lift the samples to the surface of the liquid in the test tubes due to the very fast activation of degradation in each magnesium sample and in some of the composite samples. This results in some parts to not have contact with the liquid. Therefore, the test tubes solutions were mixed each time this had happened to make the samples sink to the bottom of the test tubes. The pH tests results can be seen in Figures 15, 16, 17 and 18. Buffer and solution change can be noticed from the Figures due to the drop in pH to the level of the buffer, except for the polymer samples.

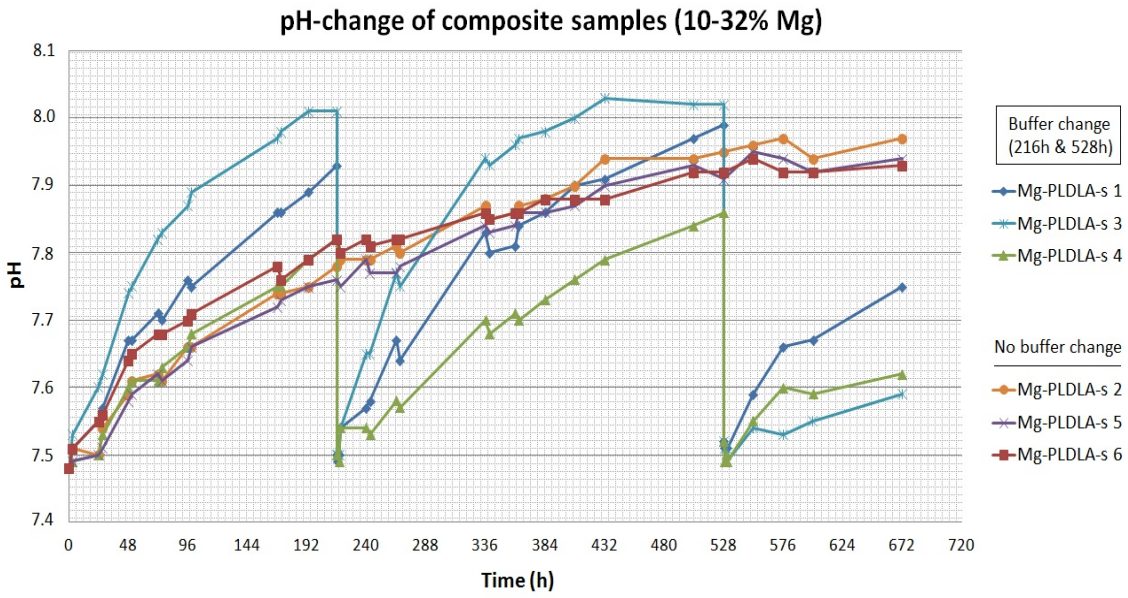

Figure 15. The pH-change for the composite samples containing 10-32 % of magnesium. Magnesium had poor coverage by the polymer.

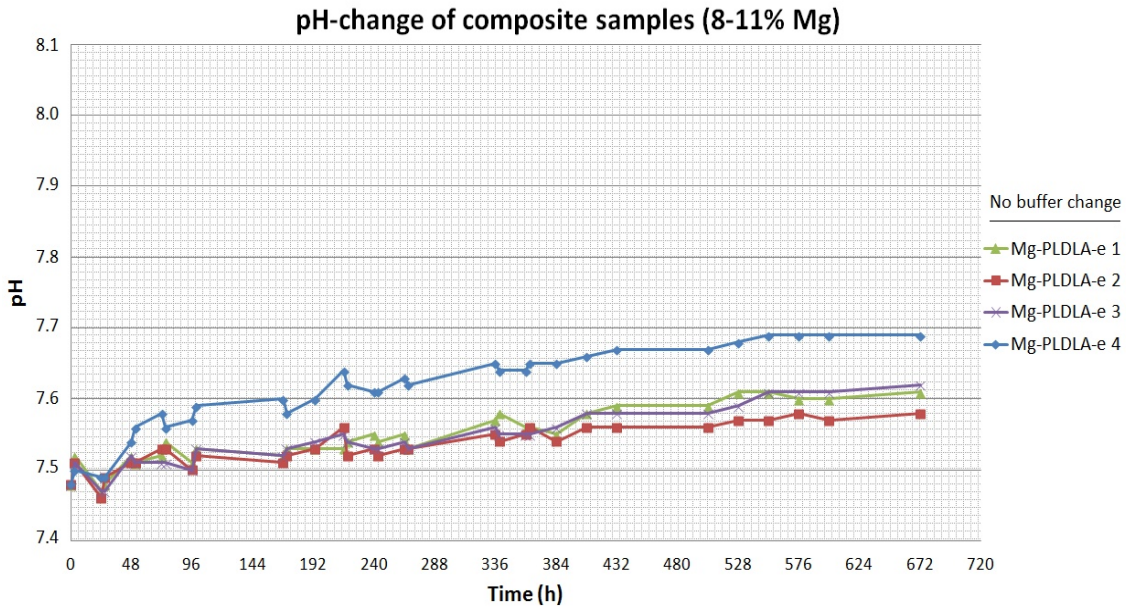

Figure 16. The pH-change for the composite samples containing 8-11 % of magnesium. Magnesium had good coverage by the polymer.

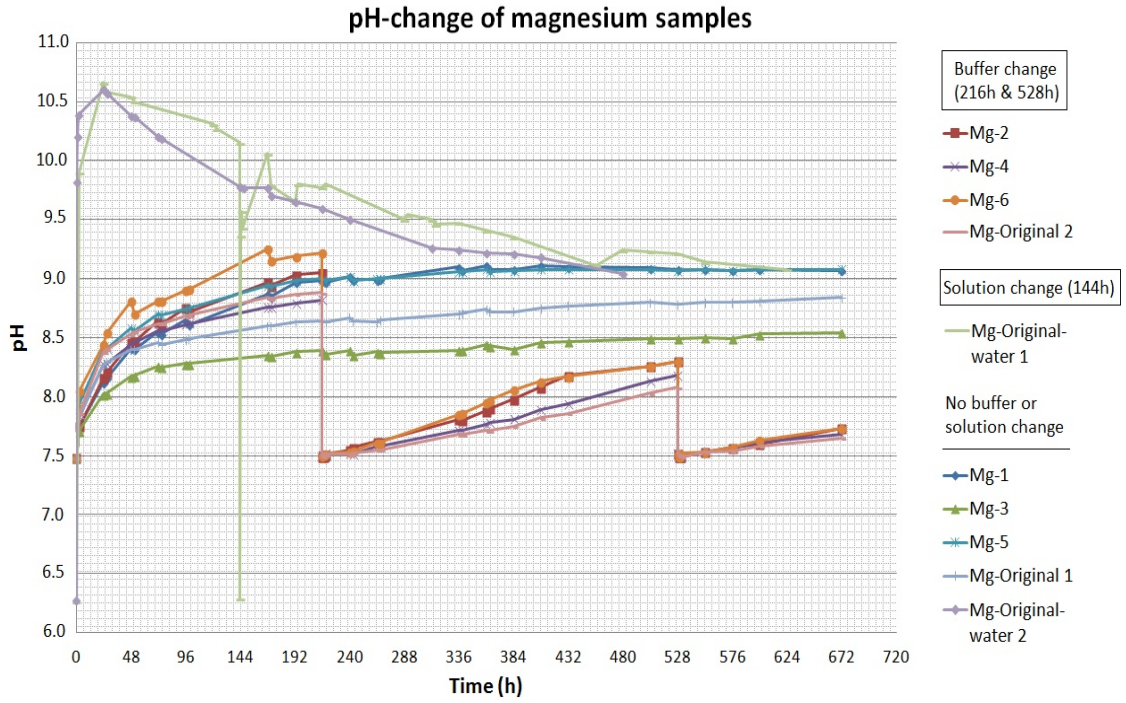

Figure 17. The pH-change for all the magnesium samples.

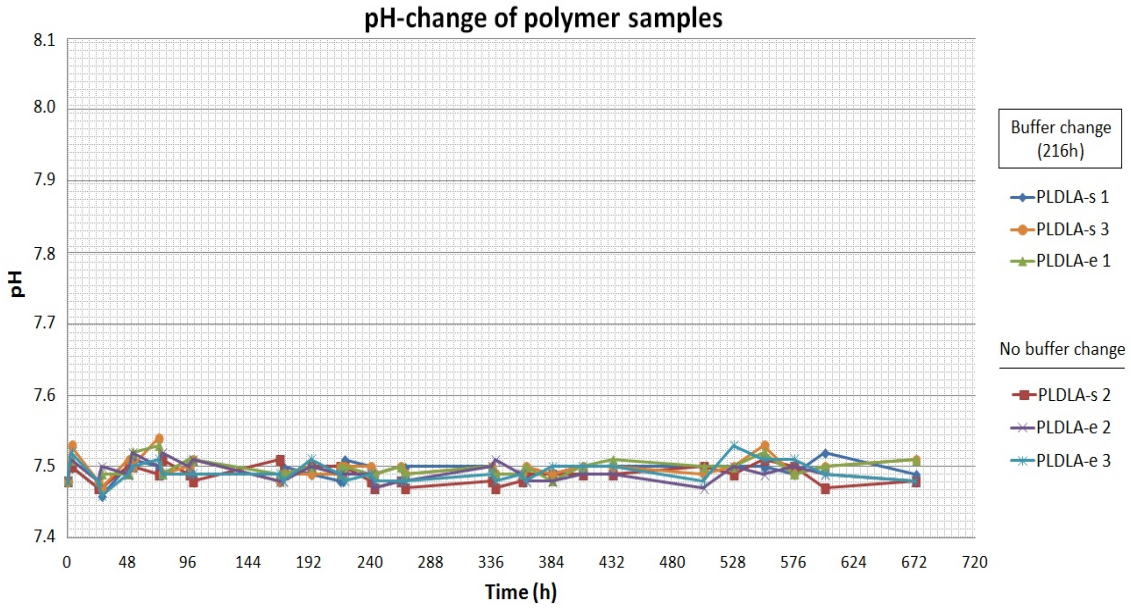

Figure 18. The pH-change for all the polymer samples.

The pH results from the degradation reactions indicate that the degradation is more active in de-ionized water than in the buffer solution. This of course is not the situation since the de-ionized water has no buffer capability. For Mg samples the buffer effect lasts for about 24 hours from immersion. In water the pH can rise up to 10.60 pH in a few hours, which is why the buffer limit is reached fast. The composite samples indicate that the degradation rate is lower due to the polymer preventing the solution from touching the magnesium material. The pH rise of composite samples containing 10 to 30 % magnesium is more clear due to the insufficient coverage of the polymer material. This yields some of the magnesium to react with the surrounding buffer and thus increase the pH of the solution. Composites containing 8 to 11 % magnesium seem to have lower degradation rates as only a few sites seem to be degrading due to the poor coverage from the polymer. Polymer sample results indicate that the polymer does not contribute effectively at to the rise or fall of the pH of the solution. Some fluctuation of the pH happens in the tests, which might be contributed to temperature, ion imbalance of the solution at the testing time and equipment errors. Additionally, the results indicate that the material amount and particle size have an effect to the degradation amount. Particle size of the magnesium samples has an effect to the degradation amount due to available surface area. The larger material amounts with some samples can cause the alloy to be tightly submerged preventing the larger surface area to have an effect on smaller particle sizes.

From the presented results the pH fluctuates with most of the samples between a given day's first reading and the second reading (3 h later). This can be explained by the temperature difference between the test times. The temperature did not change most of the times between these test points but at some points the difference was 0-0.5 ^{o}C. Temperature changes between days ranged from 0-2 ^{o}C due to the change in the lab room. More prominent reason for the pH change can be caused by an uneven

distribution of the ions in the solution. This was noticed some of the times when the pH changed due to the movement of the sensor and the solution around it. The last reason could be contributed to the reactions mentioned in formula 1. These reactions remove the free hydroxide ions from the solution to water or to the surface of the magnesium material. The $Mg(OH)_2$ layer formation was noticed in the magnesium samples in the de-ionized water as their pH started to decline after 24 hours. The formation of the protective layer slows down and can even prevent the degradation when the solution is in a pH range of 9-11.

5.5.2 Mass change results

The wet and dry weights of the composite, polymer and magnesium samples were measured with the measuring machine. These results can be seen in Figures 19, 20 and 21.

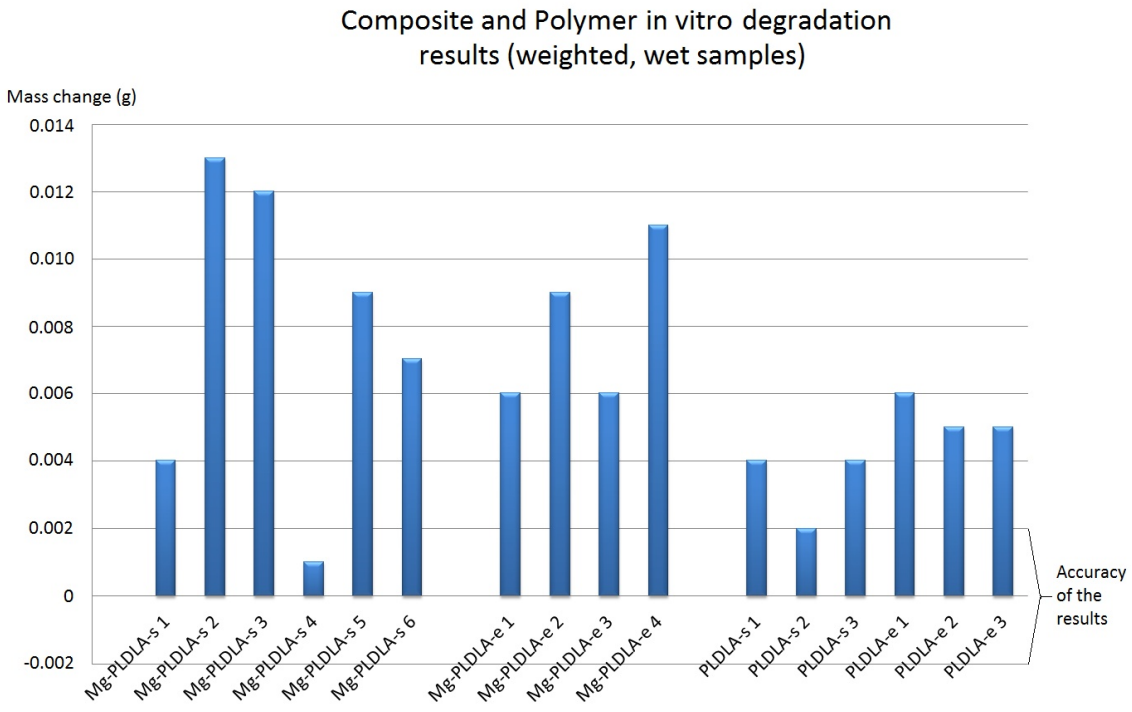

Figure 19. Wet weight mass change for all the composite and polymer samples.

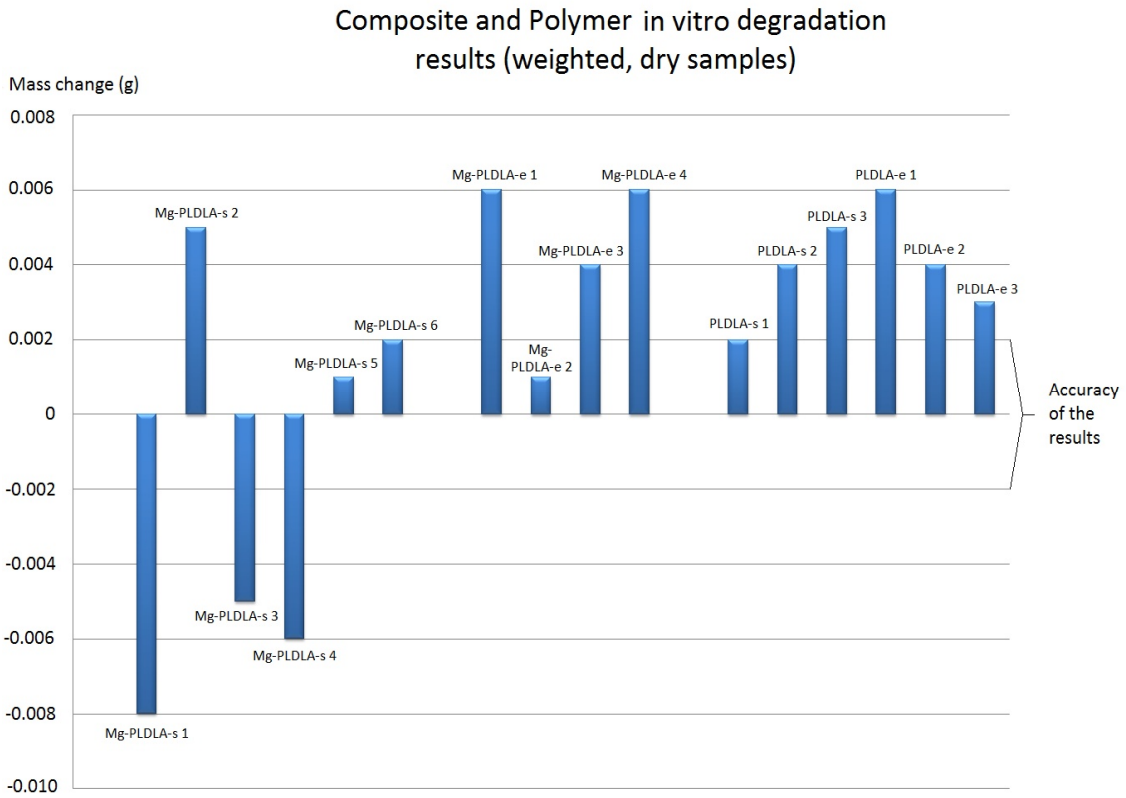

Figure 20. Dry weight mass change for composite and polymer samples.

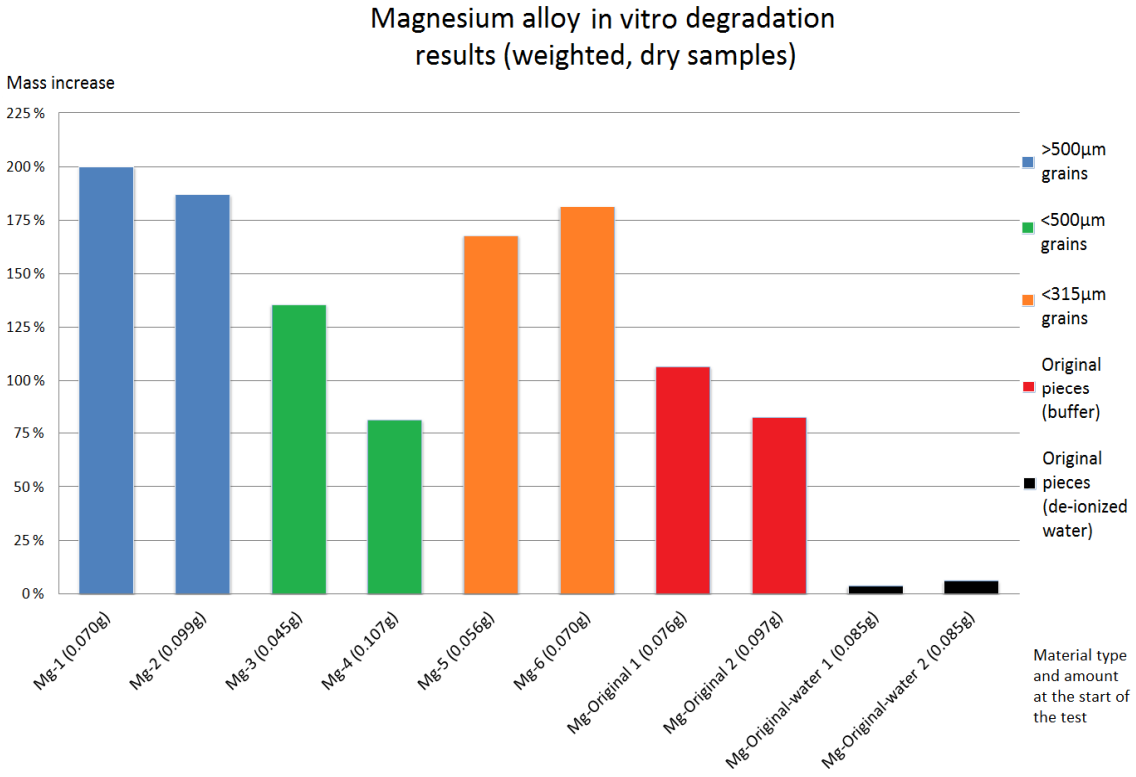

Figure 21. Mass change for magnesium samples after 72 hours of drying.

Results indicate that the weight changes only slightly with composite samples and most cases they can be considered to be close to the error margins of the measuring equipment. Wet weights show the importance of drying but also indicate that the equipments error margin can have an effect. For example, the PLDLA-s 2 sample has higher weight increase after drying. This may also indicate impurity problems during measurement. Some polymer sample results indicate that a small amount of solution is still trapped in them as they have higher mass than at the start. This indicates that the drying period was not long enough. This applies to the composite samples. Mass variations can be caused due to degradation of the material, additions of phosphate layer and the intake of solution. The intake of solution, degradation of magnesium and formation of phosphate layer might then indicate that they can balance the weight of the samples for the first few weeks. This makes degradation measurements difficult when using the weighting method. The mass increases of Mg samples are due to the phosphate layers presence, which is important to be removed before evaluating the mass change for magnesium samples. The increase in mass for magnesium samples is also difficult to estimate when including the phosphate layer as during the drying period, some of the phosphate material is stuck in the container/test tube walls and are thus left out from the weight measurements. Mg-Original-water samples did not have the phosphate layer and as such did not have any clear mass change. Change can be contributed to the measurement devices error range and the fast addition of hydroxide layer.

5.5.3 Calculation results for degradation

The buffer effect calculated according to formula (2) results to about 8.8 mg of magnesium. Once this amount is degraded the pH starts to rise according to formula 3. After this point the mass loss results are added to the final amount of degradation. The mass change results from the calculation of formula (3) and (6) were done to each sample.

The buffer effect calculated according to formula (4) results to about 8.8 ml of hydrogen gas. The loss of hydrogen from the solution is balanced by the reaction that occurs from the buffer effect. During the buffer solution, a loss of about 2 ml of solution was noticed. This loss can be contributed towards the hydrogen release and the pH testing where the sensor takes a small amount of solution with it when the calculation is done. Once the buffer effect is diminished the pH starts rising. The hydrogen release results from the calculation of formula (6) were done to each sample that contained magnesium. This was done to determine the correlation between the hydrogen evolution to the mass loss. Both mass loss and hydrogen evolution results are shown in Figures 22, 23, 24 and 25. Mass loss of polymer samples from the calculations can be seen in Figure 26.

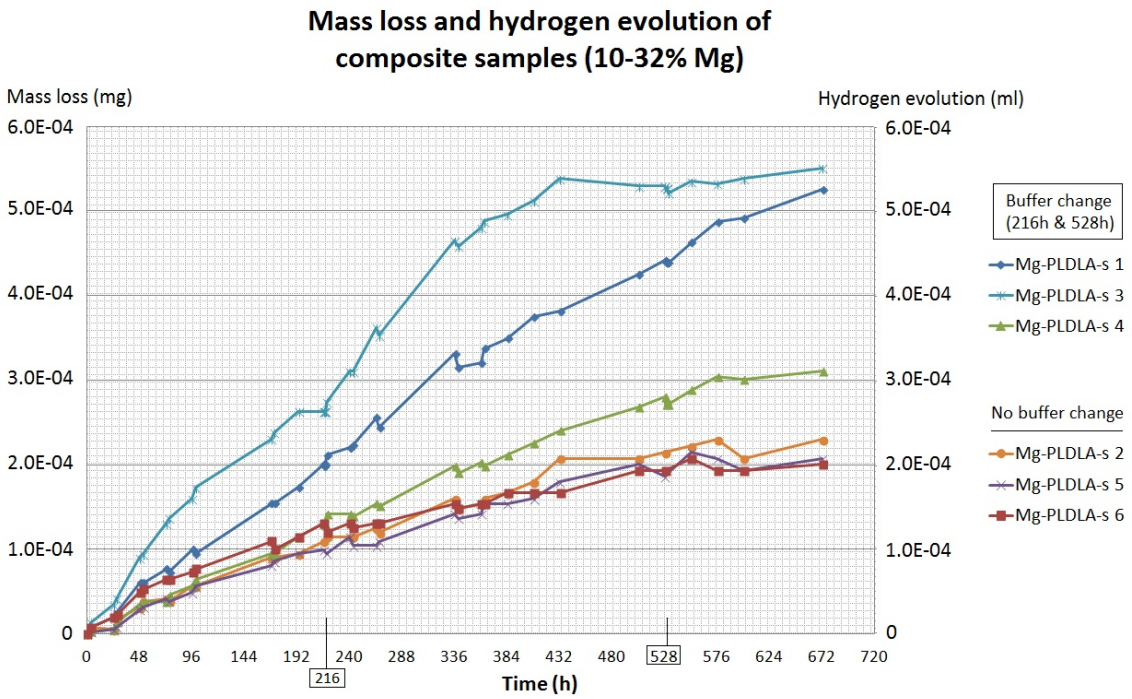

Figure 22. Mass loss and hydrogen evolution for composite samples containing about 10-32 % of magnesium. Magnesium had poor coverage by the polymer.

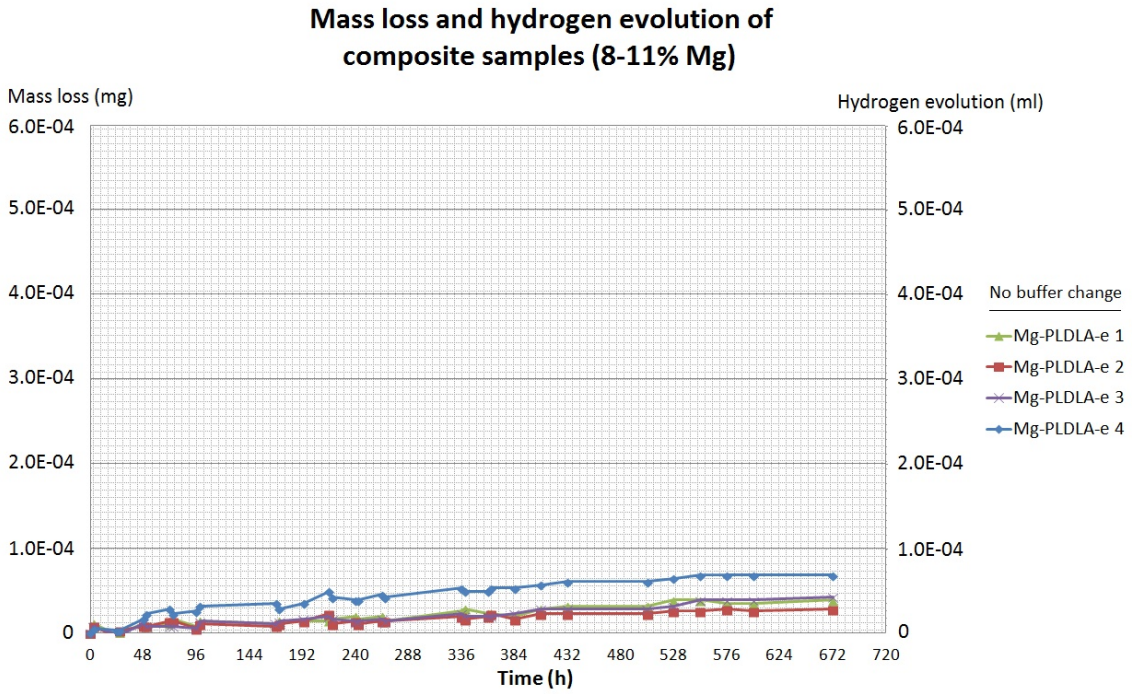

Figure 23. Mass loss and hydrogen evolution for composite samples containing about 8-11 % of magnesium. Magnesium had good coverage by the polymer.

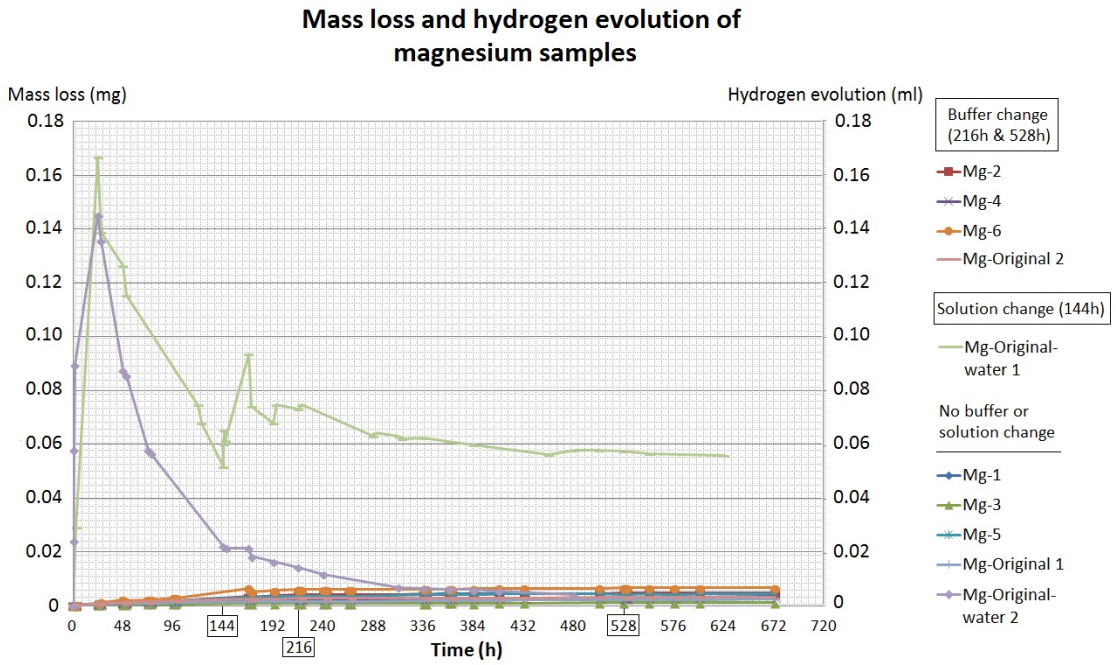

Figure 24. Mass loss and hydrogen evolution for magnesium samples including the Mg-Original-water 1 and 2 samples submerged in de-ionized water.

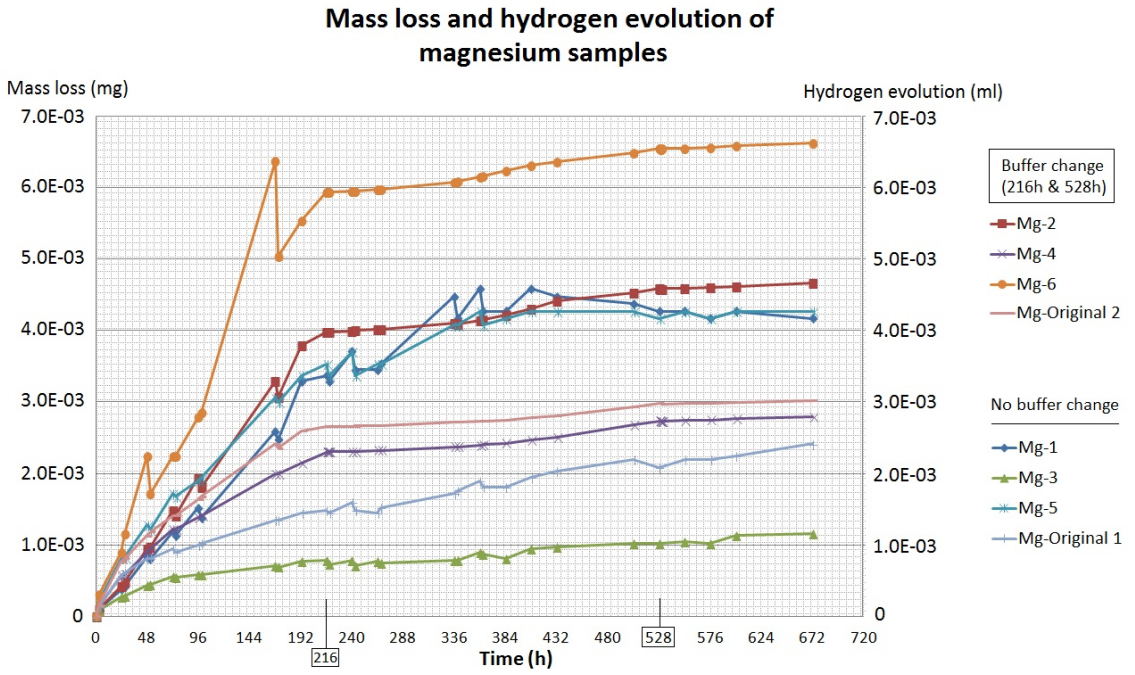

Figure 25. Mass loss and hydrogen evolution for magnesium samples without the Mg-Original-water 1 and 2 samples submerged in de-ionized water.

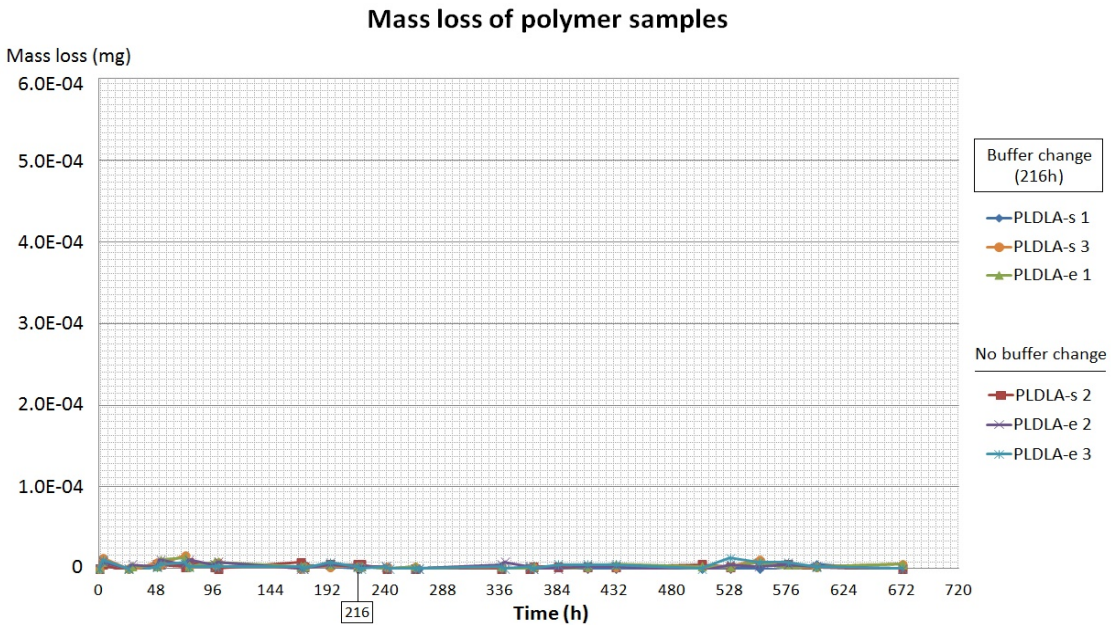

Figure 26. Mass loss for the polymer samples.

Based on the calculation results, magnesium's degradation amount with magnesium and composite samples that have noticeable pH increase is around 8.8 mg. This degradation amount happens during the buffer effect. The mass loss during pH rise in a buffer solution is a low amount that does not change this value in a significant way. The mass loss from the calculations indicates that the degradation in the buffer (8.8 mg) is more active than in de-ionized water (0.00014-0.00017 mg). This is due to the pH staying longer below the 9 to 11 range. For de-ionized water samples, the pH rises fast to 10.5-11 pH area. This hinders further active degradation and enables the formation of the protective layer, which lowers the mass loss values that are seen in Figure 24. The buffer solution thus keeps the solution in the area that benefits further degradation of the material. Additionally, due to the buffer solution containing phosphates, the surface of the magnesium materials starts to gain a phosphate coating, according to formula (1). The degradation amount after buffer change, when the buffer is limiting the pH rise, is difficult to estimate due to the degradation of the protective layers. The phosphate layer can be noticed without a microscope as it forms a white crystal type of structure around the magnesium metal. This increases the sample weight which explains why the wet and dry weight measurements do not reveal clear decrease in weight when compared to calculation results.

These results indicate the correlation between pH increase to mass loss and hydrogen release amounts. The maximum amount of hydrogen release from the calculations is not accurate as the decrease in the value does not mean hydrogen gain outside of the solution. The amount can be estimated, though, to be around 8.8 ml of hydrogen gas as the evolved amount during pH rise is low compared to the evolution during the buffer effect. For samples in de-ionized water the hydrogen amount is around 0.14-0.17 ml. These results do not provide enough information to determine if the

material is suitable or not for implant applications. They do, though, indicate that a certain amount of degraded magnesium in milligrams can release the same amount of hydrogen gas in milliliters. Accurate degradation measurement should be done through the ratio towards a surface area which was not done to the samples in this test due to random sized pieces and different particle sizes.

The pH readings indicate a slightly steeper rising curve for the samples after the first buffer change when compared to the curves after the second buffer change. With calculation results of mass loss and hydrogen evolution this is not seen so clearly as change in pH is based on a logarithmic scale. This means that a pH of 10 has ten times as much [OH^-] ions than a pH of 9, resulting to ten times higher mass loss for the degradation. This can be noticed with the Mg-Original-water 1 sample in Figure 24 as the maximum degradation amount after solution change is around four to five times lower than in the start of the test, due to pH level being lower by 0.5 units.

The degradation curve change after buffer change is not completely due to a sudden fast degradation of the sample material. The change is due to the degradation of the protective layer around the sample and the sample itself. Due to the change of the buffer and the lower pH due to it, the hydroxide and phosphate layers start to degrade which again releases the magnesium, hydroxide and phosphate materials to the solution. This in turn raises the pH much faster when compared to the original degradation rates before buffer change. This happens mainly with the first buffer change as the protective layer is not as complete as before the second buffer change. This leads to a situation where the normal magnesium degradation and the hydrogen evolving from it can destroy the layer easily. With the second buffer change, the layer is more complete and can thus prevent the degradation more readily. These reactions indicate that the pH, mass loss and hydrogen release results are not quite accurate as some of the material hydroxide ions from the degradation process are bound to a coating and sometimes these ions (from the coating) are released back to the solution. These eventually, give us lower degradation results for samples where the buffer was not changed and higher degradation results for those of which buffer was changed.

5.5.4 Results from the conductivity tests

The conductivity and resistivity tests done with the "True RMS Multimeter" machine revealed two aspects for these kinds of tests. The original material pieces gave about 0.2-1.0 Ω resistance readings from a 1 cm long material section. Due to the varying sample sizes for length and diameter size, as well as not uniform diameter in the pieces themselves, the materials conductivity values cannot be estimated. This applies to the varying particle size samples as the device does not provide readings unless the particles are pressed to create a proper contact between each particle piece. The readings with the powder samples ranged from 0-8 Ω depending on how much the material was pressed together. More force applied resulted to a lower reading. The readings also indicate that obtaining accurate reading can only be done from a solid piece that would have a fixed uniform diameter and length.

5.5.5 Imaging results

Imaging was done with a camera and a microscope to determine whether there were visual degradation effects. Two different composite samples from before immersion, after 190 h and after 672 h are presented in Figure 27. The degradation in both samples is happening in the materials surface as the material has lost some of its shine. The change is more noticeable in Mg-PLDLA-s 5 as it had less polymer covering the material. The degradation, especially with the sample Mg-PLDLA-e 4, is localized. This is referring to the pitting corrosion reaction of the alloy. This degradation is indicated in the figure using the arrows. The polymer covering these samples does prevent the solution from touching the metal completely which is why both of them experience degradation.

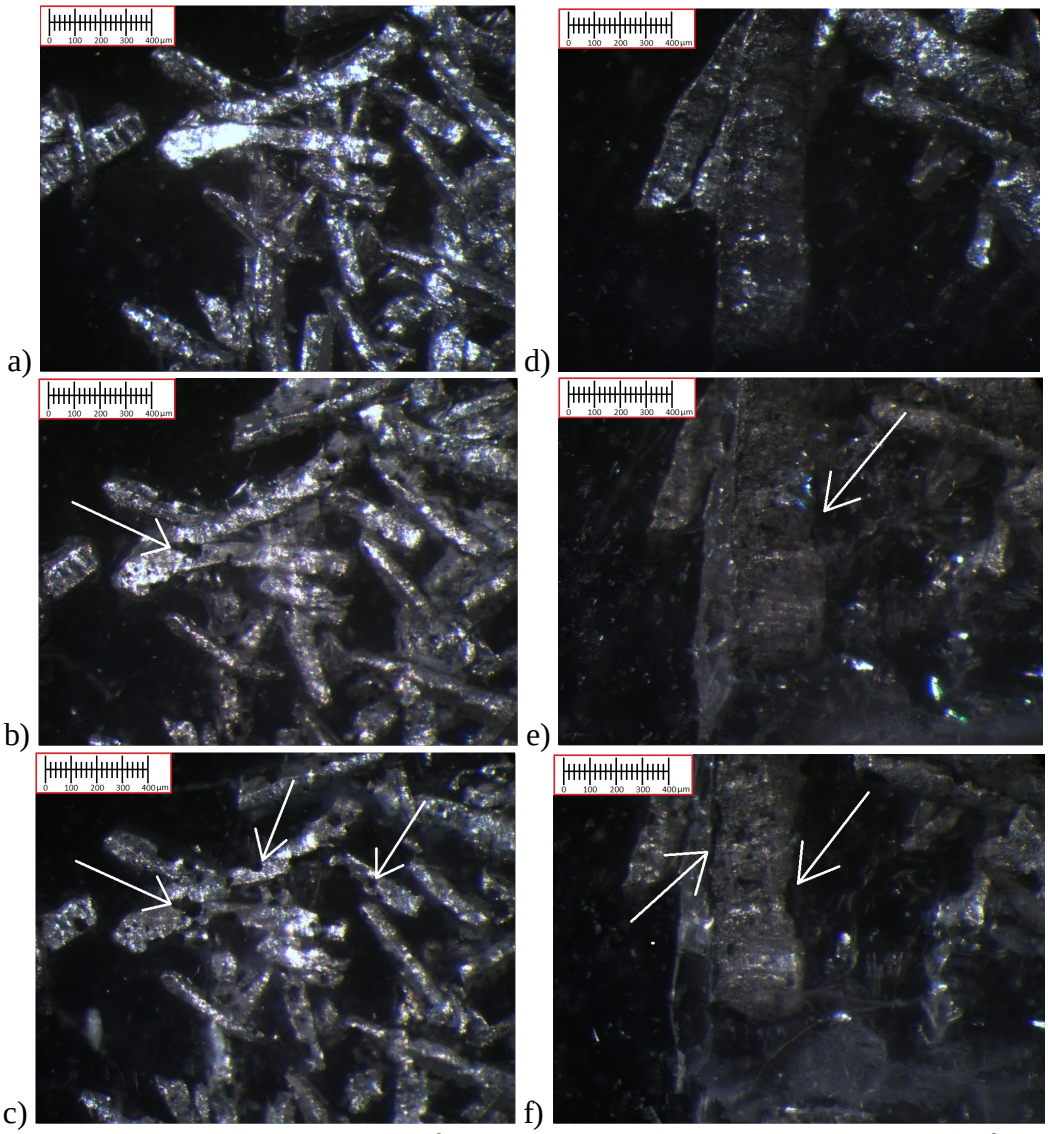

Figure 27. Degradation images of composite samples. a) Mg-PLDLA-e 4 before immersion, b) Mg-PLDLA-e 4 after 190 h, c) Mg-PLDLA-e 4 after 672 h, d) Mg-PLDLA-s 5 before immersion, e) Mg-PLDLA-s 5 after 190 h and f) Mg-PLDLA-s 5 after 672 h. Arrows indicate localized degradation.

The localized corrosion in the areas influenced by the solution is more noticeable in sample Mg-PLDLA-e 4. With Mg-PLDLA-s 5, the corrosion is more uniform due to higher exposure to the buffer solution. The samples were imaged with the same brightness in at a given time. This indicates that the surface of Mg-PLDLA-s 5 has degraded more and lost its shine. The degradation behavior was noticed more in Figure 28. These two locations indicate how the magnesium can degrade if it is directly in contact with the surrounding solution. The degraded area is thought to experience excessive degradation which results to extensive hydrogen release. The hydrogen can cause localized areas where the degradation can happen even faster which can explain the cracks in the materials surface. Additionally, these cracks might be explained by the fact that metal degradation tends to happen more easily in defect areas and in grain boundaries. The cracks later disappear due to the complete corrosion of the surface area.

a) 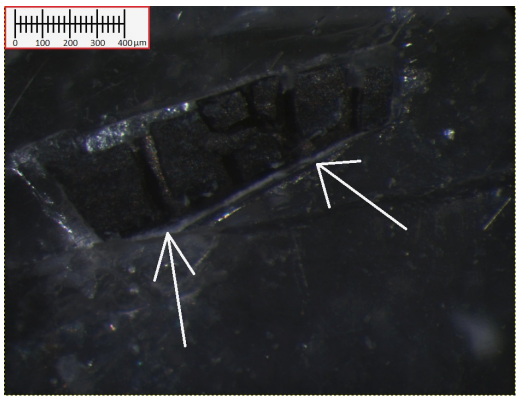 b) 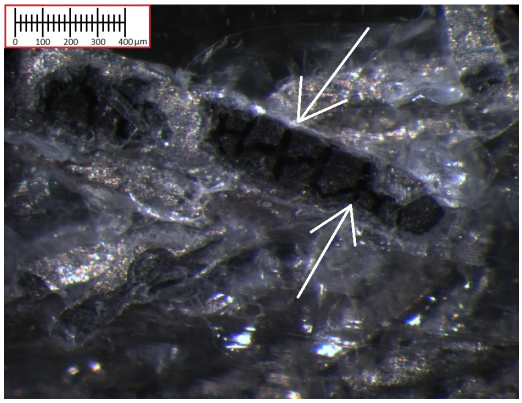

Figure 28. Degradation images of composite samples. a) Image section Mg-PLDLA-e 2 after 190 h and b) Mg-PLDLA-s 5 after 190 h. Arrows indicate localized degradation.

The formation of the phosphate layer can also be noticed through imaging. This layer creates a crystalline structure over the magnesium material. This can be seen in Figures 29, 30 and 31. The layer can be detected by the human eye and can cover the magnesium material completely if given enough time.

a) 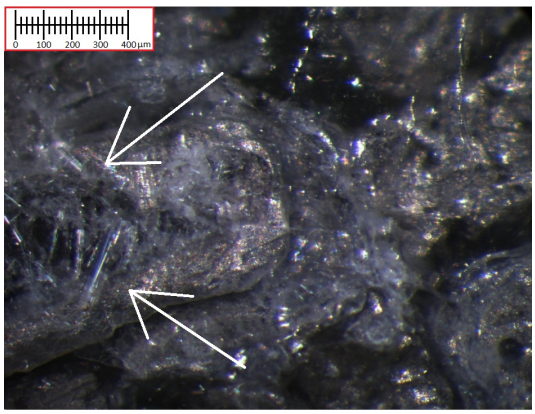 b) 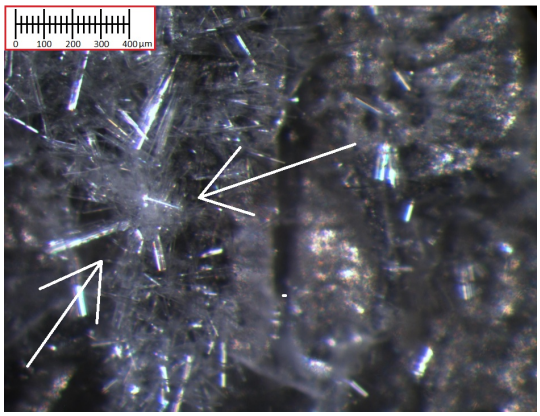

Figure 29. Degradation images of composite samples. a) Image section of Mg-PLDLA-s 1 and b) Mg-PLDLA-s 3 after 190 h. Arrows indicate locations of phosphate layer.

The phosphate layer can form around the material in a few days and continues to form until it covers it completely. After the layer has covered the material, it does not grow larger in a way that it could be noticed through imaging during the testing period.

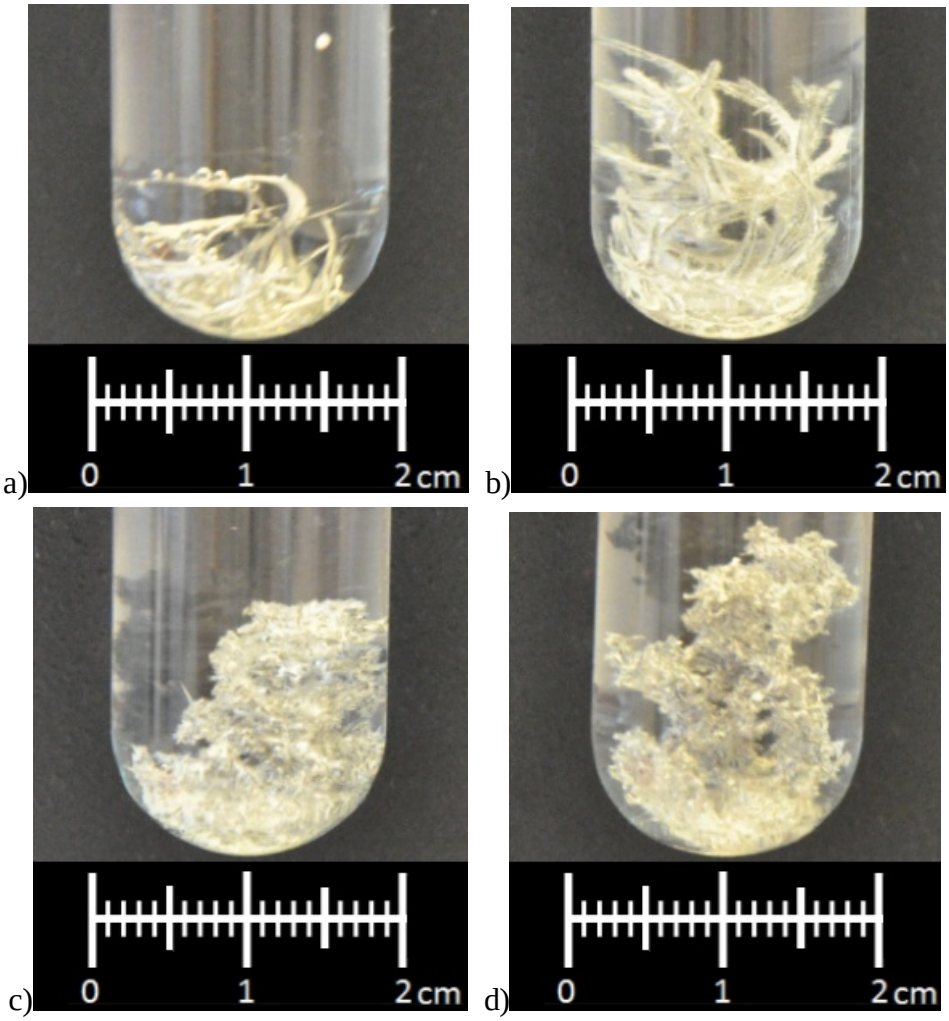

Figure 30. Degradation picture of magnesium samples. a) Mg-Original-water 1 after 144 h, b) Mg-Original 1 after 190 h, c) Mg-1 after 190 h and d) Mg-6 after 190 h.

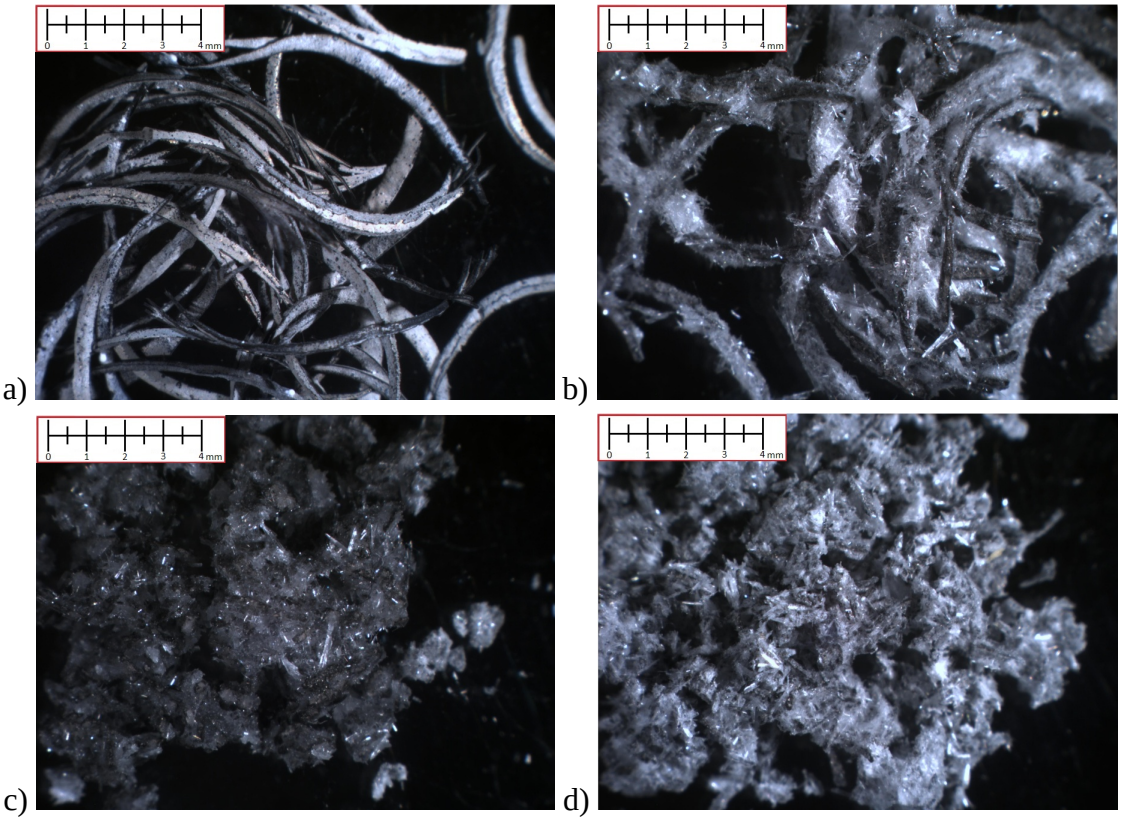

Figure 31. Degradation picture of magnesium samples. a) Mg-Original-water 1 after 624 h, b) Mg-Original 1 after 672 h, c) Mg-1 after 672 h and d) Mg-6 after 672 h. Each sample was dried for a 72h period.

Figures 30 and 31 reveal that the magnesium powder and original pieces in the buffer are formed in different forms compare to the Mg-Original-water 1 sample. This is due to the phosphate layer that covers the samples. During the degradation, the hydrogen release causes the magnesium to move with the hydrogen unless the hydrogen bubbles are shaken away from the material. This movement causes the pieces and the powder to not stay on the bottom of the test tube. As the phosphate layer starts to form during this process, it prevents the magnesium to have a compact form resulting into the shapes seen in the figures. This enables the alloy to have a larger amount surface to be in contact with the solution. This in turn enables a larger phosphate layer formation which can give higher weight results for weigh measurements.

5.6 Discussion

The benefits that can be attained when the corrosion problem of the magnesium material is solved are immense. Creating biodegradable metallic implants that could be used for temporary solutions due their mechanical, structural and production advantages with biocompatibility. The use of such material could mean alternative choices for bone healing products, where the material actually has a very close mechanical property to the bone [69].

Creating biodegradable electrical applications are also a potential side for metallic implants. This aspect could be used for temporary sensors, drug releasing applications that need some control but a specific release site and even applications for temporary tracking devices if needed in certain situations.

To obtain a biodegradable magnesium material, a few solutions have been presented. Improving the material purity is one but generally results in the lowering of mechanical properties of the material when compared to alloyed options. Increasing the material purity also results to a material that is harder to manufacture to a certain size and shape. For electrical applications, pure magnesium could be used in terms of mechanical properties but the corrosion rate is too high if it is not remedied by coating choices. Alloying has be another way to solve the degradation problem. Biocompatibility has been a problem though. The complexity of choosing a suitable alloying element for magnesium alloys has been difficult. All of the possibilities, advantages and disadvantages of the material have caused the recent interest for further study.

The metal combination in the practical study was considered to be created due to improving the corrosion resistance of the material and its machinability, without compromising the materials biocompatibility. The material amounts in the alloy stay in the limits of alloying with magnesium. The material amount provided for testing was 6 grams of the alloy from the supplier. The low amount of material created difficulties for preparation and testing. This meant that careful preparation was necessary without having too large material losses.

The shape of the alloy resulted to the need of forming the alloy to a different shape for testing. The usual form for degradation and other tests are either solid known size pieces or powders. With metals, melting the material and then solidifying it to a solid piece is a possibility. This would then be grinded to a powder if there is a need to it. For alloys, melting is not an option unless the alloying process for the metal material is known. Knowing the process and the steps would enable the replication of the alloy when creating the solid pieces. This information was not known for this research. Due to this, options were limited to cutting and grinding the alloy to a powder form as the original piece shape was more difficult to use for composite forming.

Powder forming with this material type was challenging due to the shape of the material and the mechanical strengths that it holds. The pieces are small and difficult to handle. The mechanical properties prevented the use of different types of mill equipment in the university. Ball mill equipment that uses hammering of the material to smaller pieces would increase the mechanical strength of the alloy due to metal hardening. Cutting mills did not work due to small amount of alloy and the shape of the material resulted it to stick to walls of the equipment. Additionally, the purity of the equipment was a consideration for later testing in mind. Lowering the properties with liquid nitrogen was tested unsuccessfully due to the alloy having too large resistance to forces even in lowered temperatures. Grinding the alloy with a single file that is used in some studies was difficult due to the shape of the material.

Cutting the material with utility knife was time consuming. This kind of method is not recommended with large material amounts. Preventing material loss is also difficult as it gets easily flown due to high forces of the method. The other method that used two files created various particle shapes due to material breaking. The method is slightly faster than cutting but still time consuming. Using the two files method also causes the files to grind each other which releases file material to the powder. This material needs to be removed. One way to do this is by using magnets as the file material is highly magnetic. The file material is possible to be removed from the powder with magnets but there is some material loss as parts of the alloy is magnetic due to the alloy metal additions. Completely removing the file material from the powder material is difficult, though, which takes time and may not be complete due to small sizes of the powder.

The overall material amount at the start of the particle formation was 4.829 g which resulted into about 1.023 g of material loss. Decision to use less than the full amount of material at hand was made so that the rest could be used for various testing purposes to save the powder material until the final methods for testing were decided. The material amounts indicate that the preparation methods are not optimal as one fifth of the material is lost due to various problems of the methods.

The polymer used for composites has a degradation tendency towards bulk degradation. The degradation, though, can change towards surface degradation due to the presence of $Mg(OH)_2$ which stabilizes the poly(L-lactide) structure through neutralization of the acid microclimate pH of the polymer, according to Mobedi et.al. [50]. Degradation rate is also lowered in this case if the pH of the polymer and the surrounding solution stay in neutral range. Higher pH increases the degradation rate of the polymer. The goal of using the polymer was to observe the influence of the surrounding polymer to the magnesium alloy's degradation rate.

Both materials were provided in plastic bags or containers. This was determined to be a preferred method of storing these materials, at least in the case of magnesium. This is due to the alloy material's susceptibility to static electrical forces. These forces cause the alloy to stick to the plastic bag or any surface that cannot discharge the material. Handling of the alloy was thus done with metallic or glass based materials.

During the composite forming, the magnesium ratio to the polymer amount was difficult to keep the same. This resulted to the large amount of magnesium towards the polymer amount in samples Mg-PLDLA-s 1, Mg-PLDLA-s 2 and Mg-PLDLA-s 3 when compared to the other samples. Due to the irregular magnesium amounts, the test results are not completely accurate for proper test results.

The hydrolysis test could not be done in a heating oven in this study as the samples released hydrogen that might cause problems to other samples or the equipment. The testing period for the study was determined due to interest in the first month of magnesium degradation as other studies have focused more on the long periods of hydrolysis tests that are the more common and appropriate ways of doing these tests.

Test results indicated that the polymer can lower the degradation rate of the magnesium alloy. Degradation difference between de-ionized water and buffer solution

reaction was also noticeable with the results. The formation of a phosphate layer was noticed and indicated that the layer prevents further degradation of the magnesium material. With composite samples, the phosphate layers formation is not complete for the whole alloy or composite. The reason is that the whole magnesium alloy amount in the composite sample is not completely in touch with the buffer solution. This enabled the pH of the surrounding buffer solution to rise as more of the alloy becomes in touch with the buffer. These results indicate that a coating can be used to limit the rate of the magnesium degradation. The degradation type and rate of polymer is thus important to obtain a low enough degradation rate for magnesium metal.

6 CONCLUSION

Magnesium is a very promising material according to the research done in the medical field. The degradation problem of the metal has been studied for over one hundred years now. Several methods have been suggested to either improve the material itself through improving its pureness, alloying the material with other metals or through coating the material. Each method provides a different way for the same problem. The most promising way to combat this property is through alloying and coating of the material. Alloying can improve the degradation resistance of the metal and improve the mechanical properties of it. Coatings, on the other hand, delay the degradation process of the material and can enable small amounts of the metal to degrade at a given time if chosen correctly. Literature review section resulted that releasing the degradation information should be done with different values. Reviews should use hydrogen release method if possible because of the formation of $Mg(OH)_2$ and phosphate layers. These layers can give false reading to the amount of degraded magnesium if they are not removed with appropriate solutions like mild acids. Mass loss results can be thus used if done properly.

The practical work reported that the Mg-10Gd-1Nd-1Zn magnesium alloy in testing is reactive as other magnesium alloys in a solution environment. This alloy was coated with a PLDLA 50:50 coating that slowed the degradation rate of the material when compared to magnesium samples. Additionally, the buffer had a significant effect to the pH development of the solutions when compared to de-ionized water samples. The buffer solution also enabled the magnesium material to gain a phosphate layer that covered it almost completely after 600 hours.

The tests results indicate potential for the alloy and for the composite type in question. Further studies would be needed for this alloy type to determine if it is suitable for implant solution or if it is too fast to degrade. Longer period of hydrolysis test is also needed with these test to see how long does it take for the material to start degrading more completely with composite samples. Additionally, cytotoxicity tests are needed to determine if the alloy still retains the biocompatibility of the magnesium metal. The hydrogen release effect on cells around the composite samples needs to be also tested if the degradation rate is suitable. To obtain proper hydrogen and mass release data about this material also means that the materials samples need to have a fixed size that is known and which can be related to the common ($ml/cm^2/day$) way of informing the hydrogen release rate.

The conductivity tests, additionally, resulted that the material form was not suitable for these kinds of tests. This indicates that multiple samples of same length and diameter are needed to make proper estimates about the materials conductivity values. Recent studies have concentrated on this property of the material. There can be a huge potential of creating a conductive magnesium product that could replace some of the

existing implants in the market. If there is a way to create a biocompatible solution for a biodegradable and electrically conductive implant, then a new section of applications can emerge.

The sample preparation work indicated that the methods for powder forming in the practical work were very inefficient and time consuming. These methods are not recommended when testing these irregular types of pieces unless one can find an easy and safe way to make the material in to a powder or melt it to a solid material piece.

7 REFERENCES

[1] Altun, H. and Sen, S. 2004. Studies on the influence of chloride ion concentration and pH on the corrosion and electrochemical behavior of AZ63 magnesium alloy. Materials and Design 25, pp.637-643.

[2] Andrews, E.W. 1917. Absorbable metal clips as substitutes for ligature in wound closure. JAMA 28, pp.278-281.

[3] ASTM F138-08. 2008. Standard Specification for Wrought 18 Chromium-14 Nickel-2.5 Molybdenum Stainless Steel Bar and Wire for Surgical Implants; ASTM International: West Conshohocken, PA, USA, doi: 10.1520/F0138-08.

[4] Atrens, A., Liu, M., and Abidin, N.I.Z. 2011. Corrosion mechanism applicable to biodegradable implants. Materials Science and Engineering B 176, pp.1609-1636.

[5] Aung, N.N. and Zhou, W. 2010. Effect of grain size and twins on corrosion behavior of AZ31B magnesium alloy. Corrosion Science 52, pp.589-594.

[6] Avedesian, M.M. and Baker, H. 1999. Magnesium and Magnesium Alloys. ASM International. The Materials Information Society. ISBN-13: 978-0871706577.

[7] Bonora, P.L., Andrei, M., Eliezer, A. and Gutman, E.M. 2002. Corrosion behaviour of stressed magnesium alloys. Corrosion Science 44, pp.729-749.

[8] Chowdhury, A. and Kumar, J. 2006. Morphology, surface topography and optical studies on electron beam evaporated MgO thin films. Bulletin of Material Science 29, 5, pp. 513-521.

[9] Conductivity and Resistivity Value for Aluminum & Alloys. NDT Resource Center http://www.ndt-ed.org/GeneralResources/MaterialProperties/ET/et_matlprop_index.htm, Referred at 24.09.2013.

[10] Conductivity and Resistivity Value for Copper & Alloys. NDT Resource Center http://www.ndt-ed.org/GeneralResources/MaterialProperties/ET/et_matlprop_index.htm, Referred at 24.09.2013.

[11] Conductivity and Resistivity Value for Iron & Alloys. NDT Resource Center http://www.ndt-ed.org/GeneralResources/MaterialProperties/ET/et_matlprop_index.htm, Referred at 24.09.2013.

[12] Conductivity and Resistivity Value for Magnesium & Alloys. NDT Resource Center http://www.ndt-ed.org/GeneralResources/MaterialProperties/ET/et_matlprop_index.htm, Referred at 24.09.2013.

[13] Conductivity and Resistivity Value for Titanium & Alloys. NDT Resource Center http://www.ndt-ed.org/GeneralResources/MaterialProperties/ET/et_matlprop_index.htm, Referred at 24.09.2013.

[14] Davis, J.R. 2003. Handbook of Materials for Medical Devices. ASM International. The Materials Information Society.

[15] El-Rahman SSA. 2003. Neuropathology of aluminum toxicity in rats (glutamate and GABA impairment). Pharmacological Research 47, 3, pp.189–194.

[16] Feyerabend, F., Drücker, H., Laipple, D., Vogt, C., Stekker, M., Hort, N. and Willumeit, R. 2012. Ion release from magnesium materials in physiological solutions under different oxygen tension. Journal of Materials Science: Materials in Medicine 23, pp.9-24.

[17] Fontenier, G., Freschard, R. and Mourot, M. 1975. Study of the corrosion in vitro and in vivo of magnesium amodes involved in an implantable bioelectric battery. Medical and Biological Engineering 13, 5, pp.683–689.

[18] Friedrich, H.E. & Mordike, B.L. 2006. Magnesium Technology: Metallurgy, Design Data, Applications. Springer, ISBN-13: 978-3-540-20599-3.

[19] Glass, E. 1926. Klinische und experimentelle Untersuchungen über die Payrsche Magnesiumpfeilbehandlung von Angiomen. Deut. Z. Chir. 194, 5–6, pp.352–366.

[20] Gray, J.E. and Luan, B. 2002. Protective coatings on magnesium and its alloys – a critical review. Journal of Alloys and Compounds 336, pp.88-113.

[21] Gu, X., Zheng, Y., Cheng, Y., Zhong, S. and Xi, T. 2009. In vitro corrosion and biocompatibility of binary magnesium alloys. Biomaterials 30, pp.484-498.

[22] Guan, R.G., Cipriano, A.F., Zhao, Z.Y., Lock, J., Tie, D., Zhao, T., Cui, T. and Liu, H. 2013. Development and evaluation of a magnesium-zinc-strontium alloy for biomedical applications - Alloy processing, microstructure, mechanical properties, and biodegradation. Materials Science and Engineering C: Materials for Biological Applications 33, 7, pp.3661-3669.

[23] Gupta, M. and Sharon, N.M.L. 2010. Magnesium, Magnesium alloys and Magnesium Composites. Wiley, ISBN-13: 978-0-470-49417-2.

[24] He, W., Zhang, E. and Yang, K. 2010. Effect of Y on the bio-corrosion behaviour of extruded Mg-Zn-Mn alloy in Hanks solution. Materials Science and Engineering C 30, pp.167-174.

[25] Hermawan, H., Dubé, D. and Mantovani, D. 2007a. Development of degradable Fe-35Mn alloy for biomedical applications. Advanced Material Research 15, pp.107-112.

[26] Hermawan, H., Moravej, M., Dubé, D., Fiset, M. and Mantovani, D. 2007b. Degradation behaviour of metallic biomaterials for degradable stents. Advanced Material Research 15-17, pp.113-118.

[27] Hermawan, H., Dubé, D. and Mantovani, D. 2010a. Developments in metallic biodegradable stents. Acta Biomaterialia 6, pp.1693-1697.

[28] Hermawan, H., Purnama, A., Dubé, D., Couet, J. and Mantovani, D. 2010b. Fe-Mn alloys for metallic biodegradable stents: Degradation and cell viability studies. Acta Biomaterialia 6, pp.1852-1860.

[29] Hornberger, H., Virtanen, S. and Boccaccini, A.R. 2012. Biomedical coatings on magesium alloys - A review. Acta Biomaterialia 8, pp.2442–2455.

[30] Hort, N., Huang, Y., Fechner, D., Störmer, M., Blawert, C., Witte, F., Vogt, C., Drücker, H., Willumeit, R., Kainer, K.U. and Feyerabend, F. 2010. Magnesium alloys as implant materials – Principles of property design for Mg-RE alloys. Acta biomaterialia 6, pp.1714-1725.

[31] Hwang, S.-W., Tao, H. Kim, D.-H., Cheng, H., Song, J.-K., Rill, E., Brenckle, M.A., Panilaitis, B., Won, S.M., Kim, Y.-S., Song, Y.M., Yu, K.J., Ameen, A., Li, R., Su, Y., Yang, M., Kaplan, D.L., Zakin, M.R., Slepian, M.J., Huang, Y., Omenetto, F.G. and Rogers J.A. 2012. A Physically Transient Form of Silicon Electronics. Science 337, 6102, pp.1640-1644.

[32] Höpfner, E. 1903. Ueber Gefässnaht, Gefässtransplantation und Replantation von amputirten Extremitäten. Arch. Klin. Chir. 70, pp.417-471.

[33] Ibasco, S., Tamimi, F., Meszaros, R., Nihouannen, D.L., Vengallatore, S., Harvey, E. and Barralet, J.E. 2009. Magnesium-sputtered titanium for the formation of bioactive coatings. Acta Biomaterialia 5, pp.2338-2347.

[34] Ishizaki, T., Kudo, R., Omi, T., Tenshima, K., Sonoda, T., Shigematsu, I. and Sakamoto, M. 2012. Magnesium hydroxide/magnesium phosphate compounds composite coating for corrosion protection of magnesium alloy by a combination process of chemical conversion and steam curing. Materials Letters 68, pp.122-125.

[35] Jia-Cheng, G., Sha, W., Li-Ying, Q. and Yong, W. 2008. Corrosion behavior of Mg and Mg-Zn alloys in simulated body fluid. Transactions of Nonferrous Metals Socciety China 18, pp.588-592.

[36] Johnson, I. and Liu, H. 2013. A Study on Factors Affecting the Degradation of Magnesium and a Magnesium-Yttrium Alloy for Biomedical Applications. PLoS One 14, 8, e65603. doi: 10.1371/journal.pone.0065603

[37] Ku, C.-H., Pioletti, D.P., Browne, M. and Gregson, P.J. 2002. Effect of different Ti–6Al–4V surface treatments on osteoblasts behaviour. Biomaterials 23, 6, pp.1447–1454.

[38] Lambotte, A. 1909. Technique et indications de la prothèse perdue dans la traitement des fractures. Presse. Med. Belge. 17, pp.321–323.

[39] Lambotte, A. 1923. L'utilisation du magnésium comme matériel perdu dans l'ostéosynthèse. Bull. Mém. Soc. Nat. Cir. 28, pp.1325–1334.

[40] Lespinasse, V.D. 1910. A practical mechanical method of end-to-end anastomosis of blood-vessels: using absorbable magnesium rings. JAMA 55, pp.1785-1790.

[41] Li, N. and Zheng, Y. 2013. Novel Magnesium Alloys Developed for Biomedical Application: A Review. Journal of Materials Science Technology 29, 6, pp.489-502.

[42] Li, Z., Gu, X., Lou, S. and Zheng, Y. 2008. The development of binary Mg-Ca alloys for use as biodegradable materials within bone. Biomaterials 29, pp.1329-1344.

[43] Liu, B., Zheng, Y. and Ruan, L. 2010. In vitro investigation of Fe30Mn6Si shape memory alloys as potential biodegradable metallic material. Material Letters 65, pp.540-543.

[44] Liu, M., Schmutz, P., Uggowitzer, P.J., Song, G. and Atrens, A. 2010. The influence of yttrium (Y) on the corrosion of Mg-Y binary alloys. Corrosion Science 52, pp.3687-3701.

[45] Material properties of Gadolinium. http://www.goodfellow.com/E/Gadolinium.html. Referred at 26.09.2013.

[46] Material properties of Neodymium. http://www.goodfellow.com/E/Neodymium.html. Referred at 26.09.2013.

[47] Material properties of Magnesium. http://www.goodfellow.com/E/Magnesium.html. Referred at 26.09.2013.

[48] Material properties of Zinc. http://www.goodfellow.com/E/Zinc.html. Referred at 26.09.2013.

[49] McBride, E.D. 1938. Magnesium screw and nail transfixion in fractures. Southern Medical Journal 31, 5, pp.508–515.

[50] Mobedi, H., Nekoomanesh, M., Orafaei, H. and Mivehchi, H. 2006. Studying the Degradation of Poly(L-lactide) in Presence of Magnesium Hydroxide. Iranian Polymer Journal 15, 1, pp.31-39.

[51] Moravej, M. and Mantovani, D. 2011. Biodegradable Metals for Cardiovascular Stent Application: Interests and New Opportunities. International Journal of Molecular Sciences 12, pp.4250-4270.

[52] Nicole, R. 1947. Metallschädigung bei Osteosynthesen. Hel. Chir. Acta 14, Suppl.III 2, pp.3–74.

[53] Niinomi, M. 2010. Metals for biomedical devices. Woodhead Publshing Series in Biomaterials, No.25, March. ISBN-13: 978 1 84569 434 0.

[54] Nogara, G. 1939. Sulla tolleranza dell' osso verso i metalli riassorbibili magnesio ed electron. Arch. Ital. Chir. 56, 5, pp.459–478.

[55] Payr, E. 1902. Ueber Verwendung von Magnesium zur Behandlung von Blutgefässerkrankungen. Deut. Z. Chir. 63, pp.503-511.

[56] Payr, E. 1903. Zur Technik der Behandlung kavernöser Tumoren. Zentralblatt Chir. 30, pp.233–234.

[57] Pilliar, R.M. 2009. Biomedical Materials - Chapter 2: Metallic Biomaterials. Springer, XXIV, 556p. 100 illus, Hardcover. ISBN: 978-0-387-84871-6.

[58] Qu, Q., Ma, J., Wang, L., Li, L., Bai, W. and Ding, Z. 2011. Corrosion behaviour of AZ31B magnesium alloy in NaCl solutions saturated with CO2. Corrosion Science 53, pp.1186-1193.

[59] Quach, N.-C., Uggowitzer, P.J. and Schmutz, P. 2008. Corrosion behaviour of an Mg-Y-RE alloy used in biomedical applications studied by electrochemical techniques. Comptes Rendus Chimie 11, pp.1043-1054.

[60] Rousselle, A.V., Heymann, D., Demais, V., Charrier, C., Passuti, N. and Basle, M.F. 2002. Influence of metal ion solutions on rabbit osteoclast activities in vitro. Histology and Histopathology 17, 4, pp.1025–32.

[61] Salahshoor, M. and Guo, Y.B. 2013. Process mechanics in ball burnishing biomedical magnesium-calcium alloy. International Journal of Advanced Manufacturing Technology 64, pp.133-144.

[62] Schinhammer, M., Hanzi, A.C., Loffler, J.F. and Uggowitzer, P.J. 2010. Design strategy for biodegradable Fe-based alloys for medical applications. Acta Biomaterials 6, pp.1705-1713.

[63] Sebaa M.A., Dhillon S. and Liu H. 2013. Electrochemical deposition and evaluation of electrically conductive polymer coating on biodegradable magnesium implants for neural applications. Journal of Materials Science: Materials in Medicine 24, 2, pp.307-316.

[64] Shadanbaz S., Walker J., Staiger M.P., Dias G.J. and Pietak A. 2013. Growth of calcium phosphates on magnesium substrates for corrosion control in biomedical applications via immersion techniques. Journal of Biomedical Materials Research B: Applied Biomaterials 101, 1, pp.162-172.

[65] Shi, Z., Song, G. and Atrens, A. 2006. The corrosion performance of anodized magnesium alloys. Corrosion Science 48, pp.3531-3546.

[66] Shih, T.-S. and Liu, I.-B. 2006. Thermally-Formed Oxide on Aluminum and Magnesium. Materials Transactions 47, 5, pp.1347-1353.

[67] Shingde, M., Pamphlett, R., Hughes, J., Boadle, R. and Wills, E.J. 2005. Macrophagic myofasciitis associated with vaccine-derived aluminium. Medical Journal of Australia 183, 3, pp.145-146.

[68] Song, G. 2007. Control of biodegradation of biocompatible magnesium alloys. Corrosion Science 49, pp.1696–1701.

[69] Staigera, M.P., Pietaka, A.M., Huadmaia, J., Diasb, G. 2006. Magnesium and its alloys as orthopedic biomaterials: A review. Biomaterials 27, pp.1728–1734.

[70] Sun, H.-F., Li, C.-J. and Fang, W.-B. 2011. Corrosion behavior of extrusion-drawn pure Mg wire immersed in simulated body fluid. Transactions of Nonferrous Metals Society of China 21, pp.258-261.

[71] Sun, Y., Zhang, B., Wang, Y., Geng, L. and Jiao, X. 2012. Preparation and characterization of a new biomedical Mg-Zn-Ca alloy. Materials and Design 34, pp.58-64.

[72] Tang, H., Xin, T. and Wang, F. 2013. Calcium Phosphate/Titania Sol-Gel Coatings on AZ31 Magnesium Alloy for Biomedical Applications. International Journal of Electrochemical Science 8, pp.8115-8125.

[73] The International Annealed Copper Standard. NDT Resource Center http://www.ndt-ed.org/GeneralResources/IACS/IACS.htm. Referred at 26.09.2013.

[74] Verbrugge, J. 1937. L'utilisation du magnésium dans le traitement chirurgical des fractures. Bull Mém Soc Nat Cir. 59, pp.813–823.

[75] Wang, H., Estrin, Y. and Zúberová, Z. 2008. Bio-corrosion of a magnesium alloy with different processing histories. Materials Letters 62, pp.2476–2479.

[76] Wang, Y., Wei, M., Gao, J., Hu, J. and Zhang, Y. 2008. Corrosion process of pure magnesium in simulated body fluid. Materials Letters 62, pp.2181–2184.

[77] Westengen, H. Magnesium alloys. Encyclopedia of Materials: Science and Technology, ISBN: 0-08-0431526, pp.4739-4754.

[78] Wexler, B.C. 1980. Patholophysiologic responses of spontaneously hypertensive rats to arterial magnesium-aluminum wire implants. Atherosclerosis 36, 4, pp.575-587.

[79] Wilflingseder, P., Martin, R. and Papp, C. 1981. Magnesium seeds in the treatment of lymph- and haemangiomata. Chir. Plastica 6, pp.105–116.

[80] Witecka, A., Yamamoto, A., Dybiec, H. and Swieszkowski, W. 2012. Surface characterization and cytocompatibility evaluation of silanized magnesium alloy AZ91 for biomedical applications. Science and Technology of Advanced Materials 13, 064214, 6pp.

[81] Witte, F., Kaese, V., Haferkamp, H., Switzer, E., Meyer-Lindenberg, A., Wirth, C.J. and Windhagen, H. 2005. In vivo corrosion of four magnesium alloys and the associated bone response. Biomaterials 26, pp.3557–3563.

[82] Witte, F., Fischer, J., Nellesen, J., Crostack, H.-A., Kaese, V., Pisch, A., Beckmann, F. and Windhagen, H. 2006. In vitro and in vivo corrosion measurements of magnesium alloys. Biomaterials 27, pp.1013-1018.

[83] Witte, F., Feyerabend, F., Maier, P., Fischer, J., Störmer, M., Blawert, C., Dietzel, W. and Hort, N. 2007. Biodegradable magnesium-hydroxyapatite metal matrix composites. Biomaterials 28, pp.2163-6174.

[84] Witte, F., Hort, N., Vogt, C., Cohen, S., Kainer, K.U., Willumeit, R. and Feyerabend, F. 2008. Degradable biomaterials based on magnesium corrosion. Current Opinion in solid State and Materials Science 12, pp.63-72.

[85] Witte, F. 2010. The history of biodegradable magnesium implants: A review. Acta Biomaterialia 6, pp.1680–1692.

[86] Wong, H.M., Yeung, K.W.K., Lam, K.O., Tam, V., Chu, P.K, Luk, K.D.K. and Cheung, K.M.C. 2010. A biodegradable polymer-based coating to control the performance of magnesium alloy orthopaedic implants. Biomaterials 31, pp.2084-2096.

[87] Wu, G., Dai, W., Song, L. and Wang, A. 2010. Surface microstructurization of a sputtered magnesium thin film via a solution-immersion route. Materials Letters 64, pp.475-478.

[88] Xin, Y., Hu, T. and Chu, P.K. 2011a. In vitro studies of biomedical magnesium alloys in a simulated physiological environment: A review. Acta Biomaterialia 7, pp.1455-1459.

[89] Xin, Y., Hub, T. and Chu, P.K. 2011b. Degradation behavior of pure magnesium in simulated body fluids with different concentrations of HCO^-_3. Corrosion Science 53, pp.1522-1528.

[90] Xu, L. & Yamamoto, A. 2012. In vitro degradation of biodegradable polymer-coated magnesium under cell culture condition. Applied Surface Science 258, pp.6353-6358.

[91] Xu, R., Wu, G., Yang, X., Zhang, X., Wu, Z., Sun, G., Li, G. and Chu, P.K. 2012. Corrosion behavior of chromium and oxygen plasma-modified magnesium in sulfate solution and simulated body fluid. Applied Surface Science 258, pp.8273-8278.

[92] Yang, J., Cui, F.-C., Lee, I.S. and Wang, X. 2010. Plasma surface modification of magnesium alloy for biomedical application. Surface & Coating Technology 205, pp.S182-S187.

[93] Yang, L., Hort, N., Willumeit, R. and Feyerabend, F. 2012. Effects of corrosion environment and proteins on magnesium corrosion. Corrosion Engineering, Science and Technology 47, 5, pp.335-339.

[94] Yu, X., Ning, Z., Hua, M., Wang, C. and Cui, F. 2013. Mechanical and biomedical properties of copper-containing diamond-like carbon films on magnesium alloys. Journal of Materials Chemistry B, 1, pp.4773-4780.

[95] Yun, Y.H., Dong, Z., Lee, N., Liu, Y., Xue, D., Guo, X., Kuhlmann, J., Doepke, A., Halsall, H.B., Heineman, W., Sundaramurthy, S., Schulz, M.J., Yin, Z., Shanov, V., Hurd, D., Nagy, P., Li, W. and Fox, C. 2009a. Revolutionizing biodegradable metals. Materials Today 12, 10.

[96] Yun, Y.H., Dong, Z., Yang, D., Schulz, M.J., Shanov, V.N., Yarmolenko, S., Xu, Z., Kumta, P. and Sfeir, C. 2009b. Biodegradable Mg corrosion and osteoblast cell culture studies. Materials Science and Engineering C 29, pp.1814–1821.

[97] Zeng, R.-C., Zhang, J., Huang, W.-J., Dietzel, W., Kainer, K.U., Blawert, C., and Wei, K. 2006. Review of studies on corrosion of magnesium alloys. Transactions of Nonferrous Metals Society of China 16, pp.763-771.

[98] Zhang, E., Yin, D., Xu, L., Yang, L. and Yang, K. 2009. Microstructure, mechanical and corrosion properties and biocompatibility of Mg-Zn-Mn alloys for biomedical application. Materials Science and Engineering C 29, pp.987-993.

[99] Zhang, S., Zhang, X., Zhao, C., Li, J., Song, Y., Xie, C., Tao, H., Zhang, Y., He, Y., Jiang, Y. and Bian, Y. 2010. Research on an Mg-Zn alloy as a degradable biomaterial. Acta Biomaterialia 6, pp.626-640.

[100] Zhang, W., Li, M., Chen, Q., Hu, W., Zhang, W. and Xin, W. 2012. Effects of Sr and Sn on microstructure and corrosion resistance of Mg-Zr-Ca magnesium alloy for biomedical applications. Materials and Design 39, pp.379-383.

[101] Zhao, Y., Wu, G., Jiang, J., Wong, H.M., Yeung, K.W.K. and Chu, P.K. 2012. Improved corrosion resistance and cytocompatibility of magnesium alloy by two-stage cooling in thermal treatment. Corrosion Science 59, pp.360-365.

[102] Zheng, Y.F., Gu, X.N., Xi, Y.L. and Chai, D.L. 2010. In vitro degradation and cytotoxicity of Mg/Ca composites produced by powder metallurgy. Acta Biomaterialia 6, pp.1783-1791.

[103] Zhou, W., Shen, T. and Aung, N.N. 2010. Effect of heat treatment on corrosion behaviour of magnesium alloy AZ91D in simulated body fluid. Corrosion Science 52, pp.1035-1041.

[104] Zierold, A.A. 1924. Reaction of bone to various metals. Archives of Surgery 9, 2, pp.365–412.

APPENDIX I/IV

pH measurement results

Time (h)	0	3	24	27	48	51	72	75	96	99	168
Sample:											
Mg-PLDLA-s 1	7.48	7.51	7.55	7.57	7.67	7.67	7.71	7.70	7.76	7.75	7.86
Mg-PLDLA-s 2	7.48	7.51	7.50	7.54	7.59	7.61	7.62	7.61	7.66	7.66	7.74
Mg-PLDLA-s 3	7.48	7.53	7.60	7.62	7.74	7.75	7.82	7.83	7.87	7.89	7.97
Mg-PLDLA-s 4	7.48	7.49	7.50	7.53	7.60	7.61	7.61	7.63	7.66	7.68	7.75
Mg-PLDLA-s 5	7.48	7.49	7.50	7.51	7.58	7.59	7.62	7.61	7.64	7.66	7.72
Mg-PLDLA-s 6	7.48	7.51	7.55	7.56	7.64	7.65	7.68	7.68	7.70	7.71	7.78
Mg-PLDLA-e 1	7.48	7.52	7.47	7.48	7.52	7.51	7.52	7.54	7.51	7.53	7.52
Mg-PLDLA-e 2	7.48	7.51	7.46	7.49	7.51	7.51	7.53	7.53	7.50	7.52	7.51
Mg-PLDLA-e 3	7.48	7.51	7.47	7.47	7.52	7.51	7.51	7.51	7.50	7.53	7.52
Mg-PLDLA-e 4	7.48	7.50	7.49	7.49	7.54	7.56	7.58	7.56	7.57	7.59	7.60
PLDLA-s 1	7.48	7.50	7.47	7.46	7.50	7.51	7.50	7.49	7.49	7.49	7.49
PLDLA-s 2	7.48	7.50	7.47	7.47	7.50	7.50	7.49	7.51	7.49	7.48	7.51
PLDLA-s 3	7.48	7.53	7.48	7.47	7.51	7.50	7.54	7.49	7.50	7.51	7.48
PLDLA-e 1	7.48	7.51	7.48	7.49	7.49	7.52	7.53	7.49	7.51	7.51	7.49
PLDLA-e 2	7.48	7.51	7.48	7.50	7.49	7.52	7.50	7.52	7.50	7.51	7.48
PLDLA-e 3	7.48	7.52	7.48	7.46	7.49	7.50	7.51	7.49	7.49	7.49	7.49
Mg-1	7.48	7.75	8.12	8.16	8.41	8.40	8.55	8.53	8.65	8.61	8.87
Mg-2	7.48	7.75	8.16	8.21	8.46	8.47	8.64	8.62	8.75	8.72	8.97
Mg-3	7.48	7.71	8.02	8.03	8.17	8.18	8.26	8.25	8.28	8.28	8.35
Mg-4	7.48	7.83	8.27	8.28	8.44	8.46	8.56	8.56	8.61	8.62	8.76
Mg-5	7.48	7.94	8.40	8.41	8.58	8.56	8.70	8.69	8.74	8.75	8.94
Mg-6	7.48	8.05	8.44	8.54	8.81	8.70	8.81	8.81	8.90	8.91	9.25
Mg-Original 1	7.48	7.82	8.27	8.29	8.40	8.40	8.46	8.44	8.48	8.49	8.60
Mg-Original 2	7.48	7.86	8.38	8.40	8.53	8.55	8.62	8.62	8.68	8.69	8.84
Time (h)	0	3	24	27	48	51	120	123	144	144	144.5
Sample:											
Mg-Original-water 1	6.26	9.90	10.66	10.58	10.54	10.50	10.31	10.27	10.15	6.29	9.36
Mg-Original-water 2										6.28	9.82

APPENDIX II/IV

pH measurement results

Time (h)	171	193	216	216	217	218	219	240	243	264	267
Sample:											
Mg-PLDLA-s 1	7.86	7.89	7.93	7.50	7.49	7.50	7.54	7.57	7.58	7.67	7.64
Mg-PLDLA-s 2	7.74	7.75	7.78	-	-	-	7.79	7.79	7.79	7.81	7.80
Mg-PLDLA-s 3	7.98	8.01	8.01	7.50	7.50	7.50	7.54	7.65	7.65	7.77	7.75
Mg-PLDLA-s 4	7.75	7.79	7.82	7.50	7.50	7.49	7.54	7.54	7.53	7.58	7.58
Mg-PLDLA-s 5	7.73	7.75	7.76	-	-	-	7.75	7.79	7.77	7.77	7.78
Mg-PLDLA-s 6	7.76	7.79	7.82	-	-	-	7.80	7.82	7.81	7.82	7.82
Mg-PLDLA-e 1	7.53	7.53	7.53	-	-	-	7.54	7.55	7.54	7.55	7.55
Mg-PLDLA-e 2	7.52	7.53	7.56	-	-	-	7.52	7.53	7.52	7.53	7.53
Mg-PLDLA-e 3	7.53	7.54	7.55	-	-	-	7.54	7.53	7.53	7.54	7.53
Mg-PLDLA-e 4	7.58	7.60	7.64	-	-	-	7.62	7.61	7.61	7.63	7.62
PLDLA-s 1	7.50	7.49	7.48	7.50	7.50	7.48	7.51	7.50	7.49	7.50	7.50
PLDLA-s 2	7.49	7.50	7.50	-	-	-	7.50	7.48	7.47	7.48	7.47
PLDLA-s 3	7.49	7.49	7.49	7.50	7.50	7.49	7.50	7.50	7.49	7.50	7.49
PLDLA-e 1	7.49	7.50	7.49	7.50	7.49	7.49	7.50	7.49	7.49	7.50	7.49
PLDLA-e 2	7.48	7.50	7.49	-	-	-	7.49	7.49	7.47	7.48	7.48
PLDLA-e 3	7.48	7.51	7.49	-	-	-	7.48	7.49	7.48	7.48	7.48
Mg-1	8.85	8.97	8.98	-	-	-	8.97	9.02	8.99	8.99	9.00
Mg-2	8.94	9.03	9.05	7.49	7.49	7.50	7.51	7.55	7.57	7.62	7.62
Mg-3	8.34	8.38	8.39	-	-	-	8.36	8.39	8.35	8.38	8.37
Mg-4	8.76	8.79	8.82	7.50	7.50	7.51	7.52	7.52	7.51	7.58	7.58
Mg-5	8.93	8.98	9.00	-	-	-	8.98	9.02	8.98	9.00	9.00
Mg-6	9.15	9.19	9.22	7.50	7.52	7.51	7.52	7.53	7.54	7.61	7.61
Mg-Original 1	8.60	8.63	8.64	-	-	-	8.63	8.67	8.64	8.63	8.65
Mg-Original 2	8.83	8.87	8.88	7.49	7.51	7.51	7.51	7.51	7.52	7.55	7.55

Time (h)	145	146	168	171	192	195	216	219	288	291	312
Sample:											
Mg-Original-water 1	9.57	9.43	10.06	9.79	9.65	9.80	9.77	9.80	9.50	9.54	9.50
Mg-Original-water 2	10.20	10.39	10.60	10.57	10.38	10.37	10.20	10.19	9.78	9.77	9.77

APPENDIX III/IV

pH measurement results

Time (h)	336	339	360	363	384	408	432	504	528	528	529
Sample:											
Mg-PLDLA-s 1	7.83	7.80	7.81	7.84	7.86	7.90	7.91	7.97	7.99	7.52	7.51
Mg-PLDLA-s 2	7.87	7.85	7.86	7.87	7.88	7.90	7.94	7.94	7.95	-	-
Mg-PLDLA-s 3	7.94	7.93	7.96	7.97	7.98	8.00	8.03	8.02	8.02	7.52	7.51
Mg-PLDLA-s 4	7.70	7.68	7.71	7.70	7.73	7.76	7.79	7.84	7.86	7.52	7.49
Mg-PLDLA-s 5	7.84	7.83	7.84	7.86	7.86	7.87	7.90	7.93	7.91	-	-
Mg-PLDLA-s 6	7.86	7.85	7.86	7.86	7.88	7.88	7.88	7.92	7.92	-	-
Mg-PLDLA-e 1	7.57	7.58	7.56	7.56	7.55	7.58	7.59	7.59	7.61	-	-
Mg-PLDLA-e 2	7.55	7.54	7.55	7.56	7.54	7.56	7.56	7.56	7.57	-	-
Mg-PLDLA-e 3	7.56	7.55	7.55	7.55	7.56	7.58	7.58	7.58	7.59	-	-
Mg-PLDLA-e 4	7.65	7.64	7.64	7.65	7.65	7.66	7.67	7.67	7.68	-	-
PLDLA-s 1	7.50	7.49	7.49	7.49	7.49	7.50	7.50	7.50	7.50	-	-
PLDLA-s 2	7.48	7.47	7.48	7.49	7.49	7.49	7.49	7.50	7.49	-	-
PLDLA-s 3	7.50	7.49	7.49	7.50	7.49	7.50	7.50	7.49	7.50	-	-
PLDLA-e 1	7.50	7.49	7.49	7.50	7.48	7.50	7.51	7.50	7.50	-	-
PLDLA-e 2	7.50	7.51	7.49	7.48	7.48	7.49	7.49	7.47	7.50	-	-
PLDLA-e 3	7.49	7.48	7.49	7.48	7.50	7.50	7.50	7.48	7.53	-	-
Mg-1	9.10	9.07	9.11	9.08	9.08	9.11	9.10	9.09	9.08	-	-
Mg-2	7.81	7.80	7.88	7.90	7.98	8.08	8.18	8.26	8.30	7.52	7.49
Mg-3	8.39	8.39	8.44	8.43	8.40	8.46	8.47	8.49	8.49	-	-
Mg-4	7.71	7.71	7.76	7.78	7.81	7.89	7.94	8.13	8.18	7.52	7.49
Mg-5	9.06	9.06	9.08	9.06	9.07	9.08	9.08	9.08	9.07	-	-
Mg-6	7.85	7.86	7.95	7.97	8.06	8.13	8.17	8.26	8.30	7.52	7.49
Mg-Original 1	8.70	8.71	8.74	8.72	8.72	8.75	8.77	8.80	8.78	-	-
Mg-Original 2	7.69	7.68	7.71	7.71	7.75	7.82	7.86	8.03	8.08	7.52	7.50

Time (h)	315	336	360	384	456	480	504	528	552	624
Sample:										
Mg-Original-water 1	9.46	9.47	9.41	9.35	9.11	9.24	9.23	9.21	9.14	9.08
Mg-Original-water 2	9.70	9.65	9.59	9.50	9.26	9.24	9.22	9.21	9.18	9.04

APPENDIX IV/IV

pH measurement results						
Time (h)	530	531	552	576	600	672
Sample:						
Mg-PLDLA-s 1	7.51	7.51	7.59	7.66	7.67	7.75
Mg-PLDLA-s 2	-	-	7.96	7.97	7.94	7.97
Mg-PLDLA-s 3	7.51	7.49	7.54	7.53	7.55	7.59
Mg-PLDLA-s 4	7.50	7.49	7.55	7.60	7.59	7.62
Mg-PLDLA-s 5	-	-	7.95	7.94	7.92	7.94
Mg-PLDLA-s 6	-	-	7.94	7.92	7.92	7.93
Mg-PLDLA-e 1	-	-	7.61	7.60	7.60	7.61
Mg-PLDLA-e 2	-	-	7.57	7.58	7.57	7.58
Mg-PLDLA-e 3	-	-	7.61	7.61	7.61	7.62
Mg-PLDLA-e 4	-	-	7.69	7.69	7.69	7.69
PLDLA-s 1	-	-	7.50	7.49	7.52	7.49
PLDLA-s 2	-	-	7.51	7.50	7.47	7.48
PLDLA-s 3	-	-	7.53	7.49	7.50	7.51
PLDLA-e 1	-	-	7.52	7.49	7.50	7.51
PLDLA-e 2	-	-	7.49	7.50	7.49	7.48
PLDLA-e 3	-	-	7.51	7.51	7.49	7.48
Mg-1	-	-	9.08	9.07	9.08	9.07
Mg-2	7.49	7.49	7.53	7.57	7.60	7.73
Mg-3	-	-	8.50	8.49	8.53	8.54
Mg-4	7.49	7.50	7.53	7.56	7.61	7.68
Mg-5	-	-	9.08	9.07	9.08	9.08
Mg-6	7.49	7.52	7.53	7.57	7.63	7.73
Mg-Original 1	-	-	8.80	8.80	8.81	8.84
Mg-Original 2	7.51	7.49	7.53	7.54	7.58	7.65